AD_____

Award Number: W81XWH-11-1-0227

TITLE: The Function of Neuroendocrine Cells in Prostate Cancer

PRINCIPAL INVESTIGATOR: Jiaoti Huang

CONTRACTING ORGANIZATION: University of California, Los Angeles, CA 90095

REPORT DATE: April 2013

TYPE OF REPORT: Annual Report

PREPARED FOR: U.S. Army Medical Research and Materiel Command
Fort Detrick, Maryland 21702-5012

REPORT DOCUMENTATION PAGE

Form Approved
OMB No. 0704-0188

1. REPORT DATE	2. REPORT TYPE	3. DATES COVERED
April 2013	Annual Report	1 April 2012 – 31 March 2013

4. TITLE AND SUBTITLE
The Function of Neuroendocrine Cells in Prostate Cancer

5a. CONTRACT NUMBER

5b. GRANT NUMBER
W81XWH-11-1-0227

5c. PROGRAM ELEMENT NUMBER

6. AUTHOR(S)
Jiaoti Huang

E-Mail: JiaotiHuang@mednet.ucla.edu

5d. PROJECT NUMBER

5e. TASK NUMBER

5f. WORK UNIT NUMBER

7. PERFORMING ORGANIZATION NAME(S) AND ADDRESS(ES)
University of California Los Angeles
Los Angeles, CA 90095

8. PERFORMING ORGANIZATION REPORT NUMBER

9. SPONSORING / MONITORING AGENCY NAME(S) AND ADDRESS(ES)
U.S. Army Medical Research and Materiel Command
Fort Detrick, Maryland 21702-5012

10. SPONSOR/MONITOR'S ACRONYM(S)

11. SPONSOR/MONITOR'S REPORT NUMBER(S)

12. DISTRIBUTION / AVAILABILITY STATEMENT
Approved for Public Release; Distribution Unlimited

13. SUPPLEMENTARY NOTES

14. ABSTRACT
Purpose: The goal of the project is to determine the function of neuroendocrine (NE) cells in the initiation and progression of human prostate cancer
Scope: 1) Use a pten null mouse prostate cancer model to determine if ablation of NE cells by selective expression of a toxin in these cells can delay or prevent tumor initiation and/or progression. 2) Use a human tissue recombination model to determine if depletion of NE cells from human epithelial cells can retard the initiation and progression of the recombinant tumor. 3). Demonstrating the origin and molecular basis of human small cell carcinoma
Major findings: 1). We have demonstrated that NE cells are not required for tumor initiation in a pten knockout mouse prostate cancer model. 2). Preliminary studies indicate that NE cells may play an important role in the progression of prostate cancer to the castration resistant stage in the pten knockout model. 3). With the tissue recombination model, tumors can be generated using the NE cell-depleted basal cells, suggesting that NE cells are not required for tumor initiation. 4). In the tissue recombination model, NE cells are not required for the propagation of established tumors. 5). NE cells are incapable of initiating small cell neuroendocrine carcinoma in the tissue recombination model.

15. SUBJECT TERMS
Prostate cancer, initiation, progression, neuroendocrine cells, animal model

16. SECURITY CLASSIFICATION OF:			17. LIMITATION OF ABSTRACT	18. NUMBER OF PAGES	19a. NAME OF RESPONSIBLE PERSON
a. REPORT	b. ABSTRACT	c. THIS PAGE			19b. TELEPHONE NUMBER *(include area code)*
U	U	U	UU		

Table of Contents

Page

1. Chen H, Sun Y, Wu C, Magyar E, Li X, Cheng6 L, Yao JL, Shen S, Osunkoya AO, Liang C and **Huang J**. Pathogenesis of Prostatic Small Cell Carcinoma Involves the Inactivation of the P53 Pathway. **Endocr Relat Cancer.** 2012;19:321-331. PMID: 22389383
2. Ding B, Sun Y, **Huang J**. Overexpression of SKI oncoprotein leads to P53 degradation through regulation of MDM2 sumoylation. **J Biol Chem**. 2012;287:14621-30.PMID: 22411991
3. Tai S, Sun Y, Liu N, Ding B, Hsia E, Bhuta S, Thor RK, Damoiseaux R, Liang C and **Huang J.** Combination of Rad001 (Everolimus) and Propachlor synergistically induces apoptosis through enhanced autophagy in prostate cancer cells. **Mol Cancer Ther.** 2012; 11:1320-31; PMID: 22491797

Introduction:

Despite years of study by clinicians and scientists around the world, there are still many unanswered questions in prostate cancer. A fundamental and clinically important issue is why prostate cancer responds to hormonal therapy initially but becomes resistant eventually in nearly all patients [1]. Prostate cancer is histologically heterogeneous consisting of luminal type tumor cells and a small component of neuroendocrine (NE) cells [2]. Unlike luminal type tumor cells that express androgen receptor (AR) and depend on androgen for proliferation, NE cells lack AR and are androgen-independent [3]. Hormonal therapy, while inhibiting luminal-type tumor cells, increases the number of NE cells in prostate cancer which is evident in recurrent castration-resistant prostate cancer[4]. In some patients, the recurrent tumor is composed of pure NE cells and is classified as small cell neuroendocrine carcinoma (SCNC) [5]. We hypothesize that NE cells play important roles in the initiation and progression of PC. We also hypothesize that they are the cells of origin for SCNC and p53 is the molecular target. This research proposal has the following specific aims: 1: To determine if NE cells are required for tumor initiation and/or progression in a mouse PC model; 2: To determine if NE cells are required for tumor initiation and/or progression in a human PC model; 3: Cell of origin and the molecular targets of prostatic small cell neuroendocrine carcinoma

Body:

Research accomplishments associated with Task 1: In this task, we will generate *pten*$^{loxP/loxP}$/pb-Cre/CR2-toxin+ mice by breeding pten conditional knockout mice with CR2-toxin mice. We will then observe tumor development and whether the mice develop castration-resistant tumors after castration (Time frame: Months 1 – 36)

1a: Breeding and genotyping (Time frame: Months 1 – 24)

Our goal is to determine the function of neuroendocrine cells in the initiation and progression of prostate cancer. Our approach is to compare the mice with or without NE cells in their prostate cancer formation. The hypothesis is that in the male mice, the toxin will be expressed in prostate neuroendocrine cells because of the selective activity of CR2 promoter in such cells [6-7], resulting in ablation of the neuroendocrine cells. This will give us an opportunity to definitively determine the function of neuroendocrine cells in prostate cancer.

The breeding strategy and genotyping protocol for identifying mice that are of the desired genotype was reported in last year's annual report. Since the last report period, we have found a productive strategy to derive mice of desired genotypes after we realized that male mouse with prostate deletion of *Pten* is most likely not fertile. We therefore bred male mouse carrying the floxed *Pten* allele to the female mouse carrying both the floxed *Pten* and *Cre* gene and have obtained a large number of animals with the desired genotypes.

This task has therefore been successfully completed.

1b: Observing the development of primary tumors (Time frame: Months 12 – 24)

In the first reporting period, we demonstrated that CR2-toxin gene can ablate the prostate cancer formation in TRAMP (transgenic adenocarcinoma of the mouse prostate) mouse model. Prostate tumors in TRAMP mice are composed exclusively of neuroendocrine cells. Therefore this result demonstrated that our approach to abolish neuroendocrine cells in the prostate with CR2 promoter-driven diphtheria toxin is a valid strategy, which will help us to definitively determine if neuroendocrine cells play a role in prostate cancer.

Table 1. A collection of mice of various ages.

$Pten^{loxP/loxP}$/Pb-Cre Age (wks)	*CR2-toxin+*	*CR2-toxin-*
54	2	1
43	1	2
38	2	6
33	2	2
29	2	2
25	3	2
21	3	2
total	15	17

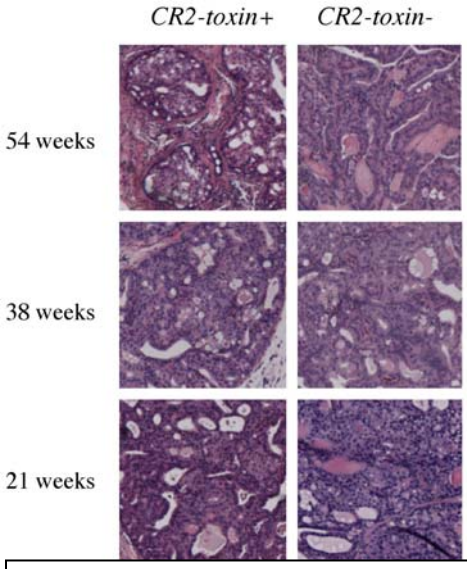

Fig. 1. Similar histologic appearance of prostate tumors in mice with or without the expression of the toxin

As outlined in Table 1, we have generated 32 mice with the desired genotypes of various ages. There were 15 mice carrying the diphtheria toxin, likely devoid of neuroendocrine cells as the toxin will ablate the target cells. There were 17 mice without the toxin genes. The prostates of those mice were dissected and whole mount H&E analyses were performed on all of those samples. As shown in Figure 1, histological analyses of those mice did not show any significant differences in the morphology of those prostates which uniformly were cancerous. Therefore, we conclude that neuroendocrine cells probably do not contribute to the development (or initiation) of prostatic adenocarcinoma.

This task is therefore completed.

1c: Castration and observation of the development of castration-resistant tumors (Time frame: Months 24-36)

The goal of this aim is to determine if neuroendocrine cells contribute to the appearance of castration-resistant prostate cancer after hormonal therapy. Most of the animals with

the appropriate genotypes have been used for aim 1b. However, we did use 4 mice (two each of toxin+ and control) and castrated them at the age of 19 weeks and continued till 33 weeks. An interesting difference was seen between the groups carrying the toxin gene vs. the control group. Both groups have smaller prostates than intact controls due to castration, and the morphology of the prostate is classified as PIN, rather than that of invasive cancer. However, the toxin group seems to have more limited PIN than the control group. Due to the limited number of mice in this preliminary study, we can not make a firm conclusion about whether the neuroendocrine cells might play a role in castration-resistant growth of the *Pten*-loss induced prostate cancer.

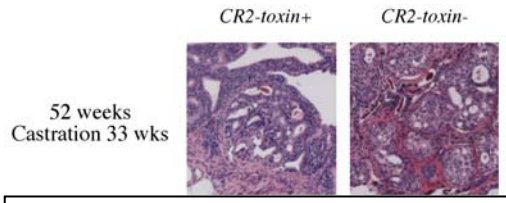

Fig. 2. Expression of the toxin appears to reduce the tumor cell proliferation.

We are continuing to collect mice with the desired genotypes to complete this aim. We will focus on the impact of castration on the prostate cancer development in these mice, and analyze them at various time periods post castration to dissect the role of neuroendocrine cells in castration-resistant development of prostate cancer.

Research accomplishments associated with Task 2: In this task, we will procure fresh human prostate cancer tissue, separate tumor from benign prostate, separate epithelial cells into NE and non-NE cells, and perform tissue regeneration experiments to determine if NE cells are essential in tumor initiation and progression

2a. Procurement of fresh human prostate cancer tissue, separate tumor from benign prostate, separate tumor cells into NE and non-NE tumor cells (Time frame: Months 1 – 36)

This task has been completed and reported in last year's annual report

2b. Tissue regeneration experiment to determine if NE cells are involved in tumor initiation (Time frame: Months 1 – 24)

In an attempt to determine the role of distinct epithelial lineages in prostate cancer development and progression, we have generated and characterized a model of human prostate cancer initiated from naïve human prostate epithelial cells transduced with the oncogenes Myc and myristoylated AKT (myrAKT). Transduction of Trop2+CD49f^{lo} CD26+ luminal cells and Trop2+ CD56+ neuroendocrine cells did not result in any detectable tumors. In contrast, Trop2+ CD49f^{hi} CD26- basal cells were efficient targets for cancer initiation. These results suggest that NE cells are not required for tumor initiation, similar to the conclusion we have drawn from the animal experiments using toxin to ablate the NE cells in pten-/- mice (aim 1b).

Interestingly, we have found that primary tumors derived from Myc/myrAKT-transformed basal cells exhibit a heterogeneous or mixed tumor response, containing

features of both adenocarcinoma and squamous cell carcinoma (Figure 3). Cells bearing both histological phenotypes are human in origin and express the oncogenes Myc and AKT. However, several markers are preferentially expressed in one or the other histological subtype. Expression of luminal-type markers Keratin 8, CD26 and androgen receptor, and the neuroendocrine marker chromogranin A are found exclusively in adenocarcinoma tumor foci. In contrast, basal cell marker Keratin 5, Keratin 14, and p63 are exclusively expressed in squamous tumor foci (Figure 3).

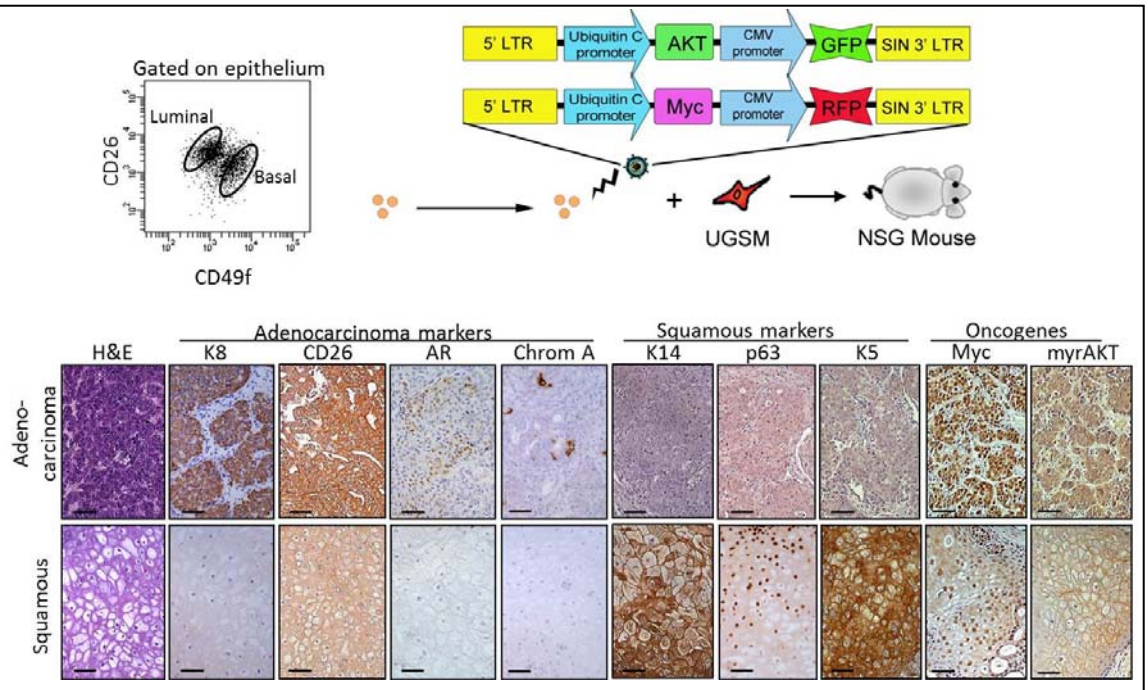

Figure 3. Schematic of naïve human prostate in vivo transformation. Top: CD45-Trop2+ epithelial cells were sorted based on CD49f and CD26 into $CD49f^{hi}CD26^{-}$ basal-enriched and $CD49f^{lo}CD26^{+}$ luminal-enriched subsets, transduced with lentivirus carrying Myc, myrAKT or both, combined with UGSM cells and transplanted into NSG mice. Bottom: Representative adenocarcinoma and squamous regions are identified based on staining for H&E and antibodies against luminal markers Keratin 8 (K8), CD26 and androgen receptor (AR), the neuroendocrine marker chromogranin A, and basal/squamous markers Keratin 14 (K14), p63 and Keratin 5 (K5), and oncogenes Myc and myrAKT/pAKT. Scale bars, 100 μm.

In addition to separate adenocarcinoma and squamous tumor foci, we also found mixed foci containing cells with both histological phenotypes. Since tumors were initiated by lentiviral delivery of oncogenes into basal cells, the viral sequence randomly integrates into the genome of the target cell and all of its progeny. We isolated DNA from neighboring adenocarcinoma and squamous cells within a mixed tumor foci, and performed PCR extending from the viral DNA into the host genome containing the lentiviral integration site. We then performed deep sequencing and aligned reads to the genome. Our analysis revealed that both histological phenotypes are derived from a common clonal cell of origin (Figure 4).

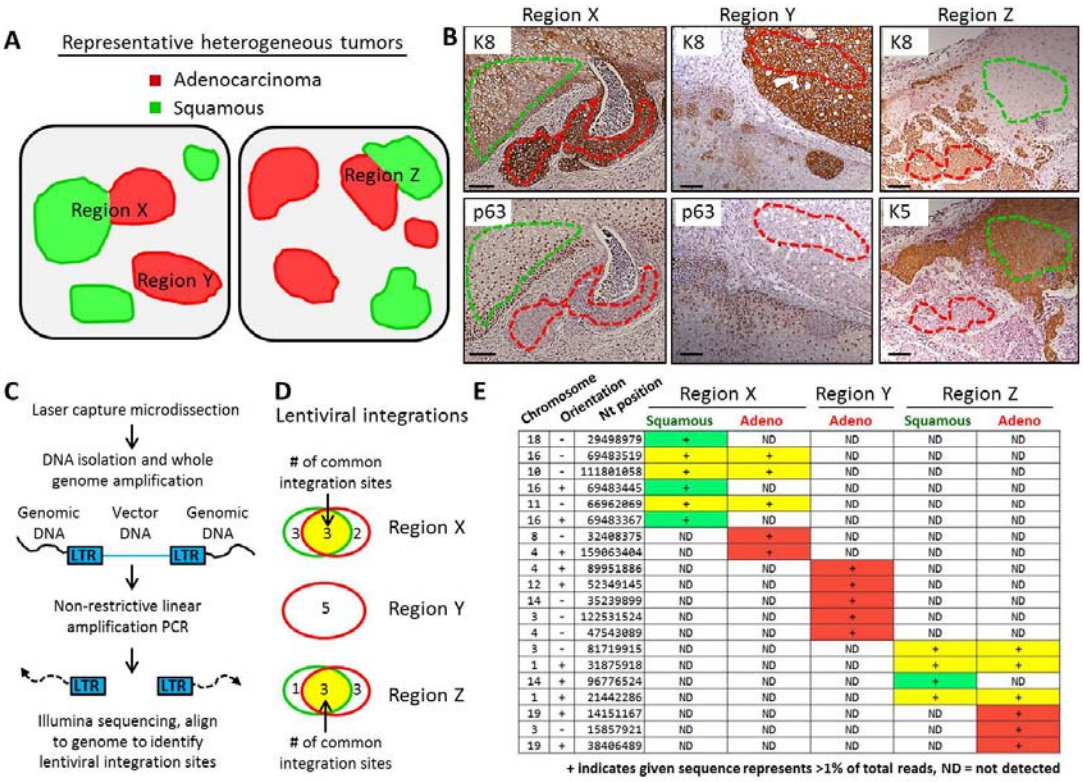

Figure 4. Distinct histological variants in heterogeneous tumors can share a clonal origin. (A) Schematic of two different heterogeneous tumors containing adenocarcinoma, squamous or both phenotypes. Regions X, Y and Z were further studied for lentiviral integration site analysis. (B) Laser capture microdissection was performed on individual glands containing both squamous and adenocarcinoma phenotypes. Representative regions X, Y and Z are shown with serial tissue sections stained with K8 to highlight adenocarcinoma and either p63 or K5 to highlight squamous regions. Dotted lines indicate region excised using laser capture microdissection. Scale bars, 100 µm. (C) Schematic of lentiviral integration site analysis. LTR: long terminal repeat (viral DNA), PCR: polymerase chain reaction. (D) Venn diagrams depict shared lentiviral integration sites in DNA isolated and amplified from neighboring adenocarcinoma (red) and squamous (green) phenotypes (region X), distinct adenocarcinoma gland (region Y), and additional neighboring adenocarcinoma and squamous phenotypes (region Z). (E) Table lists all unique integration sites (IS) with genomic location identifiers (chromosome, orientation, nucleotide position) representing at least 1% of total reads (indicated by +) in each sample. Highlighted rows in yellow represent shared IS between distinct histological phenotypes in the same region, rows in red indicate IS unique to adenocarcinoma, and green represent IS unique to squamous. Note: different regions (X, Y, Z) do not share any IS.

2c. Serial transplantation and tissue regeneration to determine if NE cells are involved in tumor progression

NE cells are continually found in tumors suggesting a role in tumor progression and maintenance [9]. As described above, we can establish aggressive primary human prostate cancer by lentivirus-mediated transduction of Myc and AKT into primary cells combined with UGSM cells in vivo in immune-deficient mice.

To determine which cell-types are capable of propagating tumors, we utilized the antigen CD49f. We first showed that CD49f was expressed highly in the basal layers of squamous tumor cells, but not in adenocarcinoma. In contrast, adenocarcinoma cells express low levels of CD49f. We then fractionated CD49f^{hi} and CD49f^{lo} cells and transplanted both into recipient mice. Both phenotypic populations were competent to propagate tumors, however the histologies represented in the tumors differed. CD49f^{hi} cells could propagate heterogeneous mixed tumors, while CD49f^{lo} cells could only transplant adenocarcinoma (Figure 5).

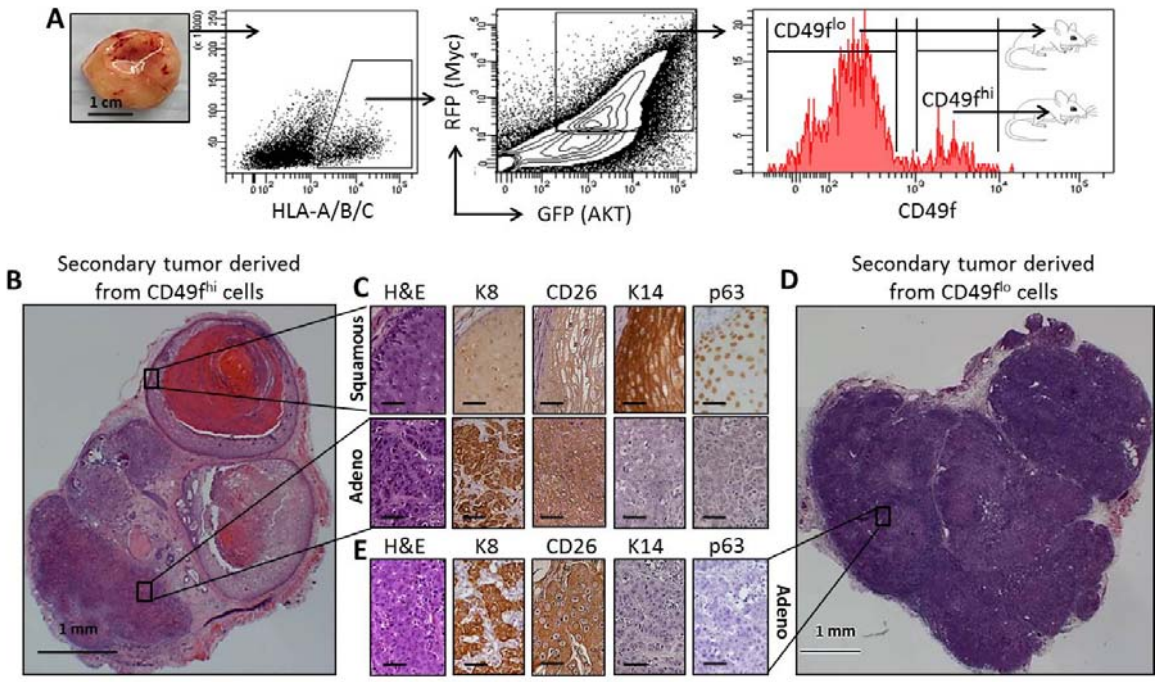

Figure 5. **Two phenotypic cell populations can propagate tumors.** (A) Tumors initiated from CD49f^{hi} cells expressing Myc and myrAKT are dissociated to single cells, stained with a pan-HLA-A/B/C human antibody and gated based on HLA+, GFP+/RFP+ from lentivirus carrying oncogenes myrAKT (GFP) and Myc (RFP), and further sorted into CD49f^{hi} and CD49f^{lo} subsets. Isolated subsets are transplanted back into recipient mice and harvested 6-12 weeks later. (B) H&E-stained overview of a representative secondary tumor from 10,000 isolated CD49f^{hi} tumor cells. (C) Both squamous and adenocarcinoma (Adeno) phenotypes are represented in secondary tumors as distinguished by stains for H&E, K8, CD26, K14 and p63. Scale bars, 50 µm. (D) H&E-stained overview of a representative secondary tumor generated from 10,000 isolated CD49f^{lo} tumor cells. (E) Only the adenocarcinoma phenotype is observed as evidenced by stains for H&E, K8, CD26, K14 and p63. Scale bars, 50 µm.

While high levels of Myc alone or AKT alone were not sufficient to drive full progression to cancer, the combination synergized to initiate large highly-proliferative tumors. Dissociated tumor cells were capable of propagating adenocarcinoma upon

transplantation into mice. Tumors maintained a phenotype that was Keratin 8+ and p63- indicating an acinar-type or luminal-like cell. Importantly, staining for chromogranin A indicated continued presence of NE cells in tumors. Therefore, we separated out the CD56+ and CD56- fraction from aggressive prostate tumors initiated by Myc and AKT, and transplanted each subset into mice. After 12 weeks, only the CD56- (NE-depleted) fraction could initiate tumors, demonstrating that in this model, NE cells may not be required for tumor propagation (Figure 6).

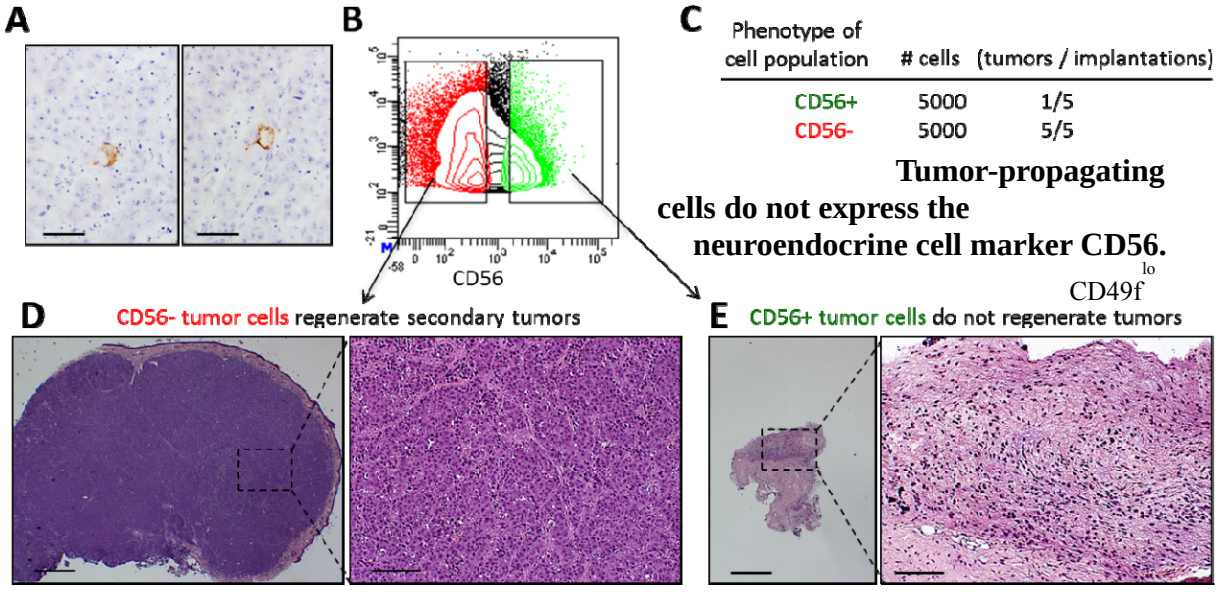

cells from primary regenerated tumors were transplanted into recipient mice to establish secondary tumors. (**A**) Secondary tumors were stained for chromogranin A to detect rare neuroendocrine-like cells. Scale bars, 50 µm. (**B**) Secondary tumor cells were sorted based on HLA+ RFP+ GFP+ and further divided into CD56+/- fractions and transplanted into recipient mice. (**C**) Tumors formed consistently from the transplantation of 5000 CD56- cells but only one tumor formed out of five transplantations of 5000 CD56+ cells. (**D**) A representative secondary tumor derived from CD56- tumor cells is stained for H&E. (**E**) A representative graft comprised of mesenchymal cells without a detectable tumor is shown, stained for H&E. Scale bars, 1 mm. Magnified image, 200 µm.

Therefore, we have successfully completed the entire Task 2.

Research accomplishments associated with Task 3: In this task, we will procure fresh human prostate cancer tissue, separate tumor from benign prostate, separate epithelial cells into NE and non-NE cells, and perform tissue regeneration experiment to determine if SV40 T antigen induces SCNC in NE cells and if p53 is the molecular targets

3a: Same as 2a (completed)

3b. Tissue regeneration experiment to determine if NE cells are the cells of origin for SCNC (Time frame: Months 1 – 24)

Dissociated naïve benign human prostate tissue was separated by FACS into CD56+ (NE-enriched) and CD56- (NE-depleted) fractions and then transduced with lentivirus carrying the SV40 Large T-antigen. Transduced cells were combined with UGSM and transplanted into mice in vivo. Dissociated cells from two different patients were tested and no growths were established from either the CD56+ (NE cells) or CD56- (non-NE) fraction. These findings suggest that the NE cells in this model are incapable of generating small cell neuroendocrine carcinoma.

This task is therefore completed.

3c. Tissue regeneration experiment to determine if p53 is the molecular target for SCNC (Time frame: Months 12 – 36)

To be performed

Key Research Accomplishments

1). We have demonstrated that neuroendocrine cells are not required for tumor initiation in a pten knockout mouse prostate cancer model.
2). Preliminary studies indicate that neuroendocrine cells may play an important role in the progression of prostate cancer to the castration resistant stage in the pten knockout model. A large number of animals are being collected to confirm this finding definitively.
3). With the tissue recombination model, tumors can be generated using the neuroendocrine cell-depleted basal cells, suggesting that neuroendocrine cells are not required for tumor initiation
4). In the tissue recombination model, NE cells are not required for the propagation of established tumors.
5). Neuroendocrine cells are incapable of initiating small cell neuroendocrine carcinoma in the tissue recombination model.

Reportable outcomes

Manuscripts, abstracts, presentations;

Manuscripts:

1. Chen H, Sun Y, Wu C, Magyar E, Li X, Cheng6 L, Yao JL, Shen S, Osunkoya AO, Liang C and **Huang J**. Pathogenesis of Prostatic Small Cell Carcinoma Involves the Inactivation of the P53 Pathway. **Endocr Relat Cancer.** 2012;19:321-331. PMID: 22389383
2. Ding B, Sun Y, **Huang J**. Overexpression of SKI oncoprotein leads to P53 degradation through regulation of MDM2 sumoylation. **J Biol Chem**. 2012;287:14621-30.PMID: 22411991
3. Tai S, Sun Y, Liu N, Ding B, Hsia E, Bhuta S, Thor RK, Damoiseaux R, Liang C and **Huang J.** Combination of Rad001 (Everolimus) and Propachlor synergistically induces apoptosis through enhanced autophagy in prostate cancer cells. **Mol Cancer Ther.** 2012; 11:1320-31; PMID: 22491797

4. Qin J, Liu X, Laffin B, Chen X, Choy G, Jeter CR, Calhoun-Davis T, Li H, Palapattu GS, Pang S, Lin K, **Huang J**, Ivanov I, Li W, Suraneni MV, Tang DG. The PSA(-/lo) Prostate Cancer Cell Population Harbors Self-Renewing Long-Term Tumor-Propagating Cells that Resist Castration. **Cell Stem Cell**. 2012;10:556-69.
5. Liu N, Tai S, Ding B, Thor RK, Bhuta S, Sun Y and **Huang J**. Arsenic trioxide synergizes with Everolimus (Rad001) to induce cytotoxicity of ovarian cancer cells through increased autophagy and apoptosis **Endocr Relat Cancer.** 2012; 19:711-23. PMID: 22919067
6. Paik DY, Janzen DM, Schafenacker AM, Velasco VS, Shung MS, Cheng D, **Huang J**, Witte ON, Memarzadeh S. Stem-Like Epithelial Cells are Concentrated in the Distal End of the Fallopian Tube: A Site for Injury and Serous Cancer Initiation. **Stem Cells**. 2012; 30:2487-97. PMID: 22911892
7. Stoyanova T, Goldstein AS, Cai H, Drake JM, **Huang J**, Witte ON. Regulated proteolysis of Trop2 drives epithelial hyperplasia and stem cell self-renewal via β-catenin signaling. **Genes Dev.** 2012; 26:2271-85. PMID: 23070813
8. Sonn GA, Natarajan S, Margolis DJ, Macairan M, Lieu P, **Huang J**, Dorey FJ, Marks LS. Targeted Biopsy in the Detection of Prostate Cancer Using an Office Based Magnetic Resonance Ultrasound Fusion Device. **J Urol.** 2012; 189:86-92. PMID: 23158413
9. Zong Y, **Huang J**, Sankarasharma D, Morikawa T, Fukayama M, Epstein JI, Chada KK, Witte ON. Stromal epigenetic dysregulation is sufficient to initiate mouse prostate cancer via paracrine Wnt signaling. **Proc Natl Acad Sci U S A**. 2012; 109:E3395-404. PMID: 23184966
10. **Huang J**, Wang JK, and Sun Y. Molecular Pathology of Prostate Cancer Revealed by Next Generation Sequencing: Opportunities for Genome-Based Personalized Therapy. **Curr Opin Urol.** 2013 Feb 4. [Epub ahead of print] PMID: 23385974
11. Li Z, Chen CJ, Wang JK, Hsia E, Squires J, Sun Y and **Huang J**. Neuroendocrine Differentiation of Prostate Cancer. **Asian Journal of Andrology** 2013 Mar 18. doi: 10.1038/aja.2013.7. [Epub ahead of print] PMID: 23503426
12. Ittmann M, **Huang J**, Radaelli E, Martin P, Signoretti S, Sullivan R[6], Simons BW, Ward JM , Robinson BD, Chu GC, Loda M, Thomas G, Borowsky A and Cardiff RD. Animal models of human prostate cancer: The Consensus Report of the New York Meeting of the Mouse Models of Human Cancers Consortium Prostate Pathology Committee. **Cancer Research** 2013 Apr 22. [Epub ahead of print] PMID: 23610450
13. An J, Liu H, Magyar CE, Guo Y, Veena MS, Srivatsan ES, **Huang J**, Rettig MB. Hyperactivated JNK Is a Therapeutic Target in pVHL-Deficient Renal Cell Carcinoma. **Cancer Res.** 2013 Feb 15;73(4):1374-85 PMID: 23393199
14. Sonn GA, Chang E, Natarajan S, Margolis DJ, Macairan M, Lieu P, Huang J, Dorey FJ, Reiter RE, Marks LS. Value of Targeted Prostate Biopsy Using Magnetic Resonance-Ultrasound Fusion in Men with Prior Negative Biopsy and Elevated Prostate-specific Antigen. Eur Urol. 2013 Mar 17. [Epub ahead of print] PMID: 23523537

Presentations:

Invited by academic institutions:

1. Tissue recombination technology in cancer research, Cancer Center, Zhejiang University School of Medicine, Hangzhou, July 2012
2. Neuroendocrine differentiation in prostate cancer, Department of Pathology, Yale University School of Medicine, August 2012
3. Neuroendocrine Differentiation in Prostate Cancer, Department of Pathology, University of California at Irvine, Irvine, CA, September 21, 2012

Invited by local, national or international conferences:

1. International session moderator, 19th Annual Meeting of Chinese Urological Association, November, 2012. Guangzhou, China
2. The annual Hangzhou Symposium on the recent development of molecular diagnosis and treatment of tumors. Hangzhou, China, April 19-21, 2013
3. International forum on translational medicine of urology, Tianjin, China, April 26-28, 2013

Posters and Platform presentations:

1. Song G, Natarajan S, Margolis D, **Huang J**, Dorey F, Macairan ML, Lieu P and Marks LS. Value of Targeted Biopsy in Detecting Prostate Cancer using an Office-Based MR-US Fusion Device. American Urologic Association Annual Meeting, Atlanta, GA, May 2012
2. Gollapudi K, Galet C, Grogan T, Zhang H, Huang J, Elashoff D, Gerber L, Freedland S, Rettig M, Aronson W. Is infiltration of tumor-associated macrophages predictive of biochemical recurrence after radical prostatectomy? American Urological Association Annual Meeting, Atlanta, GA May 20, 2012
3. Susan Kerkoutian, Yin Sun, Xinmin Li, Jason Scapa, Jiaoti Huang. Cell Type-Specific Biomarkers to Predict the Risk of Prostate Cancer in Men with Increased PSA but Negative Biopsies. United States and Canadian Academy of Pathology Annual Meeting, March 2013, Baltimore, MD
4. Karow D., White N., Huang J., Reiter R., Mattrey R., Margolis D., Raman S., Dale A. Improved Conspicuity and Delineation of High-Grade Prostate Tumors Using "Restriction Spectrum Imaging": Quantitative Comparison with High B-Value ADC. **The International Society for Magnetic Resonance in Medicine** 21st Annual Meeting & Exhibition, 20-26 April 2013, Salt Lake City, Utah, USA
5. Geoffrey Sonn, Shyam Natarajan, Daniel Margolis, Edward Chang, Malu Macairan, Patricia Lieu, Jiaoti Huang, Frederick Dorey, Leonard Marks. Prospective Evaluation of MRI-Ultrasound Fusion Biopsy to Diagnose Prostate Cancer in Men with Prior Negative Biopsies. American Urological Society Annual Meeting, May 2013, San Diego, CA
6. Geoffrey Sonn, Shyam Natarajan, Daniel Margolis, Edward Chang, Malu Macairan, Patricia Lieu, Jiaoti Huang, Frederick Dorey, Leonard Marks. Targeted Biopsy with MRI-Ultrasound Fusion. American Urological Society Annual Meeting, May 2013, San Diego, CA
7. Nils Kroeger, David B. Seligson, Sabina Signoretti, Hong Yu, Frederic D. Birkhaeuser, Clara Magyar, Jiaoti Huang, Joseph Riss, Fairooz F. Kabbinavar, Arie S. Belldegrun, Allan J. Pantuck. Investigating the association of cytoplasmic and nuclear

HIF-2 expression with cancer specific survival (CSS) in clear cell renal cell carcinoma. American Society of Clinical Oncology Genitourinary Cancers Symposium, February 2013, Orlando, FL

8. Mitchell Kamrava, Shane Mesko, Robyn Banerjee, Jiaoti Huang, D. Jeffrey Demanes, Leonard S. Marks. Quantifying the ki-67 heterogeneity profile in prostate cancer. American Society of Clinical Oncology Genitourinary Cancers Symposium, February 2013, Orlando, FL
9. Lindsay Ann Schelling; Sean Williamson; Jorge Yao; Shaobo Zhang; Mingsheng Wang; Huang, Jiaoti; Antonio Lopez; Adeboye Osunkoya; Gregory MacLennan. ERG Immunohistochemistry in Prostatic Small Cell Carcinoma: Comparison to Fluorescence in situ Hybridization. United States and Canadian Academy of Pathology Annual Meeting, March 2013, Baltimore, MD
10. Geoffrey Sonn MD, Edward Chang, Shyam Natarajan, Frederick Dorey, Daniel Margolis , Jiaoti Huang, Patricia Lieu, Malu Macairan and Leonard Marks. Impact of MR-Us Fusion Targeted Confirmatory Biopsy on Patient Selection for Active Surveillance. Society for Urologic Oncology Annual Meeting, May 2012, Atlanta, GA

Licenses applied for and/or issued:

None

Funding applied for based on work supported by this award

1. Department of Defense Prostate Cancer Research Program W81XWH-12-1-0206 (PI: L. Wu)
   Period: 07/01/2012 – 06/30/2015
   Title: Disrupting the Pro-Tumorigenic Influences of Tumor-Infiltrating Myeloid Cells by CSF1R Blockade to Augment Androgen Deprivation Therapy in Prostate Cancer
   Direct cost: $150,000/yr
   Percentage effort: 5%
   Role: co-PI

2 Stand–up-to-Cancer Dream Team Award (PI: Small and Witte)
   Period: 1/01/2013 -12/31/2015
   Title: Targeting Adaptive Pathways in Metastatic Treatment-Resistant Prostate Cancer
   Direct Cost: $10,000,000 (all 3 years)
   Percentage effort: 10%
   Role: Pathologist

3 Prostate Cancer Foundation Honorable A. David Mazzone Special Challenge Award (PI: Robert Reiter)
   Period: 01/01/2013 – 12/31/2015
   Title: Preventing Treatment Resistance by Co-Targeting Androgen Receptor and SRC/MEK1-Dependent Epithelial to Mesenchymal Transition
   Direct Cost: 2,000,000 (all 3 years)
   Percent effort: 10%

Role: Co-PI and Pathologist

CONCLUSION:

This project continues to progress well and we are on target to complete all the proposed tasks. We have demonstrated that neuroendocrine cells are not required for tumor initiation in a pten knockout mouse prostate cancer model, and our preliminary studies indicate that neuroendocrine cells may play an important role in the progression of prostate cancer to the castration resistant stage in the pten knockout model. A large number of animals are being collected to confirm this finding definitively.

Using the tissue recombination model, we have demonstrated that neuroendocrine cells are not required for tumor initiation. Similarly, they may not be required for the propagation of established tumors. In addition, neuroendocrine cells are incapable of initiating small cell neuroendocrine carcinoma in the tissue recombination model.

The support by DOD has resulted in extremely high scientific productivity from our laboratory. Since the last annual report, we have published a total of 14 papers in respected scientific journals, with the PI being the corresponding author on 6 of them. We have presented 10 abstracts in various scientific meetings and the PI has been invited to give presentations by many academic institutions and national and international conferences. We have also received more grant funding from DOD, Stand-up-to-Cancer foundation and the Prostate cancer foundation. We are very proud of the accomplishments we have made with the funding from DOD.

References:

1. Scher, H.I. and C.L. Sawyers, *Biology of progressive, castration-resistant prostate cancer: directed therapies targeting the androgen-receptor signaling axis.* J Clin Oncol, 2005. **23**(32): p. 8253-61.
2. Huang, J., et al., *Function and molecular mechanisms of neuroendocrine cells in prostate cancer.* Anal Quant Cytol Histol, 2007. **29**(3): p. 128-38.
3. Huang, J., et al., *Immunohistochemical characterization of neuroendocrine cells in prostate cancer.* Prostate, 2006. **66**(13): p. 1399-1406.
4. Sun, Y., J. Niu, and J. Huang, *Neuroendocrine differentiation in prostate cancer.* Am J Transl Res, 2009. **1**(2): p. 148-62.
5. Wagner, D. and J. Huang, *Small Cell Carcinoma of the Prostate.* eMedicine from WebMD. , 2009. **http://emedicine.medscape.com/article/1611899-overview**.
6. Garabedian, E.M., P.A. Humphrey, and J.I. Gordon, *A transgenic mouse model of metastatic prostate cancer originating from neuroendocrine cells.* Proc Natl Acad Sci U S A, 1998. **95**(26): p. 15382-7.
7. Hu, Y., et al., *Molecular characterization of a metastatic neuroendocrine cell cancer arising in the prostates of transgenic mice.* J Biol Chem, 2002. **277**(46): p. 44462-74.
8. Goldstein, A.S., et al., *Purification and direct transformation of epithelial progenitor cells from primary human prostate.* Nat Protoc, 2011. **6**(5): p. 656-67.

9. Huang, J. and P.A. diSant'Agnese, *Neuroendocrine differentiation in prostate cancer: An overview.*, in *Advances in Oncology: The Expanding Role of Octreotide.* , S. Lamberts, Editor. 2002, BioScientifica Ltd: Bristol. p. 243-262.

Appendices:

Endocrine-Related Cancer (2012) **19** 321–331

Pathogenesis of prostatic small cell carcinoma involves the inactivation of the P53 pathway

Hongbing Chen[1,2], Yin Sun[2]*, Chengyu Wu[5], Clara E Magyar[2], Xinmin Li[2,3], Liang Cheng[6], Jorge L Yao[7], Steven Shen[8], Adeboye O Osunkoya[9], Chaozhao Liang[1] and Jiaoti Huang[2,3,4]*

[1]Department of Urology, The Geriatrics Research Institute, First Affiliated Hospital of Anhui Medical University, Anhui, China
[2]Department of Pathology and Laboratory Medicine, [3]Jonsson Comprehensive Cancer Center and [4]Broad Center for Regenerative Medicine and Stem Cell Biology, David Geffen School of Medicine at UCLA, 10833 Le Conte Avenue, 13-229 CHS, Los Angeles, California 90095-1732, USA
[5]Transplant Immunology Laboratory, Albert Einstein College of Medicine, Montefiore Medical Center, Bronx, New York, USA
[6]Department of Pathology, Indiana University School of Medicine, Indianapolis, Indiana, USA
[7]Department of Pathology, University of Rochester School of Medicine, Rochester, New York, USA
[8]Department of Pathology, The Methodist Hospital, Houston, Texas, USA
[9]Department of Pathology, Emory University School of Medicine, Atlanta, Georgia, USA

(Correspondence should be addressed to J Huang at Department of Pathology and Laboratory Medicine, David Geffen School of Medicine at UCLA; Email: jiaotihuang@mednet.ucla.edu; C Liang; Email: liang_chaozhao@163.com)

*(H Chen and Y Sun contributed equally to this work)

Abstract

Small cell neuroendocrine carcinoma (SCNC) of the prostate is a variant form of prostate cancer that occurs *de novo* or as a recurrent tumor in patients who received hormonal therapy for prostatic adenocarcinoma. It is composed of pure neuroendocrine (NE) tumor cells, but unlike the scattered NE cells in benign prostate and adenocarcinoma that are quiescent, the NE cells in SCNC are highly proliferative and aggressive, causing death in months. In this study, we provide evidence that interleukin 8 (IL8)–CXCR2–P53 (TP53) signaling pathway keeps the NE cells of benign prostate and adenocarcinoma in a quiescent state normally. While P53 appears to be wild-type in the NE cells of benign prostate and adenocarcinoma, immunohistochemical studies show that the majority of the NE tumor cells in SCNC are positive for nuclear p53, suggesting that the *p53* is mutated. This observation is confirmed by sequencing of genomic DNA showing *p53* mutation in five of seven cases of SCNC. Our results support the hypothesis that *p53* mutation leads to inactivation of the IL8–CXCR2–p53 signaling pathway, resulting in the loss of an important growth inhibitory mechanism and the hyper-proliferation of NE cells in SCNC. Therefore, we have identified potential cells of origin and a molecular target for prostatic SCNC that are very different from those of conventional adenocarcinoma, which explains SCNC's distinct biology and the clinical observation that it does not respond to hormonal therapy targeting androgen receptor signaling, which produces short-term therapeutic effects in nearly all patients with prostatic adenocarcinoma.

Endocrine-Related Cancer (2012) **19** 321–331

Introduction

Prostate cancer (PC) is the most common malignancy in men and the second leading cause of cancer-related deaths (Cooperberg *et al*. 2004). Normal prostate epithelium contains luminal epithelial cells, basal cells, and a minor component of neuroendocrine (NE) cells that are scattered throughout the prostate (Vashchenko & Abrahamsson 2005, Huang *et al*. 2007, Yuan *et al*. 2007, Sun *et al*. 2009). The majority of PCs are classified as adenocarcinomas characterized by absence of basal cells and uncontrolled proliferation of malignant tumor cells with luminal cell features

DOI: 10.1530/ERC-11-0368
1351–0088/12/019–321
Online version via http://www.endocrinology-journals.org

including glandular formation and expression of androgen receptor (AR) and prostate-specific antigen (PSA). Interestingly, every case of prostatic adenocarcinoma also contains a small population (usually ~1%) of NE cells (Vashchenko & Abrahamsson 2005, Huang *et al*. 2007, Yuan *et al*. 2007, Sun *et al*. 2009). The NE cells in adenocarcinoma share many important features with those in the benign prostate. In contrast to the luminal-type non-NE tumor cells, the NE tumor cells do not express AR and PSA (Bonkhoff 2001, Huang *et al*. 2006). Importantly, unlike the bulk, non-NE tumor cells, NE cells in benign prostate and adenocarcinoma are normally quiescent (Bonkhoff 2001, Huang *et al*. 2006).

While adenocarcinomas comprise the majority of PC, there are variant forms among which small cell neuroendocrine carcinoma (SCNC) is an important histological subtype that is often seen in patients with advanced disease. Prostatic SCNC is composed of tumor cells with NE phenotype (Grignon 2004). In comparison to adenocarcinoma, which usually shows glandular formation, SCNC has a solid, sheet-like growth pattern but no glandular formation. Tumor cells are small with fine chromatin pattern, scant cytoplasm, and nuclear molding. Mitotic figures, crush artifact, and tumor necrosis are frequent findings (Yao *et al*. 2006, Huang *et al*. 2007, Wang & Epstein 2008). Although SCNCs may arise *de novo*, such tumors are often seen as recurrent tumors after hormonal therapy for conventional adenocarcinomas of the prostate (Miyoshi *et al*. 2001, Tanaka *et al*. 2001). The prevalence of this disease is likely underestimated because patients with advanced and metastatic diseases usually do not undergo tissue diagnosis. Accurate diagnosis of SCNC is important as such tumors do not respond to hormonal therapy targeting the AR signaling pathway (Brown *et al*. 2003), which produces a short-term therapeutic effect in nearly all cases of prostatic adenocarcinoma (Scher 2003).

The NE tumor cells in prostatic SCNCs share many features with those in benign prostate and prostatic adenocarcinoma. For example, they contain dense-core secretory granules when examined by electron microscopy and are usually positive for NE markers chromogranin A (CgA) and synaptophysin by immunohistochemistry. However, unlike the NE cells in benign prostate and prostatic adenocarcinoma that are quiescent, the NE tumor cells in prostatic SCNCs are highly proliferative, leading to early metastasis (Erasmus *et al*. 2002), and the patients usually die within months of diagnosis. The molecular mechanisms responsible for the aggressive biological behavior of the NE tumor cells in prostatic SCNC remain unknown. Here, we provide evidence that the interleukin 8 (IL8)–CXCR2–p53 (TP53) pathway may be important in keeping the NE cells in benign prostate and prostatic adenocarcinoma in a quiescent state, and inactivation of the pathway due to *p53* mutation may be responsible for the rapid proliferation of NE cells in prostatic SCNC.

Materials and methods

Cell culture and transfection

LNCaP cells were maintained in RPMI-1640 medium supplemented with 10% fetal bovine serum, 2 mM L-glutamine, penicillin (100 U/ml), and streptomycin (100 μg/ml) in a humidified atmosphere of 5% CO_2 maintained at 37 °C. pcDNA3 vector or pcDNA3-CXCR2 was transfected into LNCAP cells with Lipofectamine 2000 (Invitrogen), and stable clones were selected with G418 at 300 μg/ml for 30 days. For siRNA transfection, Dharmafect #2 was used with siRNA at 100 nM for *p53* (duplex sequences are 5′-rCrCrA rCrCrArUrCrCrArCrUrArCrArArCr-UrArCrArUrGTG-3′, 5′-rCrArCrArUrGrUrArGrUr-UrGrUrArGrUrGrGrArUrGrGrUrGrGrUrA-3′). For expression of *p53* in PC3 cells, GFP expression plasmid with a ratio of 9:1 to CMV-driven *p53* plasmid were transfected with Fugene 6, 3 days later, IL8 was added, and the number of GFP-positive cells were counted using Acumen laser cytometer.

Immunoblot analysis

Cells were washed with PBS and lysed in RIPA buffer (50 mM Tris, pH 7.4, 150 mM NaCl, 1% Triton X-100, 0.5% deoxycholate, 0.1% SDS) containing protease inhibitor cocktail for 15 min at 4 °C. Cell lysates were centrifuged and supernatants were collected. Equal amounts of proteins were resolved on SDS–PAGE gels and transferred to polyvinylidene fluoride (PVDF) membranes. The resulting blots were blocked in 5% nonfat dry milk for 30 min followed by incubation with primary antibody against CXCR2 (Cat. no. 555932; BD Biosciences, San Diego, CA, USA). HRP-conjugated secondary antibody and supersignal west pico chemiluminescent substrate (Thermo Fisher Scientific, Waltham, MA, USA) were used to visualize antigen–antibody complexes.

Flow cytometry analysis

Flow cytometry analysis was performed as described previously (Palapattu *et al*. 2009) using a fluorescein

isothiocyanate (FITC) conjugated anti-CXCR2 antibody (BD Biosciences).

Cell proliferation assay

Cells were seeded into 96-well microplates and 10 nM IL8 were added to the culture 24 h after seeding for 6 days with the cell number determination at days 0, 2, 4, and 6 using CellTiter Glo assay (Promega) according to the manufacture's protocol.

RNA isolation and quality control and microarray hybridization

Total RNA was isolated using the RNeasy Mini Kit (Qiagen) according to the manufacturer's instructions. RNA integrity was evaluated using an Agilent 2100 Bioanalyzer (Agilent Technologies, Palo Alto, CA, USA) and purity/concentration was determined using a NanoDrop 8000 (NanoDrop Products, Wilmington, DE, USA). Microarray targets were prepared using MessageAmp Premier RNA Amplification Kit (Ambion) and hybridized to the Affymetrix GeneChip U133plus 2.0 Array (Affymetrix, Inc., Santa Clara, CA, USA) according to the manufacturers' instructions. The arrays were washed and stained with streptavidin phycoerythrin in Affymetrix Fluidics Station 450 using the Affymetrix GeneChip protocol and then scanned using an Affymetrix GeneChip Scanner 3000.

Microarray data analysis

The acquisition and initial quantification of array images were conducted using the AGCC Software (Affymetrix, Inc.). The subsequent data analyses were performed using Partek Genomics Suite version 6.4 (Partek, Inc., St. Louis, MO, USA). Differentially expressed genes were selected at ≥ 1.5-fold and $P < 0.05$. Cluster analyses and principal component analysis were conducted with Partek default settings. Biofunctional analysis was performed using Ingenuity Pathways Analysis Software version 7.6 (Ingenuity Systems, Redwood City, CA, USA).

Construction of tissue microarrays and immunohistochemical staining

Construction of tissue microarray (TMA) and immunohistochemical staining has been described previously (Huang *et al*. 2005). Three hundred cases of prostatectomy specimens were reviewed and representative cancer and benign areas were circled. The cancer and benign prostate tissues were then transferred from donor blocks to recipient blocks to construct tissue microarray blocks. H&E sections were prepared from the top for quality control.

For immunohistochemical studies, paraffin sections of 5 μm thickness were prepared from regular histological blocks or from tissue microarrays. The sections were deparaffinized with xylene and rehydrated through graded ethanol. Endogenous peroxidase activity was blocked with 3% hydrogen peroxide in methanol for 10 min. Heat-induced antigen retrieval (HIER) was carried out for all sections in 0.01 M citrate, pH = 6.00, using a vegetable steamer at 95 °C for 25 min. Mouse monoclonal anti-p53 antibody (clone 1801, Oncogene, OP09-100 μg, used at 1:50) and mouse monoclonal anti-CgA antibody (clone DAK-A3, M0869, used at 1:1000; DakoCytomation Carpinteria, CA, USA) were used as primary antibodies. MACH2 Mouse HRP-Polymer (Cat no. #MHRP520L, Biocare Medical, Concord, CA, USA) was used as the secondary antibody. For double staining of p53 and CgA, the two antibodies were used sequentially. 3,3'-diaminobenzidine (DAB, brown) and alkaline phosphatase (AP, red) were used as chromogens.

Genomic sequencing of p53 exons

Based on microscopic examination, small cell carcinoma regions in paraffin section were scraped off and collected from the slides followed by deparaffinization and overnight proteinase K digestion. The genomic DNA was purified through ethanol precipitation after phenol and chloroform extraction. Exons 5–10 of *p53* were amplified by PCR followed by gel electrophoresis analysis. The PCR products were either directly used for sequencing if there is specific amplification or gel purified and sequenced by one of the amplifying primers. Primers for amplifications are as follows: exon 5 forward 5′-GCCCTGTCGTCTCTCCAG-3′, reverse 5′-GACTTTCAACTCTGTCTCCTTCC-3′; exon 6 forward 5′-CTTAACCCCTCCTCCCAGAG-3′, reverse 5′-CAGGCCTCTGATTCCTCACT-3′; exon 7 forward 5′-GTGTGCAGGGTGGCAAGT-3′, reverse 5′-CGACAGAGCGAGATTCCATC-3′; exons 8 and 9 forward 5′-CGGCATTTTGAGTGTTAGACTG-3′, reverse 5′-GCCTCTTGCTTCTCTTTTCC-3′, exon 10 forward 5′-TGCATGTTGCTTTTGTACCG-3′, reverse 5′-GGAGTAGGGCCAGGAAGG-3′.

Results

Establishing LNCaP cell lines stably expressing IL8 receptor CXCR2

We have previously shown that NE cells in benign prostate and prostatic adenocarcinoma express IL8 and its receptor CXCR2 (Huang *et al*. 2005). We hypothesized that the autocrine action of IL8–CXCR2

may be responsible for certain function of NE cells (Huang *et al*. 2005), but the exact consequence of this autocrine action was unclear. A more recent publication showed that activation of CXCR2 by IL8 leads to cellular senescence, a state of stable proliferative arrest, via a p53-dependent mechanism (Acosta *et al*. 2008). Thus, we further hypothesized that IL8–CXCR2–p53 pathway may also be active in NE cells in benign prostate and prostatic adenocarcinoma, which maintains these cells in a quiescent state.

In human PC tissue, NE cells are positive for IL8 and its receptor CXCR2 while luminal cells are negative for both (Huang *et al*. 2005). LNCaP cells have features of prostatic cancer cells with luminal (non-NE) features in that they express luminal differentiation markers AR and PSA but not NE markers CgA and neuron-specific enolase (NSE) (Palapattu *et al*. 2009). Accordingly, there is no detectable expression of IL8 and a very low level of CXCR2 in LNCaP cells.

In order to study the function and signaling pathway of CXCR2, we transfected LNCaP cells with pcDNA3-CXCR2 plasmid to obtain LNCaP cells that stably overexpress CXCR2. Figure 1 (A, B and C) shows that we have established LNCaP cells that overexpress CXCR2 (LNCaP/CXCR2 cells), as confirmed by immunoblot as well as flow cytometric analysis with antibodies against CXCR2.

Activation of CXCR2 by IL8 inhibits cell proliferation

In a genetic screen to identify molecules that are critical for replicative senescence, it was found that activation of CXCR2 by IL8 leads to cellular senescence, which is mediated by p53 (Acosta *et al*. 2008). Thus, we hypothesized that in NE cells of benign prostate and adenocarcinoma, the IL8–CXCR2–p53 pathway may be responsible for keeping the cells in a quiescent state normally. To test this hypothesis, we used LNCaP and LNCaP/CXCR2 cells and examined their proliferative responses to IL8. As shown in Fig. 1D, IL8 inhibited the proliferation of LNCaP/CXCR2 cells but not the parental LNCaP cells, a finding that supports our hypothesis. We also examined the transcriptional responses to IL8 by comparing the transcriptional profiles of cells with or without IL8 treatment. As shown in Fig. 1E, IL8 stimulation induced similar changes in transcriptional profiles at 1 and 12 h, with up- or downregulation of a variety of genes. Interestingly, activation of CXCR2 by IL8 led to altered expression of many genes involved in p53 signaling. Functional gene family analysis showed that among the genes whose expression increased significantly in response to IL8 stimulation were those controlling the G1/S and G2/M transition check points. As an important function of p53 is in the cell cycle control and growth inhibition, these results suggest that growth inhibition of LNCaP/CXCR2 cells after activation of CXCR2 by IL8 may involve the p53 pathway.

P53 is required for the growth inhibitory function of the IL8–CXCR2 autocrine pathway

P53 was shown to be critical in mediating the IL8–CXCR2 signaling to induce cellular senescence (Acosta *et al*. 2008). Similarly, p53 may also be essential in the growth suppression after activation of CXCR2 by IL8 treatment in LNCaP/CXCR2 cells, as suggested by our microarray studies. To directly test this hypothesis, we attempted to abrogate p53 function in LNCaP/CXCR2 cells to determine whether a loss of P53 activity would change the growth response toward IL8 treatment. P53 protein is of wild-type in LNCaP cells (van Bokhoven *et al*. 2003), thus inactivation of p53 activity can be achieved through reduction of the endogenous wild-type protein. We used a transient transfection method to introduce siRNA to reduce the endogenous P53 level in LNCaP/CXCR2 cells. As shown in Fig. 2A, we were able to significantly reduce the P53 level by siRNA method. Importantly, IL8 treatment of the cells with reduced P53 levels resulted in an increase in cell number while the control cells showed reduced cell numbers in response to IL8 treatment, suggesting that P53 is critically important for the growth inhibition after activation of CXCR2 by IL8. The results also suggest that in the absence of functional P53, activation of CXCR2 by IL8 may stimulate cell proliferation via a different signaling pathway.

Our group has recently demonstrated that another commonly used PC cell line, PC3, possesses features of prostatic SCNC in that these cells are negative for luminal differentiation markers AR and PSA but positive for NE markers (Tai *et al*. 2011). Similar to NE cells in benign prostate and prostatic adenocarcinoma, PC3 cells express IL8 (Ma *et al*. 2009) and CXCR2 (Reiland *et al*. 1999). Contrary to NE cells in benign prostate and prostatic adenocarcinoma, PC3 cells are highly proliferative NE cells similar to human prostatic SCNC. We hypothesized that loss of the growth inhibitory function of the IL8–CXCR2–p53 pathway may be responsible for the rapid proliferation and aggressive behavior of PC3 cells. In support of our hypothesis, it has been reported that PC3 cells, unlike LNCaP cells, contain a *p53* mutation

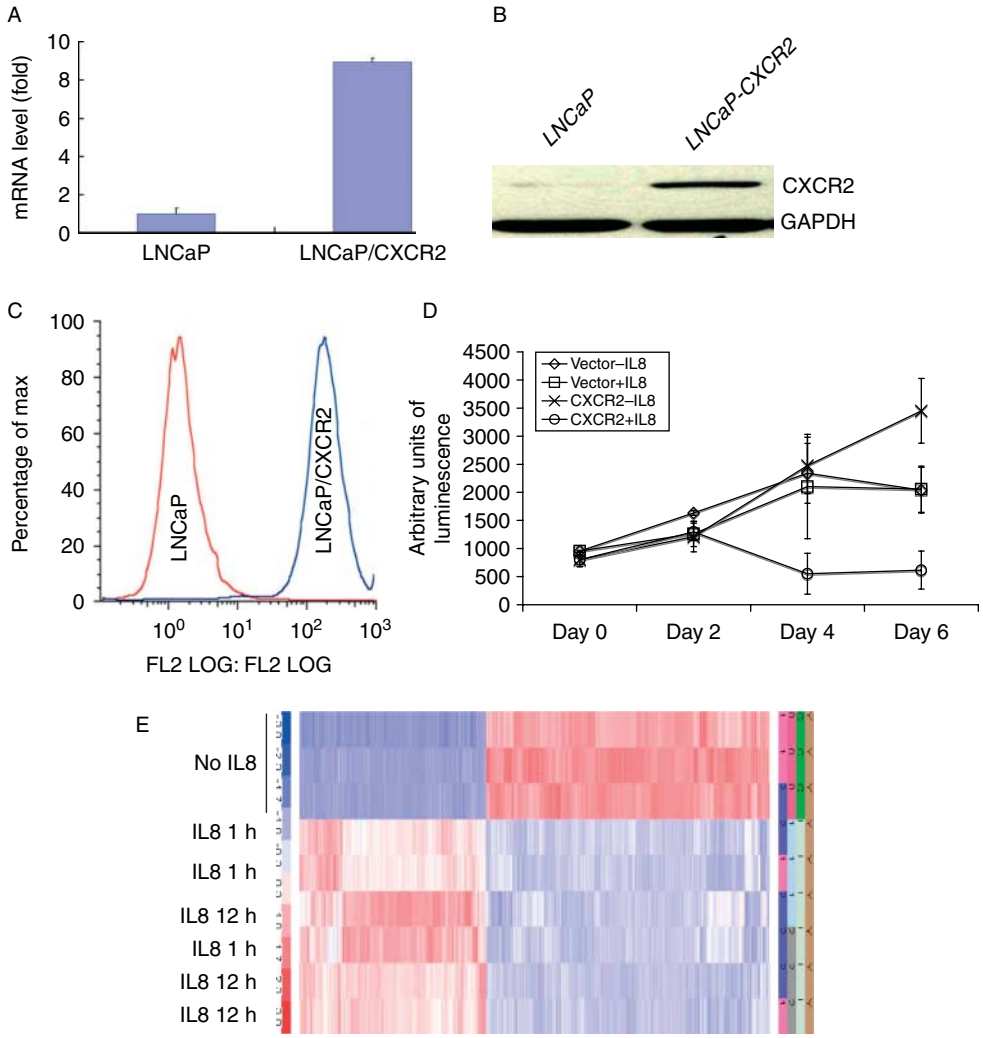

Figure 1 Activation of CXCR2 by IL8 inhibits cell proliferation and induces changes in gene expression profile. LNCaP cells were stably transfected with a plasmid-expressing CXCR2, a receptor for IL8. Real-time PCR (A), western blot (B), and flow cytometry (C) analyses show that CXCR2 is not expressed in the parental LNCaP cells but highly overexpressed in the stable cell line. (D) LNCaP cells transfected with vector control or CXCR2 were cultured in the absence or presence of IL8. IL8 significantly inhibits the proliferation of LNCaP cells expressing CXCR2. (E) Microarray analysis shows that IL8 stimulation of LNCaP/CXCR2 cells results in significant changes of gene expression profile. Similar changes were observed at 1 and 12 h after IL8 treatment.

(van Bokhoven *et al*. 2003). Therefore, we tested whether forced expression of wild-type P53 may restore the function of the IL8–CXCR2–P53 pathway resulting in inhibition of cellular proliferation. Similar to what was reported previously (Isaacs *et al*. 1991), introduction of wild-type P53 significantly slowed the growth of PC3 cells. Additionally, in contrast to control PC3 cells, IL8 treatment of PC3 cells expressing wild-type P53 led to reduced cell numbers. These data suggest that IL8–CXCR2–p53 pathway plays a central role in mediating growth suppression normally, and loss of function of this pathway (such as a P53 mutation) can lead to increased proliferation in NE cells.

Mutation of *P53* in NE tumor cells of prostatic SCNC

NE cells in benign human prostate and prostatic adenocarcinoma are quiescent (Huang *et al*. 2007) but those in prostatic SCNC, whether arising *de novo* or as a recurrent tumor in patients treated with hormonal therapy for adenocarcinoma, are highly proliferative and biologically very aggressive (Yao *et al*. 2006, Wang & Epstein 2008). The underlying molecular mechanism responsible for such a difference is unclear. The results presented above are consistent with the model that the intact IL8–CXCR2–P53 pathway may be responsible for keeping the NE cells

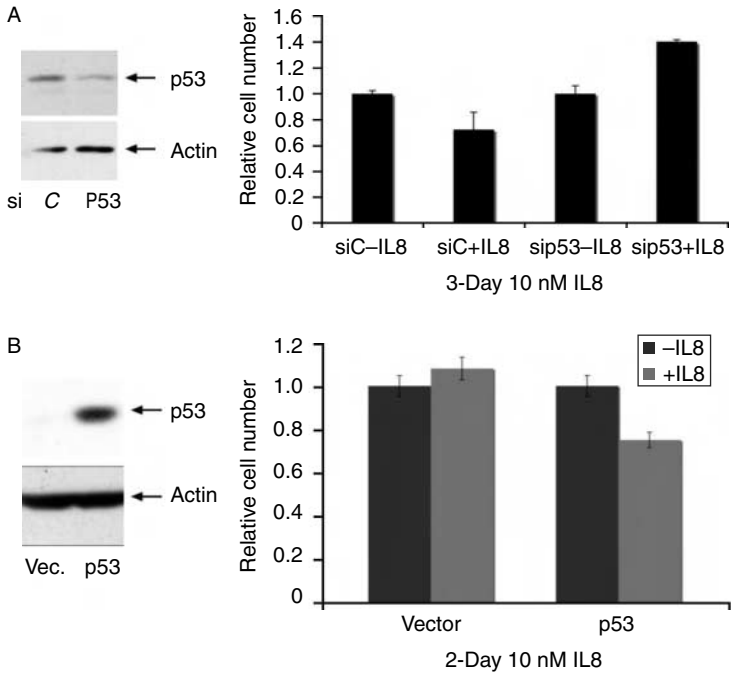

Figure 2 p53 is important for mediating IL8 activity in LNCAP and PC3 cells. (A) Knocking down endogenous p53 in CXCR2-expressing LNCaP cells leads to increase in cell proliferation in response to IL8 treatment. (B) Expression of p53 renders PC3 cells responsive to growth inhibition of IL8. GFP-positive cells were counted using laser microplate cytometer as equivalent to p53 expression in PC3 cells. The ratio of the number of cells in the presence or absence of IL8 was tabulated.

under a state of quiescence, a mechanism that has been reported in senescent cells (Acosta *et al*. 2008). Therefore, we further hypothesized that the reason the NE tumor cells in prostatic SCNC are highly proliferative and biologically aggressive is because this important growth-inhibitory pathway is inactivated in such cells. As mutation of *P53* represents the most common genetic alteration of human malignancies, we further hypothesized that *P53* mutation is a fundamental molecular change responsible for the aggressive biological behavior of prostatic SCNC as has been observed in PC3 cells, a cell line that is characteristic of human prostatic SCNC (Tai *et al*. 2011).

It is well known that *p53* mutation causes prolonged half-life and subsequent nuclear accumulation of the p53 protein, which then becomes detectable by immunohistochemistry (Schlomm *et al*. 2008, Kudahetti *et al*. 2009). Therefore, we performed immunohistochemistry to observe p53 nuclear staining in NE cells of benign prostate, prostatic adenocarcinoma, and SCNC. Adjacent sections were prepared from tissue microarrays containing 150 cases (300 cores) of prostatic adenocarcinoma and an equal number of benign prostate from the same patients. We had shown that the two adjacent sections prepared in this manner contained essentially identical cells and such sections are useful in identifying proteins specifically expressed in prostatic NE cells (Huang *et al*. 2005, 2006, Wu *et al*. 2006). To determine whether NE cells in benign prostate tissue and adenocarcinoma are positive for nuclear p53 staining, the first sections from the tissue microarrays were stained with an anti-CgA antibody to highlight NE cells as CgA is widely considered the most sensitive and specific marker for prostatic NE cells (Vashchenko & Abrahamsson 2005, Huang *et al*. 2007, Yuan *et al*. 2007) and the second sections stained with an anti-p53 antibody. The stained slides were scanned and analyzed using the Ariol SL-50 scanner with thresholds applied for RGB algorithms, shapes, and sizes. The number of nuclei and positively stained cells were counted and separately recorded. Benign cores ($n=300$) in the TMAs contained 1353 NE cells (representing 0.33% of total cells) and 3297 p53+ cells (representing 0.84% of total nuclei); cancer cores ($n=300$) had 1331 NE cells (representing 0.23% of total cells) and 4646 p53+ cells (representing 0.9% of total nuclei). As has been described previously, the NE cells were present as individual cells or small clusters (Huang *et al*. 2007). The p53-positive cells in benign prostate appear to be mostly basal cells while in adenocarcinoma, the p53-positive cells were

mostly individual tumor cells. Importantly, when the corresponding cores in the two TMA sections were matched and compared, there was no overlap between CgA+ and p53+ cells, supporting the conclusion that the NE cells were negative for p53 nuclear staining and the scattered nuclear p53+ cells were not the NE cells (Fig. 3A and B). To confirm this finding, we also performed double staining for CgA and p53 on the same TMA section. We again showed that CgA staining (cytoplasmic) and p53 staining (nuclear) did not exist in the same cells (Fig. 3C). These results suggest that in benign prostate and prostatic adenocarcinoma, the NE cells likely have wild-type p53.

To determine whether *p53* mutation may be present in prostatic SCNC, we used immunohistochemistry to study *p53* expression in 31 cases of prostatic SCNC using regular histological sections. Unlike NE cells in benign prostate or prostatic adenocarcinoma, the NE tumor cells in prostatic SCNCs were positive for p53, with 74% (23/31) of the cases showing positivity in 50–100% cells and the remaining 26% (8/31) of the cases with positivity in 5–50% cells (Fig. 4A and B). As nuclear staining of p53 results from prolonged half-life of the protein after mutations, these results suggest that most, if not all, prostatic SCNCs contain mutations in the *p53* gene.

To directly examine the possible mutations of the *p53* gene in the SCNC, we obtained formalin-fixed, paraffin-embedded tissue from seven cases of prostatic SCNC and extracted genomic DNA from them. Exons 5–10 of *p53* were amplified by PCR followed by direct sequencing. As shown in Fig. 4C, this analysis indicated that five out of seven tumor samples contain an identical allele of a missense transition converting G to A at position 747, changing negatively charged aspartic acid to hydrophilic amino acid asparagine at amino acid 184, again supporting our hypothesis that

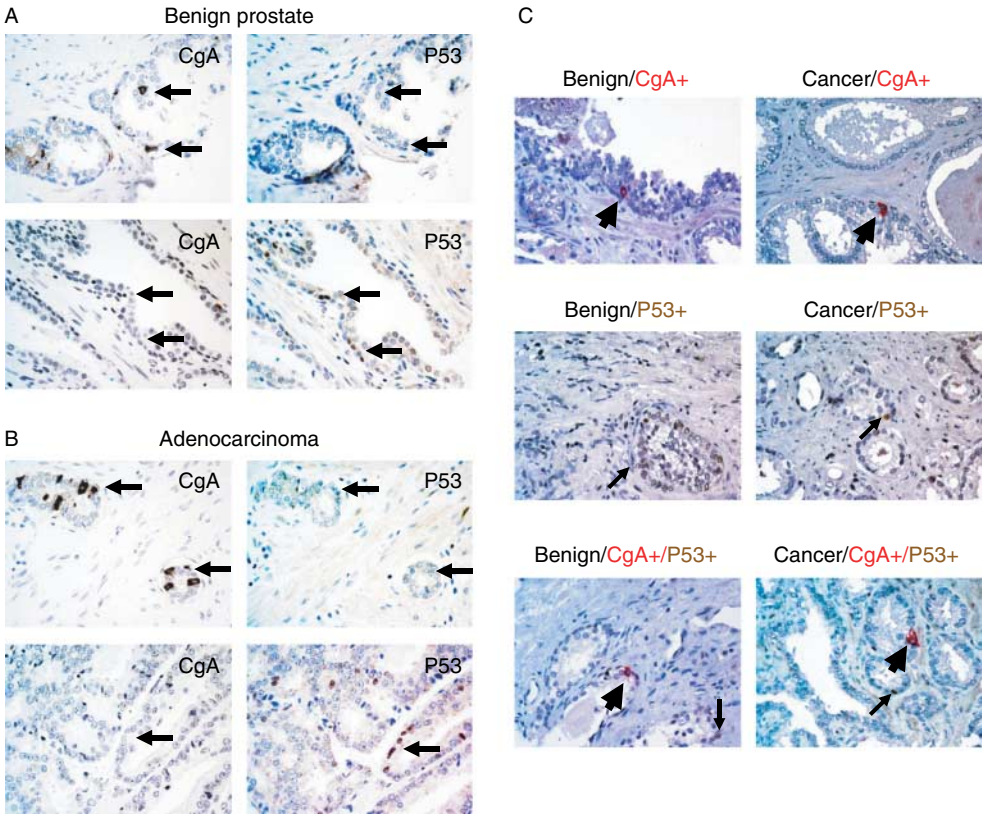

Figure 3 NE cells in benign and adenocarcinoma of prostate are negative for nuclear P53 staining. (A) Adjacent sections of benign prostate were stained with anti-CgA and anti-P53 antibodies respectively. The upper panel shows that NE cells (CgA+, arrows) are negative for nuclear P53. The lower panel shows that the scattered P53+ cells (arrows) were not NE cells (CgA−). (B) Adjacent sections of prostate adenocarcinoma were stained with anti-CgA and anti-P53 antibodies respectively. The upper panel shows that NE cells (CgA+, arrows) are negative for nuclear P53. The lower panel shows that the scattered P53+ cells (arrows) were not NE cells (CgA−). (C) Sections of benign prostate and prostate adenocarcinoma were doubly stained for CgA (cytoplasmic, red, thick arrow) and P53 (nuclear, brown, thin arrow). The pictures on the left show benign prostate with NE cells (thick arrow, top), P53+ cells (thin arrow, middle), and both (lower). The right panel shows the same in adenocarcinoma. Importantly, cytoplasmic CgA staining and nuclear P53 staining do not occur in the same cells.

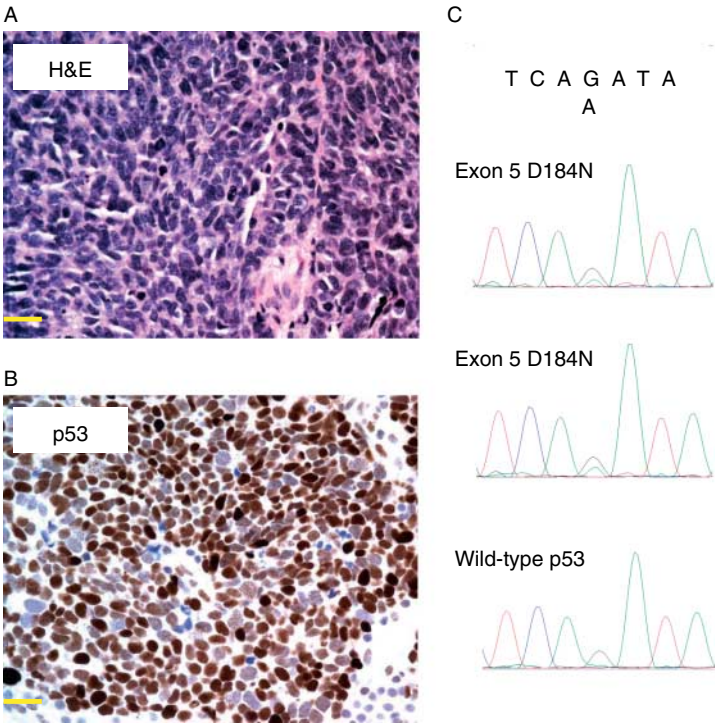

Figure 4 SCNC shows diffuse nuclear P53 staining and contains P53 mutation. (A) H&E slide of SCNC composed of pure NE tumor cells with characteristic morphological features including scant cytoplasm, fine nuclear chromatin pattern, and nuclear molding. (B) Immunohistochemistry shows diffuse nuclear P53 staining in SCNC. (C) Sequencing data from SCNC. The two examples in the top and middle panels show p53 mutation in exon 5 resulting in replacement of aspartic acid at position 184 by asparagine. The bottom panel shows wild-type P53 sequence in the same region.

a *p53* mutation inactivates the IL8–CXCR2–p53 pathway that normally keeps the NE cells in a quiescent state, resulting in hyper-proliferation and aggressive behavior, features that are characteristic of the tumor cells in SCNC.

Discussion

NE cells are normally present as a minor component in benign prostate and prostatic adenocarcinomas and their functions remain unclear. It has been observed that in cultured LNCaP cells, a cell line with luminal cell features, androgen withdrawal induces differentiation toward a NE phenotype (Burchardt *et al*. 1999), suggesting that hormonal therapy in PC patients may drive luminal-type cancer cells into NE cancer cells. One interesting hypothesis is that the normally quiescent NE tumor cells may provide growth signals to the adjacent non-NE cancer cells through a paracrine mechanism, contributing to therapeutic failure and the progression to castration-resistant state (Vashchenko & Abrahamsson 2005, Huang *et al*. 2007, Yuan *et al*. 2007, Sun *et al*. 2009). Occasionally, the recurrent tumor contains pure populations of highly aggressive NE tumor cells and is classified as SCNC, although SCNC can also be seen in patients without a history of adenocarcinoma. With the advent of novel drugs such as Abiraterone and MDV3100 that show superior efficacy in the inhibition of AR signaling, we expect that the incidence of prostatic SCNC will only increase.

The cell of origin and the molecular basis for prostatic adenocarcinoma remain controversial. These issues are even less clear for prostatic SCNC. Our results are consistent with a model in which the NE cells in benign prostate and prostatic adenocarcinoma are normally quiescent due to the growth inhibitory function of an autocrine mechanism involving the IL8–CXCR2–p53 pathway. Mutation of *p53* leads to inactivation of the above pathway leading to hyper-proliferation of NE cells with the resultant SCNC as shown in Fig. 5. In fact, in the absence of functional P53, activation of CXCR2 by IL8 appears to stimulate cell growth (Fig. 2), suggesting that CXCR2 may elicit both growth inhibitory and growth stimulatory pathways. Normally, the P53-mediated growth-inhibitory pathway may dominate. Once P53 is mutated, CXCR2 activation becomes growth promoting and oncogenic. This hypothesis is supported by previous reports showing

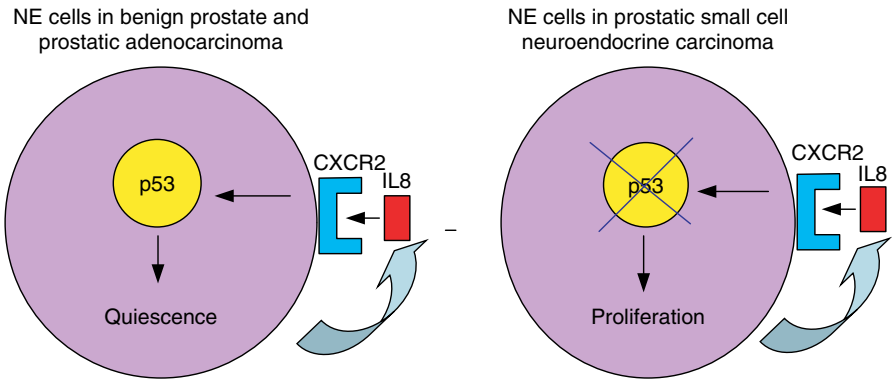

Figure 5 The function of IL8–CXCR2–p53 pathway in controlling the proliferation of NE cells in benign prostate, adenocarcinoma, and SCNC. The model on the left suggests that autocrine activation of CXCR2 by IL8 activates the p53 pathway, which keeps NE cells of benign prostate and prostate adrenocarcinoma in a quiescent state. The model on the right suggests that p53 mutation inactivates the IL8–CXCR2–p53 pathway, leading to rapid proliferation and aggressive biological behavior of NE tumor cells in SCNC.

that a CXCR2-neutralizing antibody can inhibit PC3 cell proliferation (Reiland *et al.* 1999) and deletion of CXCR2 inhibits TRAMP tumors (Shen *et al.* 2006).

Therefore, we have identified a potential cell-of-origin as well as a molecular target for prostatic SCNS. It is unclear whether the NE cells in both benign prostate and adenocarcinoma can be the cells of origin for SCNS. It is possible that pure SCNC arising *de novo* may result from *p53* mutation in NE cells of benign prostate, although we cannot exclude the possibility that SCNC always arises from NE cells of adenocarcinoma, but in some cases, the rapidly proliferating tumor NE cells have completely overtaken the slow-growing adenocarcinoma, resulting in the histological appearance of a pure SCNC. For those SCNCs that coexist with prostatic adenocarcinoma and those that are recurrent tumors in patients with a history of adenocarcinoma treated with hormonal therapy, the most likely mechanism appears to be *p53* mutation in the NE cells of adenocarcinoma. For these patients, a likely scenario is that within the adenocarcinoma, a *p53* mutation occurs in NE cell(s) during the course of hormonal therapy leading to the development of SCNC. The rapidly proliferating NE cells of SCNC can coexist with adenocarcinoma initially but eventually become the only component as adenocarcinoma cells usually have a low proliferation rate and this component can be completely overtaken by SCNC. Because of its distinct cell of origin and molecular alteration, SCNC is an entirely different disease from adenocarcinoma. In contrast to adenocarcinoma, prostatic SCNC is a disease of NE differentiation, likely has its cell of origin in NE cells of benign prostate and/or adenocarcinoma, with *p53* mutation as the underlying molecular mechanism, and does not respond to hormonal therapy, which has proven to be effective, at least initially, in nearly all patients with prostatic adenocarcinomas.

Our results are consistent with findings in cell line models. We have shown that PC3 cells, a PC cell line originally derived from a patient's bone metastasis, have NE features in that they express NE markers CgA and NSE (Palapattu *et al.* 2009). Like NE cells in human prostate and prostatic adenocarcinoma, PC3 cells express IL8 (Ma *et al.* 2009) and IL8 receptor CXCR2 (Reiland *et al.* 1999) and are positive for CD44 (Palapattu *et al.* 2009). Unlike NE cells in benign prostate and adenocarcinoma, PC3 cells are highly proliferative and biologically aggressive, features shared by SCNCs. Consistent with this notion, it has been shown that PC3 cells contain a *p53* mutation and restoration of p53 function inhibits tumor cell growth (Isaacs *et al.* 1991). Therefore, we have proposed that PC3 cells may actually represent a cell line of SCNC (Tai *et al.* 2011).

Our model is supported by animal models of PC. Transgenic mice expressing SV40 early genes including T antigen (TRAMP) develop aggressive carcinomas with abundant NE tumor cells similar to human prostatic SCNC (Greenberg *et al.* 1995, Masumori *et al.* 2001, 2004), as do $p53^{-/-}Rb^{-/-}$ double knockout mice (Zhou *et al.* 2006). In both models, the AR-responsive probasin promoter was used to drive the expression of the transgene or the Cre recombinase. Although AR is not usually expressed in NE cells, it is possible that a low level of AR is present in NE cells at some point of mouse prostate development and is sufficient to activate the probasin promoter. We hypothesize that in these animals, inactivation of p53 in NE cells of the prostate leads to malignant transformation and rapid proliferation of

NE cells, resulting in the development of a malignant tumor with abundant NE tumor cells mimicking human prostatic SCNC. Notably, in both models, there are also areas of glandular formation resembling adenocarcinoma, which probably results from inactivation of p53 and/or Rb in luminal epithelial cells. In most of the TRAMP tumor tissues we have examined, NE tumor cells predominate, likely reflecting the highly proliferative nature of the malignant NE tumor cells.

The findings described here are also consistent with a previous report by De Marzo's group who reported positive nuclear staining for p53 and a *p53* mutation in a case of SCNC intermixed with adenocarcinoma (Hansel *et al*. 2009). The *p53* mutation discovered in their study differs from that identified in our cases, suggesting that a variety of *p53* mutations may be found if a large number of SCNCs are sequenced.

It is noteworthy that SV40 T antigen inactivates both p53 and Rb in TRAMP tumors and the Nikitin group has shown that both p53 and Rb need to be inactivated in order for invasive tumors to develop (Zhou *et al*. 2006). It is possible that, inactivation of Rb as well as p53 in NE cells is required for the development of prostatic SCNC in men. However, unlike p53 for which mutations are usually associated with protein accumulation in the nucleus detectable by immunohistochemistry, assaying for the inactivation of Rb pathway is not straightforward. Therefore, additional studies need to be performed to determine whether the Rb pathway, which appears to be important for prostatic adenocarcinoma (Balk & Knudsen 2008), is also involved in the pathogenesis of prostatic SCNC in men.

Declaration of interest

The authors declare that there is no conflict of interest that could be perceived as prejudicing the impartiality of the research reported.

Funding

J Huang is supported by Department of Defense Prostate Cancer Research Program (PC1001008), UCLA SPORE in prostate cancer (PI: R Reiter), a challenge award from the Prostate Cancer Foundation (PI: O Witte), a creativity award from Prostate Cancer Foundation (PI: M Rettig), and NIH 1R01CA158627 (PI. L Marks).

Author contribution statement

H Chen, Y Sun, L Cheng, C Wu, J L Yao, S Shen, A O Osunkoya, C Liang, and J Huang designed the study; H Chen, Y Sun, and C Wu performed the experiments; Y Sun, C E Magyar, X Li, and J Huang analyzed the data; J Huang wrote the manuscript.

Acknowledgement

We thank Dr Schraufstatter of La Jolla Institute for Molecular Medicine for providing the *CXCR2* cDNA and Ms Qi Yang, Ngan Doan, and Ko Kiehle for performing immunohistochemical studies.

References

Acosta JC, O'Loghlen A, Banito A, Guijarro MV, Augert A, Raguz S, Fumagalli M, Da Costa M, Brown C, Popov N *et al.* 2008 Chemokine signaling via the CXCR2 receptor reinforces senescence. *Cell* **133** 1006–1018. (doi:10.1016/j.cell.2008.03.038)

Balk SP & Knudsen KE 2008 AR, the cell cycle, and prostate cancer. *Nuclear Receptor Signaling* **6** e001.

van Bokhoven A, Varella-Garcia M, Korch C, Johannes WU, Smith EE, Miller HL, Nordeen SK, Miller GJ & Lucia MS 2003 Molecular characterization of human prostate carcinoma cell lines. *Prostate* **57** 205–225. (doi:10.1002/pros.10290)

Bonkhoff H 2001 Neuroendocrine differentiation in human prostate cancer. Morphogenesis, proliferation and androgen receptor status. *Annals of Oncology* **12** (Suppl 2) S141–S144. (doi:10.1093/annonc/12.suppl_2.S141)

Brown JR, Wieczorek TJ, Shaffer K & Salgia R 2003 Small-cell cancers, and an unusual reaction to chemotherapy. Case 1. Extrapulmonary small-cell carcinoma arising in the prostate. *Journal of Clinical Oncology* **21** 2437–2438. (doi:10.1200/JCO.2003.081.03)

Burchardt T, Burchardt M, Chen MW, Cao Y, de la Taille A, Shabsigh A, Hayek O, Dorai T & Buttyan R 1999 Transdifferentiation of prostate cancer cells to a neuroendocrine cell phenotype *in vitro* and *in vivo*. *Journal of Urology* **162** 1800–1805. (doi:10.1016/S0022-5347(05)68241-9)

Cooperberg MR, Park S & Carroll PR 2004 Prostate cancer 2004: insights from national disease registries. *Oncology* **18** 1239–1247 (discussion 1248–1250, 1256–1258).

Erasmus CE, Verhagen WI, Wauters CA & van Lindert EJ 2002 Brain metastasis from prostate small cell carcinoma: not to be neglected. *Canadian Journal of Neurological Sciences* **29** 375–377.

Greenberg NM, DeMayo F, Finegold MJ, Medina D, Tilley WD, Aspinall JO, Cunha GR, Donjacour AA, Matusik RJ & Rosen JM 1995 Prostate cancer in a transgenic mouse. *PNAS* **92** 3439–3443. (doi:10.1073/pnas.92.8.3439)

Grignon DJ 2004 Unusual subtypes of prostate cancer. *Modern Pathology* **17** 316–327. (doi:10.1038/modpathol.3800052)

Hansel DE, Nakayama M, Luo J, Abukhdeir AM, Park BH, Bieberich CJ, Hicks JL, Eisenberger M, Nelson WG, Mostwin JL *et al.* 2009 Shared *TP53* gene mutation in morphologically and phenotypically distinct concurrent primary small cell neuroendocrine carcinoma and adenocarcinoma of the prostate. *Prostate* **69** 603–609. (doi:10.1002/pros.20910)

Huang J, Yao JL, Zhang L, Bourne PA, Quinn AM, di Sant'Agnese PA & Reeder JE 2005 Differential

expression of interleukin-8 and its receptors in the neuroendocrine and non-neuroendocrine compartments of prostate cancer. *American Journal of Pathology* **166** 1807–1815. (doi:10.1016/S0002-9440(10)62490-X)

Huang J, Yao JL, di Sant'agnese PA, Yang Q, Bourne PA & Na Y 2006 Immunohistochemical characterization of neuroendocrine cells in prostate cancer. *Prostate* **66** 1399–1406. (doi:10.1002/pros.20434)

Huang J, Wu C, di Sant'Agnese PA, Yao JL, Cheng L & Na Y 2007 Function and molecular mechanisms of neuroendocrine cells in prostate cancer. *Analytical and Quantitative Cytology and Histology* **29** 128–138.

Isaacs WB, Carter BS & Ewing CM 1991 Wild-type p53 suppresses growth of human prostate cancer cells containing mutant p53 alleles. *Cancer Research* **51** 4716–4720.

Kudahetti S, Fisher G, Ambroisine L, Foster C, Reuter V, Eastham J, Moller H, Kattan MW, Cooper CS, Scardino P *et al.* 2009 p53 immunochemistry is an independent prognostic marker for outcome in conservatively treated prostate cancer. *BJU International* **104** 20–24. (doi:10.1111/j.1464-410X.2009.08407.x)

Ma J, Ren Z, Ma Y, Xu L, Zhao Y, Zheng C, Fang Y, Xue T, Sun B & Xiao W 2009 Targeted knockdown of EGR-1 inhibits IL-8 production and IL-8-mediated invasion of prostate cancer cells through suppressing EGR-1/NF-kappaB synergy. *Journal of Biological Chemistry* **284** 34600–34606. (doi:10.1074/jbc.M109.016246)

Masumori N, Thomas TZ, Chaurand P, Case T, Paul M, Kasper S, Caprioli RM, Tsukamoto T, Shappell SB & Matusik RJ 2001 A probasin-large T antigen transgenic mouse line develops prostate adenocarcinoma and neuroendocrine carcinoma with metastatic potential. *Cancer Research* **61** 2239–2249.

Masumori N, Tsuchiya K, Tu WH, Lee C, Kasper S, Tsukamoto T, Shappell SB & Matusik RJ 2004 An allograft model of androgen independent prostatic neuroendocrine carcinoma derived from a large probasin promoter-T antigen transgenic mouse line. *Journal of Urology* **171** 439–442. (doi:10.1097/01.ju.0000099826.63103.94)

Miyoshi Y, Uemura H, Kitami K, Satomi Y, Kubota Y & Hosaka M 2001 Neuroendocrine differentiated small cell carcinoma presenting as recurrent prostate cancer after androgen deprivation therapy. *BJU International* **88** 982–983. (doi:10.1046/j.1464-4096.2001.00936.x)

Palapattu GS, Wu C, Silvers CR, Martin HB, Williams K, Salamone L, Bushnell T, Huang L-S, Yang Q & Huang J 2009 Selective expression of CD44, a putative prostate cancer stem cell marker, in neuroendocrine tumor cells of human prostate cancer. *Prostate* **69** 787–798. (doi:10.1002/pros.20928)

Reiland J, Furcht LT & McCarthy JB 1999 CXC-chemokines stimulate invasion and chemotaxis in prostate carcinoma cells through the CXCR2 receptor. *Prostate* **41** 78–88. (doi:10.1002/(SICI)1097-0045(19991001)41:2<78::AID-PROS2>3.0.CO;2-P)

Scher HI 2003 Prostate carcinoma: defining therapeutic objectives and improving overall outcomes. *Cancer* **97** 758–771. (doi:10.1002/cncr.11151)

Schlomm T, Iwers L, Kirstein P, Jessen B, Kollermann J, Minner S, Passow-Drolet A, Mirlacher M, Milde-Langosch K, Graefen M *et al.* 2008 Clinical significance of p53 alterations in surgically treated prostate cancers. *Modern Pathology* **21** 1371–1378. (doi:10.1038/modpathol.2008.104)

Shen H, Schuster R, Lu B, Waltz SE & Lentsch AB 2006 Critical and opposing roles of the chemokine receptors CXCR2 and CXCR3 in prostate tumor growth. *Prostate* **66** 1721–1728. (doi:10.1002/pros.20476)

Sun Y, Niu J & Huang J 2009 Neuroendocrine differentiation in prostate cancer. *American Journal of Translational Research* **1** 148–162.

Tai S, Sun Y, Squires JM, Zhang H, Oh WK, Liang CZ & Huang J 2011 PC3 is a cell line characteristic of prostatic small cell carcinoma. *Prostate* **71** 1668–1679. (doi:10.1002/pros.21383)

Tanaka M, Suzuki Y, Takaoka K, Suzuki N, Murakami S, Matsuzaki O & Shimazaki J 2001 Progression of prostate cancer to neuroendocrine cell tumor. *International Journal of Urology* **8** 431–436 (discussion 437). (doi:10.1046/j.1442-2042.2001.00347.x)

Vashchenko N & Abrahamsson PA 2005 Neuroendocrine differentiation in prostate cancer: implications for new treatment modalities. *European Urology* **47** 147–155. (doi:10.1016/j.eururo.2004.09.007)

Wang W & Epstein JI 2008 Small cell carcinoma of the prostate: a morphologic and immunohistochemical study of 95 cases. *American Journal of Surgical Pathology* **32** 65–71. (doi:10.1097/PAS.0b013e318058a96b)

Wu C, Zhang L, Bourne PA, Reeder JE, di Sant'agnese PA, Yao JL, Na Y & Huang J 2006 Protein tyrosine phosphatase PTP1B is involved in neuroendocrine differentiation of prostate cancer. *Prostate* **66** 1125–1135. (doi:10.1002/pros.20412)

Yao JL, Madeb R, Bourne P, Lei J, Yang X, Tickoo S, Liu Z, Tan D, Cheng L, Hatem F *et al.* 2006 Small cell carcinoma of the prostate: an immunohistochemical study. *American Journal of Surgical Pathology* **30** 705–712. (doi:10.1097/00000478-200606000-00005)

Yuan TC, Veeramani S & Lin MF 2007 Neuroendocrine-like prostate cancer cells: neuroendocrine transdifferentiation of prostate adenocarcinoma cells. *Endocrine-Related Cancer* **14** 531–547. (doi:10.1677/ERC-07-0061)

Zhou Z, Flesken-Nikitin A, Corney DC, Wang W, Goodrich DW, Roy-Burman P & Nikitin AY 2006 Synergy of p53 and Rb deficiency in a conditional mouse model for metastatic prostate cancer. *Cancer Research* **66** 7889–7898. (doi:10.1158/0008-5472.CAN-06-0486)

Received in final form 17 February 2012
Accepted 29 February 2012
Made available online as an Accepted Preprint
2 March 2012

THE JOURNAL OF BIOLOGICAL CHEMISTRY VOL. 287, NO. 18, pp. 14621–14630, April 27, 2012

Overexpression of SKI Oncoprotein Leads to p53 Degradation through Regulation of MDM2 Protein Sumoylation*[S]

Received for publication, September 7, 2011, and in revised form, March 9, 2012 Published, JBC Papers in Press, March 12, 2012, DOI 10.1074/jbc.M111.301523

Boxiao Ding[‡], Yin Sun[‡1], and Jiaoti Huang[‡§¶2]

From the [‡]Department of Pathology and Laboratory Medicine, [¶]Jonsson Comprehensive Cancer Center, and [§]Broad Center for Regenerative Medicine and Stem Cell Research, David Geffen School of Medicine, UCLA, Los Angeles, California 90095

Background: SKI is an oncoprotein with partial understanding of its molecular mechanisms.
Results: Through regulation of Ubc9, SKI can increase MDM2 sumoylation to enhance p53 degradation.
Conclusion: Up-regulation of Ubc9 is a novel biochemical function of SKI and is essential for its transforming activity.
Significance: This is a first example that an oncoprotein can transform cells through regulation of Ubc9, a critical component of cellular sumoylation.

Protooncogene *Ski* was identified based on its ability to transform avian fibroblasts *in vitro*. In support of its oncogenic activity, *SKI* was found to be overexpressed in a variety of human cancers, although the exact molecular mechanism(s) responsible for its oncogenic activity is not fully understood. We found that SKI can negatively regulate p53 by decreasing its level through up-regulation of MDM2 activity, which is mediated by the ability of SKI to enhance sumoylation of MDM2. This stimulation of MDM2 sumoylation is accomplished through a direct interaction of SKI with SUMO-conjugating enzyme E2, Ubc9, resulting in enhanced thioester bond formation and mono-sumoylation of Ubc9. A mutant SKI defective in transformation fails to increase p53 ubiquitination and is unable to increase MDM2 levels and to increase mono-sumoylation of Ubc9, suggesting that the ability of SKI to enhance Ubc9 activity is essential for its transforming function. These results established a detailed molecular mechanism that underlies the ability of SKI to cause cellular transformation while unraveling a novel connection between sumoylation and tumorigenesis, providing potential new therapeutic targets for cancer.

Ski was found more than 20 years ago as the only transforming oncogene discovered through *in vitro* viral replication assay (1). It was shown to be able to transform chicken and quail embryo fibroblasts as evidenced by the overgrowth of virally infected cells in monolayer culture and anchorage-independent colony formation in soft agar, hallmarks of cellular transformation. Consistent with its role as an oncoprotein, SKI was found to be overexpressed in a variety of human cancers, including melanoma (2), leukemia (3), colorectal (4), pancreatic (5), esophageal (6), and gastric (7) cancers. Although there is scarce evidence to suggest that SKI can transform mammalian cells except melanocytes (8), a reduction of SKI through small interfering RNA technology lessens the tumorigenic properties of cancer cells (9). Transgenic mice overexpressing *Ski* show overgrowth of type II muscle fibers but no enhanced tumor formation (10). Mice lacking the *Ski* gene result in early postnatal lethality with exencephaly caused by failed closure of the cranial neural tube during neurulation as well as a host of developmental abnormalities (11). Humans diagnosed with a haploid deficiency of *SKI* due to 1p36 deletion display similar phenotypes as shown in mice with a constitutional lack of *Ski* gene (12).

The connection of the SKI oncoprotein with the TGFβ signaling pathway was established a decade ago by the finding that SKI can physically interact with Smad proteins, including Smad2, -3, and -4 (13–15). Smad proteins are the central mediators of TGFβ signaling pathways transmitting signals of the activated receptor at the plasma membrane to the nucleus (16). Upon activation of receptor through ligand binding, type I receptor kinase is activated and phosphorylates Smad protein that subsequently oligomerizes with Smad4, and the complex translocates to the nucleus to regulate target gene transcription. SKI regulates the TGFβ signaling at multiple levels; it interacts with the Smad proteins and inhibits the transcriptional activation of target genes, likely by recruiting the nuclear corepressor complex. Indeed, SKI has been found to be a component of the nuclear corepressor complex capable of inhibiting the transcriptional activation of reporter constructs (17). In addition, it has also been found that SKI can interact with the type I TGFβ receptor directly and can lead to repression of the receptor activity (18). Because TGFβ signaling is a major cellular pathway that negatively regulates epithelial cell proliferation, the transforming capability of SKI is at least partially derived from its ability to neutralize the inhibition of cell proliferation by the TGFβ pathway. However, in the initial characterization of *Ski* oncogene in avian fibroblast cells, TGFβ signaling was thought to be promoting *Ski*-induced transformation by inhibiting *Ski*-induced myogenic differentiation (19).

* This work was supported, in whole or in part, by National Institutes of Health Grant RO1 CA093848 (to Y. S.).
[S] This article contains supplemental Figs. 1–4.
[1] To whom correspondence may be addressed. E-mail: yinsun@mednet.ucla.edu.
[2] Supported by Department of Defense Prostate Cancer Research Program Grant PC1001008, UCLA SPORE in Prostate Cancer (to R. Reiter), a challenge award from the Prostate Cancer Foundation (to O. Witte), a creativity award from Prostate Cancer Foundation (to M. Rettig), and National Institutes of Health Grant 1R01CA158627 (to L. Marks). To whom correspondence may be addressed. E-mail: jiaotihuang@mednet.ucla.edu.

Thus, TGFβ signaling cooperates with *Ski* to transform avian fibroblast cells. This apparent contradiction of the role of TGFβ signaling in *Ski*-induced cellular transformation has not been fully reconciled.

Small ubiquitin-like modifier (SUMO)[3] has been found to be involved in a variety of cellular processes, including intracellular trafficking, stress response, DNA replication, DNA damage repair, as well as transcriptional regulation (20). Four versions of SUMO, 1–4, have been identified. SUMO1–3 is expressed in the precursor forms and requires proteolytic activation to expose the invariant Gly-Gly motif at the C terminus of the mature SUMO for target conjugation. Much like the cellular ubiquitination process, SUMO activation enzyme E1, SUMO-conjugating enzyme E2, and SUMO ligase enzyme E3 are required to transfer the SUMO moiety to target proteins. SUMO E1 activates the SUMO through thioester bond formation between C-terminal Gly of SUMO and the catalytic cysteine residue of E1; the activated SUMO is then transferred to E2 with a similar thioester bond. Although E2 itself can transfer SUMO to target proteins, SUMO ligase E3 through enhancing efficiency and substrate specificity facilitates this process by transferring SUMO from the high energy bond to the ϵ-position of lysine of the target protein. Unlike ubiquitin modification, the main function of sumoylation is not a signal of destruction of the target through proteasomal degradation, instead it plays a role in a variety of cellular processes. SUMO modification in some cases has been shown to antagonize ubiquitination through competitive modification (21–23). Another difference between ubiquitination and sumoylation is their respective core enzymes that carry out the modifications. It appears that there is only one E2 enzyme for sumoylation, although there are many E2s that can fulfill the ubiquitin-conjugating activity. Similar to regulation by ubiquitination, there are also proteases, sentrin-specific proteases, that can hydrolytically remove the SUMO moiety, and thus reverse the modification of sumoylation. These sentrin-specific proteases are also responsible for the activation of SUMO precursor by removing their C-terminal peptides to expose the Gly-Gly motif. Like many biological processes, the core machinery of SUMO modification has also been found to be regulated by other proteins. For example, RSUME and SF2/ASF have been found to enhance SUMO E2 enzyme Ubc9 to regulate target sumoylation (24, 25), although Rhes can enhance cross-sumoylation between E1 and Ubc9 (26).

Several prominent proteins involved in tumorigenesis have been found to be modified by sumoylation. For example, p53 can be modified by sumoylation with either enhancement or reduction of its activity (27). Similarly, MDM2, the main ubiquitin E3 ligase for p53, has been found to be sumoylated (28), and this sumoylation was shown to be associated with increased activity of MDM2 (29). MDM2 can be self-ubiquitinated and degraded. Sumoylation of MDM2 decreases its self-ubiquitination and degradation, whereas de-sumoylation leads to enhanced MDM2 self-ubiquitination. UV damage can decrease MDM2 sumoylation through a SUMO protease SUSP4. MDM2 sumoylation requires its N-terminal domain of amino acids 40–59 (30).

We report here that SKI is capable of regulating sumoylation of MDM2 through its ability to interact with and regulate SUMO E2 enzyme Ubc9, resulting in enhanced MDM2 activity and decreased p53 protein. This novel function of SKI is likely a major molecular mechanism for its oncogenic activity as p53 is an important tumor suppressor, and a mechanism that leads to its destruction will greatly contribute to cellular transformation.

EXPERIMENTAL PROCEDURES

Culture of Mammalian Cells—LNCaP was cultured in RPMI 1640 medium; H1299, U2OS, HEK293, 293T, HepG2, and mink lung epithelial cells were cultured in Dulbecco's modified Eagle's medium; HCT116 and HCT116 p53$^{-/-}$ cells were in McCoy's 5A medium, and all were supplemented with 10% fetal calf serum, 2 mM glutamine, penicillin, and streptomycin at 37 °C with 5% CO_2.

Nucleic Acids—Chemical siRNA for *Ski, PIAS1,* and *PIAS3* were from IDT Inc. with the following sequences: *Ski*, sense 5′-rCrCrArGrUrArArGrGrArGrArCrUrUrGrArArArUrUrC-rAGA-3′ and antisense 5′-rUrCrUrGrArArUrUrUrCrArArG-rUrCrUrCrCrUrUrArCrUrGrGrUrU-3′; *PIAS1*, sense 5′-rUr-GrGrUrUrArUrGrArGrCrCrUrUrArGrArGrUrUrUrCrUG-A-3′ and antisense 5′-rUrCrArGrArArArCrUrCrUrArArGrG-rCrUrCrArUrArArCrCrArUrU-3′; and *PIAS3*, sense 5′-rCrA-rCrUrGrArUrCrArArGrGrArGrArArUrUrUrGrArCrUGC-3′ and antisense 5′-rGrCrArGrUrCrArArUrUrUrCrUrCrCrUr-UrGrArUrCrArGrUrGrCrC-3′. Dharmafect was used to transfect siRNA into cells. Expression plasmids were introduced into cells with BioT transfection reagent (Bioland Inc.) according to the instruction of the vendor, and empty vector DNA was used to provide equal amount of DNA in each transfection. PCR primers for p53 target gene quantification are as follows: *p21,* forward 5′-CTGGAGACTCTCAGGGTCGAA-3′ and reverse 5′-GGATTAGGGCTTCCTCTTGGA-3′; *Noxa*, forward 5′-CTCTTTCCTCCTCGCCACTT-3′ and reverse 5′-CGTGCA-CCTCCTGAGAAAAC-3′; *Tsp1,* 5′-GGGAAGAAAATCAT-GGCTGA-3′ and reverse 5′-GGTCGCACGTTCTAGGAGT-C-3′; *Mdm2* mRNA (p2 promoter), forward 5′-CGATTGGA-GGGTAGACCTGT-3′ and reverse 5′-GGTCTCTTGTTCC-GAAGCTG-3′; *Mdm2* (last exon), forward 5′-CAGACGGGG-ACTAGCTTTTG-3′ and reverse 5′-AGGTTGCAGTGA-GCCAAGAT-3′; and *Gapdh*, forward 5′-CATGGGTGTGAA-CCATGAGA-3′ and reverse 5′-CAGTGATGGCATGGACT-GTG-3′. RNA was isolated using Qiagen RNeasy kit, and cDNA was generated using SuperscriptII reverse transcriptase (Invitrogen).

Biochemical and Cell Biological Reagents and Procedures—Anti-SKI, p53, and Ubc9 antibodies were from Santa Cruz Biotechnology. Anti-FLAG M2 antibody was from Sigma (A1205). Anti-HA antibody was from Roche Applied Science. Anti-SUMO1 antibody was from Epitomics. For immunoprecipitation and immunoblotting, cells were collected by scraping or trypsinization and lysed in lysis buffer (20 mM KCl, 150 mM NaCl, 1% IGEPAL, 50 mM Tris-HCl (pH 7.5), 50 mM NaF, 1 mM EGTA, 1 mM DTT, and 1× protease inhibitor mixture (Roche

[3] The abbreviation used is: SUMO, small ubiquitin-like modifier.

Applied Science) and 10% glycerol). Immunoprecipitations were performed with appropriate antibody and protein A- or G-Sepharose (Upstate Biotechnology). Beads were washed three times in lysis buffer, and immunoprecipitated proteins were separated on SDS-PAGE followed by Western blotting with primary and horseradish peroxidase-conjugated secondary antibodies (Bio-Rad). Immunoreactive proteins were visualized by enhanced chemiluminescence (SuperSignal West Femto, Pierce). CellTiter Glo (Promega Inc.) was used to measure relative cell number according to the manufacturer. For FACS analysis to gauge the sub-G_1 DNA content, the cells were collected and fixed in 70% ethanol followed by RNase treatment and 1 μg/ml propidium iodide staining, and the cells were then analyzed by FACS.

MDM2 Sumoylation Assay—Expression plasmid for His_6-MDM2 was transfected into 293T cells together with other expression plasmids. 40 h after transfection, cells were collected and lysed in 150 μl of RIPA buffer (regular buffer + 0.1% SDS + 0.5% sodium deoxycholate) followed by centrifugation. The supernatant was mixed with 8 M guanidine hydrochloride to obtain 6 M guanidine hydrochloride with 20 mM sodium phosphate buffer (pH 7.5), 20 mM imidazole, 1 mM DTT. This lysate was centrifuged at room temperature for 10 min, and the supernatant was mixed with 20 μl of nickel-nitrilotriacetic acid beads in 50% bead slurry. After binding for 3 h, the beads were washed three times with urea buffer (8 M urea with 20 mM sodium phosphate buffer (pH 7.5)) followed by incubation with sample buffer at 95 °C for 10 min. The supernatant was then separated by SDS-PAGE followed by immunoblot analysis.

RESULTS

Overexpression of SKI Leads to Decreased p53—SKI is a transforming oncoprotein for chicken embryo fibroblast cells upon overexpression. Previously, we and others have established that SKI can interact with Smad proteins and negatively regulate TGFβ signal transduction (13–15), and it was widely thought that this inhibition of TGFβ signaling is the underlying mechanism of its transforming activity. Although this mechanistic explanation is plausible, we suspected that other mechanism(s) might also be involved in the oncogenic activity of SKI. Therefore, we examined in cells with overexpression of SKI the abundance of p53 protein, one of the essential tumor suppressor proteins in regulating cell proliferation and differentiation. As shown in Fig. 1*A*, overexpression of SKI in mink lung epithelial cells leads to a decrease of p53, and this reduction is independent of the status of TGFβ signaling (data not shown). Consistent with this reduction, the protein level of $p21^{waf1}$, one of the p53 target genes, also decreases. Moreover, this reduced p53 level is likely a result of decreased metabolic stability as its half-life is apparently reduced in cells with overexpression of SKI (Fig. 1*B*). These findings therefore suggested the possibility that a higher level of SKI results in a reduction of p53, thus resulting in cellular transformation. We further tested whether in a transient overexpression system SKI can also cause a reduction of p53. As shown in Fig. 1*C*, in human colorectal carcinoma HCT-116 cells with or without endogenous *Tp53* (see supplemental Fig. 1), overexpression of SKI by itself cannot decrease p53 levels; however, SKI can enhance the reduction of p53 caused by the wild type MDM2, the main ubiquitin E3 ligase for p53, but not the RING finger mutant of MDM2 (C464A) (31). These results suggest that a higher level of SKI can result in an MDM2-dependent p53 reduction likely through enhanced p53 degradation. To rule out the possibility that SKI can only regulate p53 in an overexpression system, we also examined the impact of SKI depletion on endogenous p53 activity. As shown in Fig. 1*D*, siRNA-mediated loss-of-function of SKI in the prostate cancer cell line LNCaP results in elevated p53 levels and enhanced apoptosis as determined by cell number enumeration through measurement of ATP levels as well as of sub-G_1 DNA content in a fluorescent-activated cell sorter (FACS) analysis (Fig. 1, *E* and *F*). Consistent with these findings, we also found that a subset of p53 target genes are up-regulated in response to a reduction of SKI and up-regulation of p53 (Fig. 1*G*). Taken together, these results strongly suggest that SKI with both physiological and quasi-physiological expressions can negatively regulate p53 through MDM2, and this aspect of SKI is likely a major contributor for its transforming activity.

SKI Enhances p53 Ubiquitination—p53 is a major tumor suppressor protein that is inactivated in many human cancers. Nearly half of the human cancers harbor mutations of *Tp53*, whereas p53 is inactivated in a large proportion of tumors without *Tp53* mutation through a multitude of mechanisms. For example, overexpression of MDM2, loss of the $p14^{Arf}$ protein, which is a negative regular of MDM2, and expression of viral oncoproteins, including HPV16 E6, adenovirus E1A, and SV40 large T antigen (32), can all lead to p53 inactivation. Although several ubiquitin E3 ligases have been shown to regulate p53 levels (33), the genetically modified mouse without *Mdm2* has unequivocally demonstrated the centrality of Mdm2 in regulating the p53 protein level (34). As described earlier, we found that SKI can enhance the MDM2-mediated p53 decrease (Fig. 1, *A* and *C*); therefore, we examined whether SKI can positively regulate MDM2-mediated ubiquitination of p53. As shown in Fig. 2*A*, although expression of MDM2 alone enhanced the ubiquitination of p53, co-expression of SKI dramatically increased the p53 ubiquitination shown both by the ubiquitin in the p53 immunoprecipitation as well as p53 in the immunoprecipitation of ubiquitin (supplemental Fig. 2). These results suggest that SKI can enhance MDM2-mediated p53 ubiquitination and thus proteasomal degradation, which likely results in a decreased p53 level. It has been shown that a mutant SKI with an insertion of four amino acids, alanine, arginine, proline, and glycine (ARPG) replacing aspartic acid at position 181, inactivated the transforming function of SKI in chicken embryo fibroblast cells (35), and we therefore tested whether the transforming capacity of SKI is correlated with its ability to enhance ubiquitination of p53. As shown in Fig. 2*B*, *lane 4*, expression of the SKI mutant ARPG, at a comparable level of wild type SKI protein, did not enhance, if reduced, p53 ubiquitination, suggesting that the transforming ability of SKI is tightly associated with its interaction with MDM2 to result in p53 ubiquitination. In addition, we also tested whether SKI at a physiological level can regulate MDM2-mediated p53 ubiquitination. As shown in Fig. 2*C*, siRNA-mediated reduction of endogenous SKI protein also reduced p53 ubiquitination conferred upon by MDM2 expression. These results suggest that SKI at both normal and

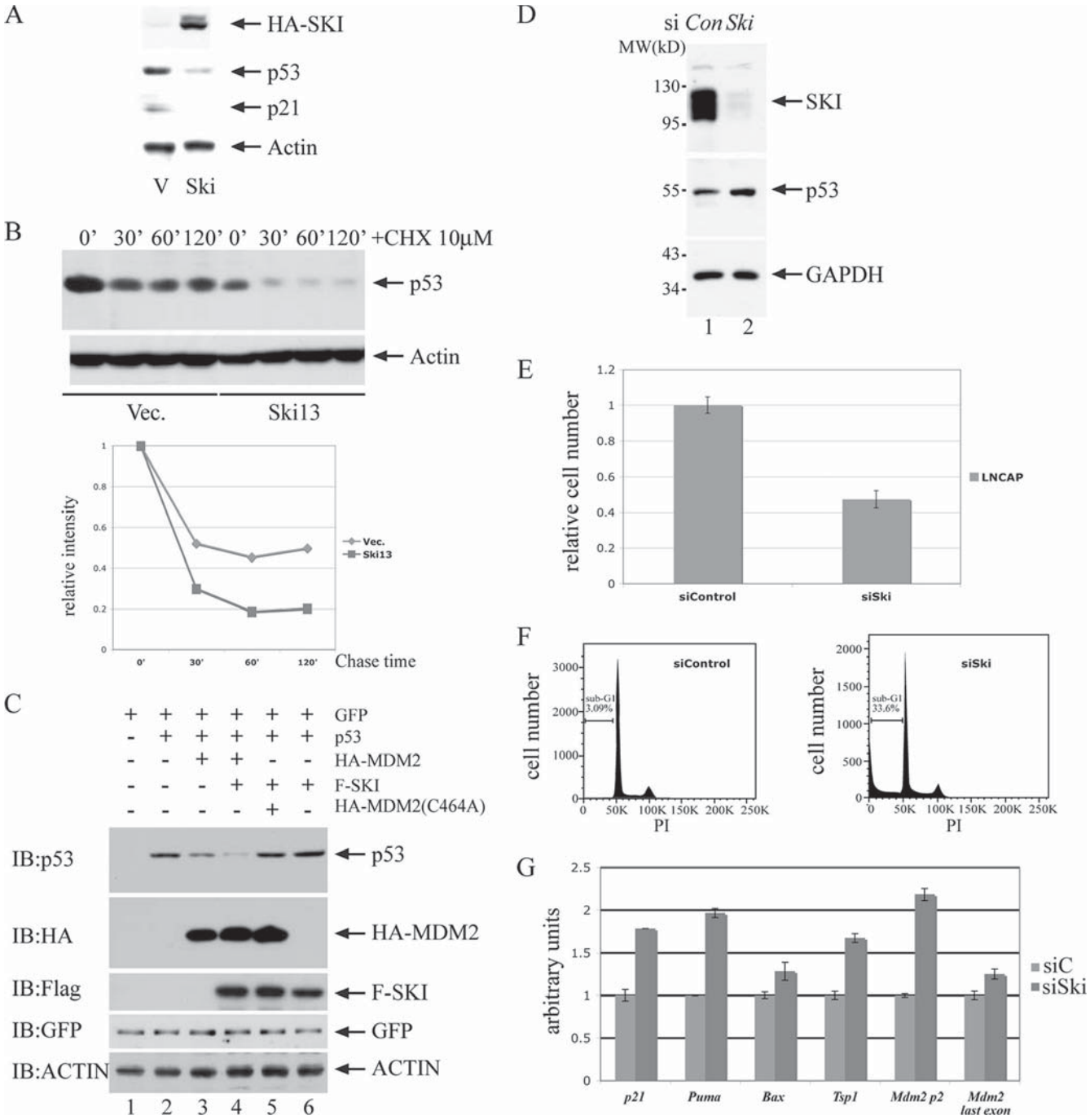

FIGURE 1. **SKI negatively regulates p53.** *A,* overexpression of SKI leads to a decrease of p53. p53, $p21^{waf1}$ level was examined with immunoblot analysis in mink lung epithelial cells overexpressing *SKI* (Ski13) or vector control. *B,* half-life of p53 was decreased in Ski13 cells. *C,* SKI enhances decrease of p53 by MDM2 but not by mutant MDM2. Various expression plasmids were introduced into HCT116 cells without *Tp53*, and the p53 was examined by immunoblot (*IB*) analysis with anti-p53 antibody. The mutant MDM2 has alanine at amino acid 464 instead of cysteine (C464A). The amount of plasmids was made equal by adding vector DNA, and the transfection efficiency was monitored with GFP expression. MDM2 and SKI expression were monitored with anti-HA and anti-FLAG antibodies. *CHX*, cycloheximide. *D,* reduction of SKI results in an increase of p53 level. siRNA for *SKI* was introduced into LNCaP cells, and the levels of SKI, p53 and GAPDH were examined by immunoblot analysis. *E* and *F,* reduction of SKI results in a decrease of cell number and an increase of apoptosis. 48 h after siRNA for *SKI* was introduced into LNCaP cells, the cell number was measured using CellTiter Glo (*E*), and the sub-G_1 content was measured with FACS analysis (*F*). *G,* reduction of SKI results in an increase of several p53 target genes. SYBR quantitative PCR was used to measure the quantity of transcript level of p53 target genes in cells with transfection of control siRNA or siRNA for *SKI*. The level in control cells was arbitrarily set as 1 followed by correction with relative total RNA level using *GAPDH* measurements.

overexpression levels is capable of enhancing MDM2-mediated ubiquitination of p53, and this activity is tightly associated with the transforming function of SKI.

SKI Positively Regulates MDM2 through Sumoylation—The ability of SKI to enhance MDM2-mediated ubiquitination of p53 suggests several possible modes of action of SKI in the regulation of p53. It is possible that SKI directly regulates p53's propensity of being ubiquitinated by MDM2 followed by proteosomal degradation. It is also possible that SKI can positively enhance the activity of MDM2 through direct physical interac-

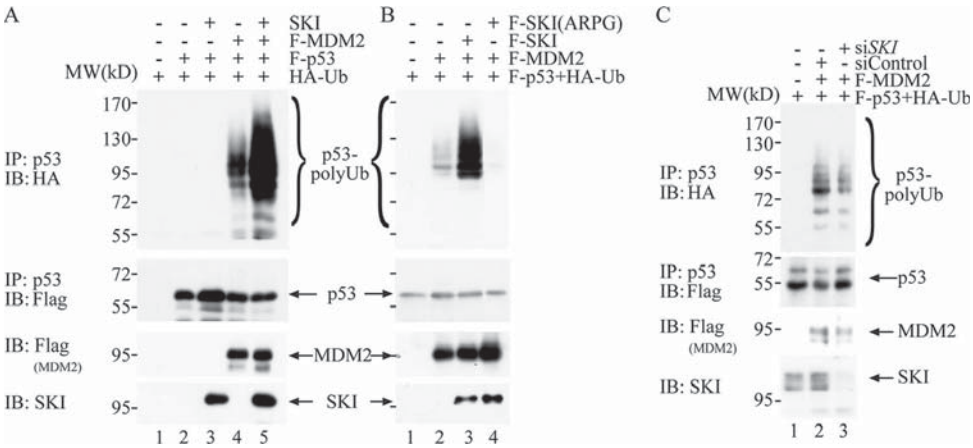

FIGURE 2. **SKI enhances MDM2-mediated p53 ubiquitination.** *A,* SKI increases p53 ubiquitination by MDM2. Various plasmids were introduced into H1299 cells, and the amount of plasmids was equalized with empty vector. 40 h after transfection, the cells were treated with 20 μM MG-132 for 4 h, lysed with 2% SDS buffer, and heated at 95 °C for 5 min followed by dilution with regular buffer to 0.1% SDS and centrifugation. The supernatant was immunoprecipitated (*IP*) with anti-p53 antibody, followed by the immunoblot (*IB*) analysis with anti-HA antibody. The blot was stripped and probed again with anti-FLAG antibody to gauge the p53 level. A separate portion of the lysate was used to analyze the expression level of MDM2 and SKI with immunoblot analysis. *B,* wild type but not mutant SKI enhances p53 ubiquitination by MDM2. The experiment was done essentially as in *A* in H1299 cells. *C,* endogenous SKI was crucial for MDM2-mediated p53 ubiquitination. The experiment was done essentially as in *A* except with introduction of siRNA for *SKI*.

tion with MDM2; alternatively, SKI can regulate MDM2 through post-translational modification without direct physical interaction. We established that in an overexpression system, SKI could physically interact with MDM2 (supplemental Fig. 3). However, repeated attempts in a variety of cell types failed to demonstrate this physical interaction at endogenous expression levels. Nevertheless, we can clearly demonstrate that overexpression of SKI increases the abundance of MDM2, consistent with its ability to decrease the p53 level (Fig. 3, *A*, and *middle panel* of *B*). Conversely, a depletion of SKI by siRNA in HepG2 cells can decrease endogenous MDM2 levels (Fig. 3*B, right panel*), supporting the view that SKI can positively regulate the abundance of MDM2. Moreover, the increased level of MDM2 by SKI is likely a result of increased stability of MDM2 as shown in Fig. 3*C*, whereas the SKI mutant ARPG fails to increase the stability of MDM2 (Fig. 3*C, right panel*). These results suggest that SKI can functionally enhance MDM2, likely its protein level or activity, yet it does not do so through high affinity or direct physical interaction with MDM2.

It is known that MDM2 can be broadly regulated by two biochemical mechanisms as follows: one involves post-translational modification, and the other involves proteinaceous regulators that modulate its cellular localization and activity (36–41). For the former, protein kinase B (AKT) can phosphorylate MDM2 and result in its nuclear translocation (42), which is crucial for its ability to degrade p53. In addition, sumoylation of MDM2 has been shown to enhance the MDM2 level and activity (29). Thus, it is possible that SKI can regulate MDM2 activity through these modifications. We tested the latter possibility, and found, as shown in Fig. 4, *A* and *B*, that SKI can clearly increase MDM2 sumoylation mediated by SUMO E3 ligases, PIAS1 and PIAS3 (protein inhibitors of activated STAT1 and -3). PIAS1 has been shown to enhance MDM2 sumoylation (28), although its impact on MDM2 activity is not clear. PIAS3 is known to interact with and sumoylate Smad4 protein (43), which has also been shown to interact with SKI (13), thus it is plausible that SKI can alter the substrate specificity of PIAS3 leading to sumoylation of MDM2. In limited cases, protein sumoylation has been found to antagonize ubiquitination thus increasing substrate protein abundance, although hypersumoylation has also been associated with sumoylation-induced ubiquitination with a consequent reduction of target protein abundance (44–46). MDM2 has been shown to be modified by sumoylation, which results in increased MDM2 activity presumably as a result of an increased protein level (29). The ability of SKI to enhance MDM2 sumoylation is thus consistent with its function to enhance MDM2 levels as well as to increase MDM2-mediated p53 ubiquitination. To provide further evidence that SKI can increase MDM2 activity through enhanced sumoylation of MDM2, we examined whether reduction of PIAS1 and/or PIAS3 can result in abrogation of the ability of SKI to up-regulate MDM2 activity. As shown in Fig. 4*D*, siRNA against PIAS1 or PIAS3 alone does not reduce MDM2-mediated p53 ubiquitination; however, combined reduction of PIAS1 and PIAS3 results in a drastic reduction of p53 ubiquitination by MDM2, suggesting that different PIAS proteins might be able to compensate each other in mediating MDM2 sumoylation and that SKI can communicate with both of them, potentially with different potencies. The potency of the siRNA for *PIAS1* and *-3* was demonstrated in Fig. 4*E, lower panel,* where respective siRNA can decrease PIAS1 and -3 protein levels. This result thus suggests that overexpression of SKI positively regulates ubiquitination of p53 by MDM2, likely through the latter's sumoylation by PIAS1 and -3. Consistent with the notion that MDM2 sumoylation by SKI is critical for the transforming ability of SKI, the SKI mutant (ARPG) fails to enhance MDM2 sumoylation as shown in Fig. 4*C*, providing a mechanistic explanation for the failure of ARPG to enhance MDM2-mediated p53 ubiquitination as demonstrated in Fig. 2*B*. To examine whether SKI can regulate endogenous p53 through regulation of MDM2 sumoylation, we examined the level of p53 in LNCaP cells in response to reduction of SKI as well as PIAS1 and PIAS3. As shown in Fig. 4*E*, reduction of SKI, PIAS1, and PIAS3 individually does not lead to a change of p53 protein

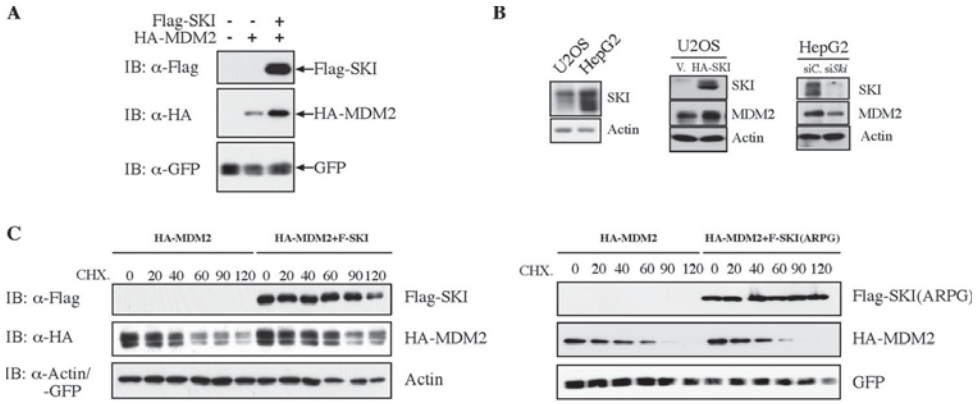

FIGURE 3. **SKI positively regulates MDM2 protein.** *A,* overexpression of SKI leads to an increase of MDM2 levels. 293T cells were transfected with expression plasmids for SKI and/or MDM2, and the exogenous MDM2 protein level was examined by immunoblot (*IB*) analysis. *B,* overexpression and reduction of SKI leads to an increase or decrease of endogenous MDM2 protein. Stable expression of SKI in U2OS cells results in increased MDM2 levels compared with the vector cells, although siRNA for *SKI* in HepG2 cells results in a decrease of MDM2 level. *C,* SKI increases the metabolic stability of MDM2 protein. 40 h after transfection with expression plasmids for SKI, SKI(ARPG), and MDM2, 293T cells were treated with cycloheximide for the indicated time, and MDM2 protein level was analyzed by immunoblot analysis.

levels, possibly due to limited reduction of the individual protein by the siRNA; however, a combined reduction of SKI and PIAS1 or PIAS3 results in increased p53 levels, concomitant with a reduction of MDM2 levels. This result supports the notion that SKI and PIAS1 or PIAS3 operate in a linear pathway in that SKI through PIAS1 or PIAS3 can result in increased MDM2 levels through sumoylation, and a combined reduction of both components leads to a reduction of MDM2 sumoylation severe enough to cause a reduction of protein levels with a consequent increase of p53 levels. Similarly, we also found that in human embryonic kidney HEK293 cells, exogenous expression of SKI leads to a reduction of endogenous p53 levels, likely through enhanced MDM2 sumoylation and activity as this reduction of p53 level can be reversed by co-expression of siRNA for *PIAS3*, but not by *PIAS1*, suggesting that SKI through PIAS3 can regulate endogenous p53 levels by modulating MDM2 sumoylation. The reason for the failure of PIAS1 to reverse the effect of SKI, despite its collaboration with SKI to enhance MDM2 sumoylation (Fig. 4*A*) and collaborate with SKI to maintain MDM2 levels (Fig. 4*E*), remains obscure. We can speculate that additional factors in HEK293 cells might have altered the substrate specificity such that PIAS1 behaves differently when it is in the context of overexpression with SKI as shown in Fig. 4*A*. These data together strongly suggest that SKI can cause down-regulation of endogenous p53 by up-regulating MDM2 activity through enhanced sumoylation of MDM2 by PIAS1 or PIAS3. It is also clear that because SKI is a modulator of MDM2 through PIAS1 or PIAS3, depending on the particular cellular context, alteration of SKI alone may not be sufficient to modulate the level or activity of MDM2 and ultimately the level of p53.

SKI Positively Regulates Ubc9 Activity—The unique feature of mammalian sumoylation is that there is a single SUMO-conjugating enzyme, Ubc9, that controls the general protein sumoylation. Thus, if a protein like SKI can directly regulate Ubc9, it can broadly regulate substrate sumoylation. We examined this possibility by performing a GST pulldown experiment with GST-Ubc9 and cellular SKI protein. We generated a recombinant GST-Ubc9 fusion protein as well as the control GST protein. As shown in Fig. 5*A*, when the same amount of these recombinant proteins was incubated with lysates prepared from 293T cells overexpressing SKI or its mutant ARPG protein, SKI as well as the ARPG mutant is capable of interacting with the Ubc9 protein, but not with GST protein, suggesting that SKI can directly interact with Ubc9 protein. This interaction can also be confirmed *in vivo* with the presence of SKI protein in the immunoprecipitate of anti-Ubc9 antibody as shown in the *lower panel* of Fig. 5*A*. Moreover, we found that SKI, but not the mutant ARPG protein, can enhance auto-sumoylation of Ubc9 in a transient expression system (Fig. 5*B*). We also monitored the *in vivo* sumoylation profile with expression of Ubc9 in the absence or presence of SKI or its mutant. As shown in Fig. 5*C*, expression of SKI, but not the ARPG mutant, significantly enhances the detectable protein sumoylation marked by epitope-tagged SUMO1 protein, suggesting that SKI can enhance Ubc9-mediated cellular sumoylation, possibly through direct interaction with Ubc9. This enhancement of Ubc9 is directly linked with its transforming ability as the transformation-defective mutant ARPG fails to do so. To examine the molecular mechanism of this enhanced sumoylation by SKI protein, we reconstituted Ubc9 modification with the SKI protein *in vitro*. We purified the SKI protein or ARPG mutant by releasing it through FLAG peptide competition from immunoprecipitates of these proteins expressed in 293T cells (Fig. 5*D*). We then incubated the recombinant Ubc9 protein with SUMO E1 as well as activated SUMO1 protein in the presence of ATP as the energy source. As shown in Fig. 5*E*, SKI can significantly increase the thioester bond formation of Ubc9 with SUMO1 as the thioester bond between Ubc9 and SUMO1 is sensitive to the reducing agent in the reaction, thus allowing us to monitor their abundance by their disappearance in response to dithiothreitol (DTT). The SUMO1-Ubc9 thioester bond formation serves as an intermediate for Ubc9 before substrate sumoylation, and thus more thioester bond formation will translate into more substrate modification. We also reconstituted this Ubc9 modification using GST-Ubc9 as a substrate. We noticed a higher basal activity of this Ubc9 protein in mediating its SUMO modification (data not shown), presumably due to the

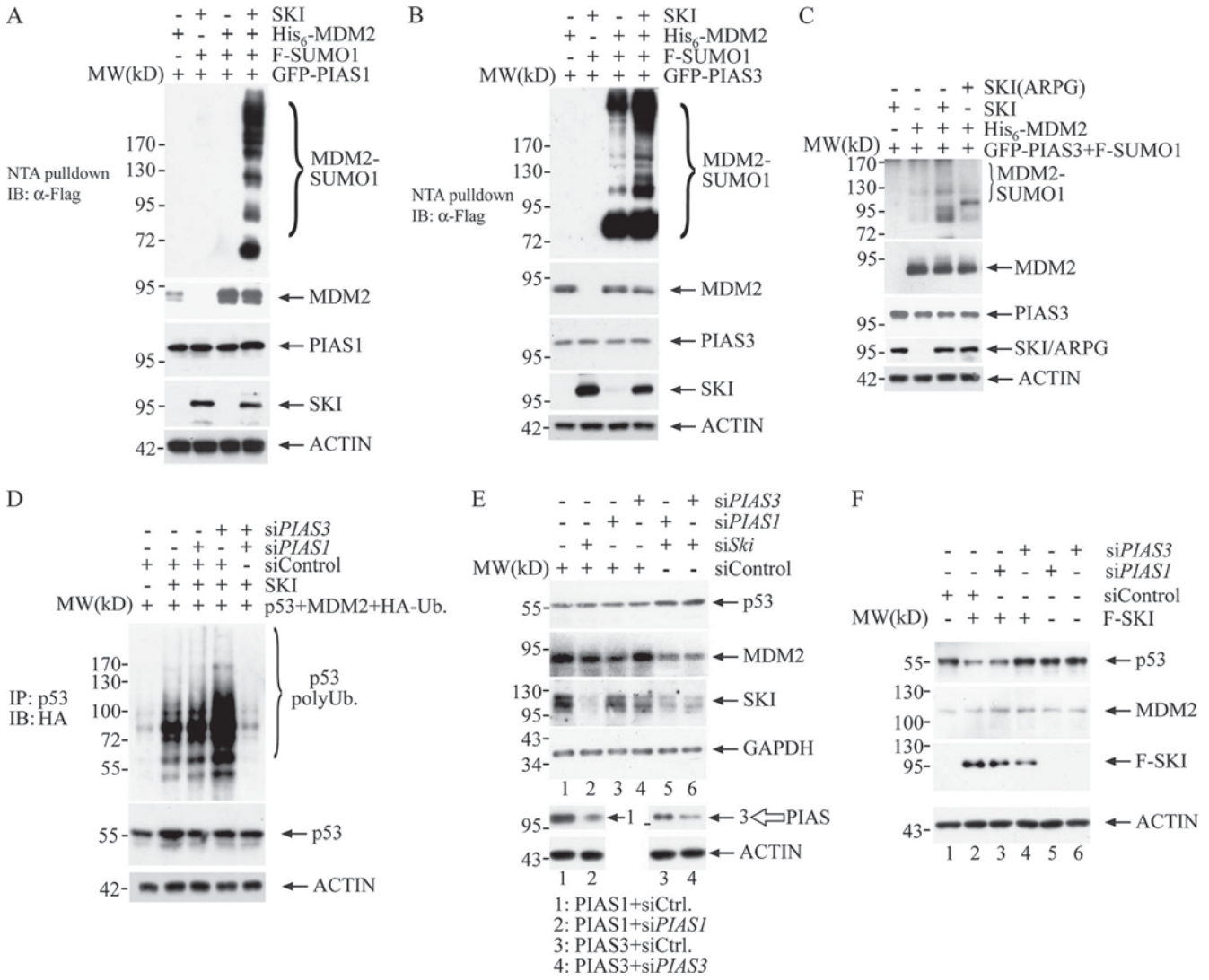

FIGURE 4. **SKI regulates MDM2 through sumoylation to result in a decrease of endogenous p53.** *A,* SKI can enhance MDM2 sumoylation through PIAS1. 24 h after expression, plasmids were introduced into 293T cells, and cells were lysed in RIPA buffer, and the supernatant was diluted into denaturing buffer. The MDM2 was isolated through nickel-nitrilotriacetic acid (*NTA*) beads followed by immunoblot (*IB*) analysis with anti-FLAG antibody to reveal MDM2 sumoylation. The blot was stripped and probed with anti-MDM2 antibody to reveal the MDM2 level. Separate lysate was used to examine PIAS1 and SKI expression levels using anti-PIAS1 and anti-SKI antibody, respectively. *B,* SKI can enhance MDM2 sumoylation through PIAS3. 40 h after transfection, cells were processed as in *A*. A portion of the lysate was analyzed to gauge the protein expression through immunoblot with anti-PIAS3 and anti-SKI antibody. *C,* SKI mutant ARPG fails to increase MDM2 sumoylation. 40 h after transfection, cells were processed as in *A*. A portion of the lysate was analyzed to gauge the protein expression through immunoblot with anti-PIAS3 and anti-SKI antibody. *D,* SKI enhances p53 ubiquitination through PIAS1 and -3. H1299 cells were transfected with various combinations of expression plasmids as well as siRNAs. The cells were processed as in Fig. 2. The effectiveness of siRNA for *PIAS1* or *-3* is shown in *E*. *E,* SKI and PIAS1 or -3 are required for maintaining the p53 level in LNCaP cells. Various siRNAs were introduced into LNCaP cells, and 40 h later, cells were lysed, and endogenous p53 as well as other proteins were examined by immunoblot analysis. The effectiveness of siRNA for PIAS1 or -3 was shown by the reduction of PIAS1 or -3 in 293T cells transfected with the expression plasmid alone or with the respective siRNA shown in the *lower panel*. *F,* down-regulation of p53 by overexpression of SKI can be reversed by a reduction of PIAS3. Expression plasmids for SKI and siRNAs were introduced into HEK293 cells, and 40 h later, cells were lysed, and endogenous p53 and MDM2 were examined by immunoblot analysis.

artificial dimerization of Ubc9 by the GST moiety. Using GST-Ubc9 as the substrate, as shown in Fig. 5*F*, SKI but not the ARPG protein can clearly increase Ubc9-mono-sumoylation as evidenced by the DTT-resistant Ubc9-SUMO1 conjugate. It has been reported that sumoylation of Ubc9 can alter substrate sumoylation by Ubc9 (47), and thus an increase of Ubc9 sumoylation likely will result in an enhanced sumoylation of certain substrate proteins. Taken together, we conclude that SKI can directly interact with Ubc9 and enhance its thioester bond formation as well as its own modification with SUMO1, resulting in increased activity of Ubc9. To our knowledge, this is the first demonstration that an oncoprotein can directly enhance Ubc9 activity through up-regulation of its biochemical activity. We also noted that there is a clear difference between wild type SKI and the ARPG mutant in that SKI protein can dramatically increase the mono-sumoylation of Ubc9, whereas ARPG mutant lacks this activity, strongly supporting the notion that the transforming capability of SKI at least partially derives from its up-regulation of Ubc9 activity through enhancing Ubc9 mono-sumoylation.

DISCUSSION

A multitude of molecular mechanisms has been put forward to explain the oncogenic activity of SKI. The most notable one

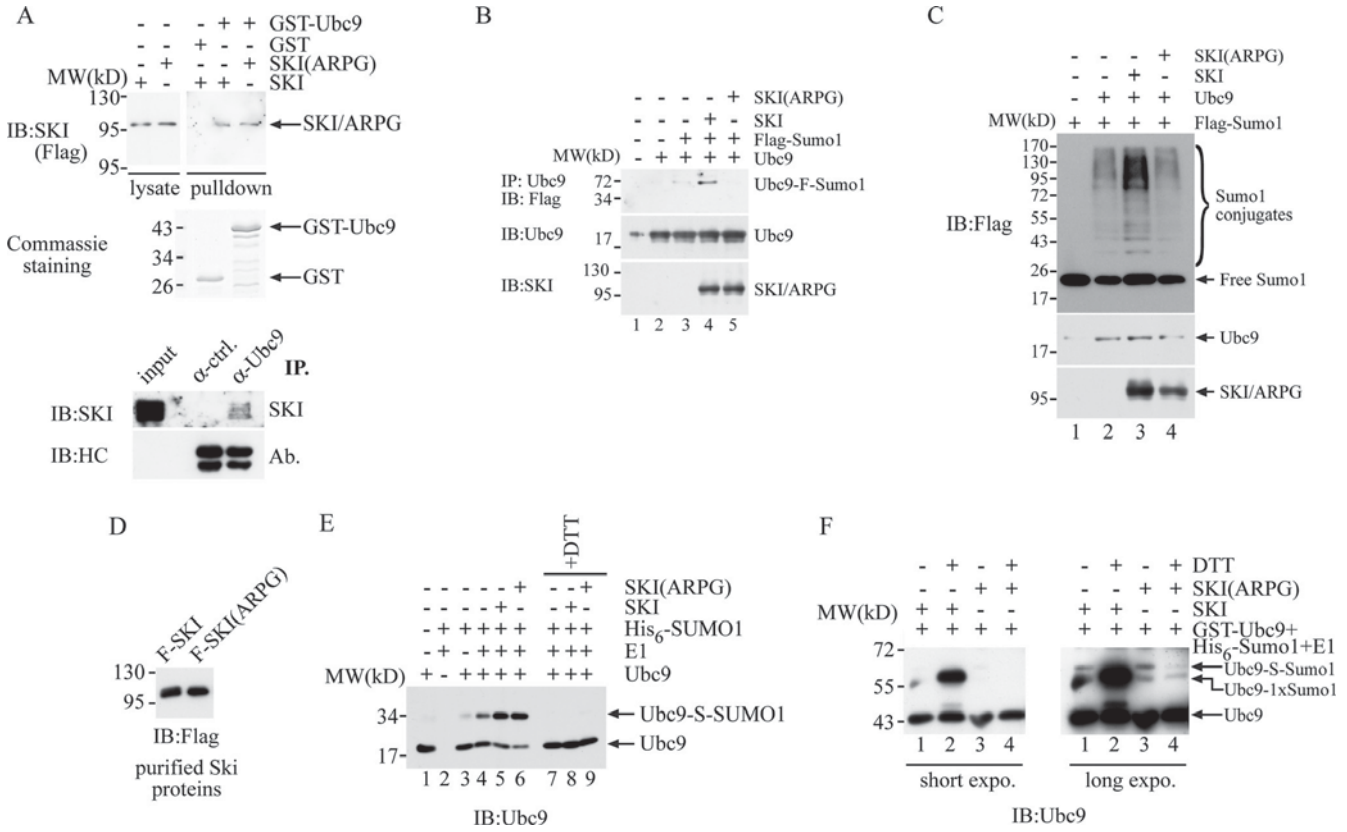

FIGURE 5. **SKI positively regulates Ubc9 both *in vivo* and *in vitro*.** *A,* SKI can directly interact with Ubc9. Approximately equal amounts of GST or GST-Ubc9 protein was mixed with lysate prepared from 293T cells with expression of FLAG-SKI, FLAG-SKI(ARPG), or control transfection. The GST fusion protein was retrieved with glutathione-Sepharose beads and washed three times with lysis buffer. The bead-bound proteins were analyzed by immunoblot (*IB*) analysis with anti-FLAG antibody to reveal the presence of SKI/ARPG protein in the GST-Ubc9 pulldown. The exposure time for the lysate protein was about 1/10 of that for the pulldown. In the *lower panel*, LNCaP cells were treated with paraformaldehyde for 10 min before collection, and lysed and immunoprecipitated (*IP*) with anti-Ubc9 antibody or control antibody. The immunoprecipitates were analyzed together with 10 μg of input lysate with SDS-PAGE followed by immunoblot with anti-SKI antibody or antibody for heavy chain. *B,* SKI enhances Ubc9 sumoylation *in vivo*. 293T cells were transfected with various plasmids, and the Ubc9 protein was immunoprecipitated with anti-Ubc9 antibody followed by immunoblot with anti-FLAG antibody to reveal the extent of the Ubc9 sumoylation. *C,* SKI enhances Ubc9-mediated sumoylation *in vivo*. 293T cells were transfected with various combinations of expression plasmids, and *in vivo* sumoylation was determined by immunoblot analysis with anti-FLAG antibody using the total lysate after SDS-PAGE. *D,* purified SKI and SKI(ARPG) protein. SKI and SKI(ARPG) were first immunoprecipitated with anti-FLAG antibody from 293T cells expressing FLAG-Ski or FLAG-Ski(ARPG), and then the immunoprecipitates were washed and incubated with FLAG peptide. The proteins were then quantitated by immunoblot with anti-FLAG antibody. *E,* SKI increases thioester bond formation of Ubc9 *in vitro*. 30 ng of Ubc9 protein was mixed with 60 ng of E1, 250 ng of His_6-Sumo1, and purified SKI/ARPG protein in 15 μl at 37 °C for 30 min. The reaction mixture was then separated by SDS-PAGE in the presence or absence of DTT in the sample buffer followed by immunoblot analysis with anti-Ubc9 antibody. *F,* SKI increases mono-sumoylation of Ubc9 *in vitro*. 10 ng of GST-Ubc9 protein was mixed with 110 ng of E1, 600 ng of His_6-Sumo1 as in *E* followed by immunoblot analysis with anti-Ubc9 antibody. The designation of Ubc9 conjugated with one SUMO1 molecule is based on its molecular weight increase and resistance to DTT.

is its connection with TGFβ signaling by its physical interaction with and inhibition of transcriptional activation by Smad proteins (13–15). It has also been found that SKI is capable of inhibiting transcriptional repression mediated by retinoblastoma tumor suppressor through complex formation (48). Its connection with Sirt1 and SKIP provides additional possibilities that potentially underlie its transforming capability (49, 50). We provided evidence that SKI can interact with the central component of cellular sumoylation machinery, Ubc9, and enhance Ubc9-mediated protein sumoylation. More specifically, SKI can enhance PIAS1- and PIAS3-mediated sumoylation of MDM2 and in this manner increase MDM2 levels and enhance MDM2-mediated p53 ubiquitination and proteasomal degradation. This is the most direct route for SKI to neutralize one of the essential tumor suppressor proteins in the cell and likely the major molecular mechanism that is responsible for its ability to cause cellular transformation.

A lack of transformation of mammalian cells by SKI raises an intriguing question. Overexpression of MDM2 has been shown to readily collaborate with several oncogenes to cause cellular transformation (51), and if SKI is capable of enhancing MDM2, then it should also readily collaborate with other oncogenes to cause transformation. Yet repeated attempts to demonstrate the transforming capability of *Ski* in mammalian cells yielded inconclusive results at best. Indeed, there are several reports suggesting that SKI is a tumor suppressor rather than an oncoprotein. For example, mouse embryo fibroblasts with a haploid deficiency of *Ski* grow faster in culture than cells with wild type *Ski* (52). In light of our evidence that SKI interacts with and enhances the activity of Ubc9, we can now rationalize the transforming ability of SKI in this broad context of cellular sumoylation. In this regard, p53 has also been shown to be sumoylated (53), and SKI can also enhance its sumoylation in mammalian cells through overexpression (supplemental Fig. 4). If sumoyla-

tion can compete against ubiquitination, it is conceivable that SKI in this manner can also enhance p53 stability. Thus, SKI can cause opposing effects in regulating p53 activity. On the one hand, more MDM2 sumoylation leads to more protein and activity and thus a reduced p53 level; on the other hand, SKI can directly enhance the p53 level through sumoylation-mediated stabilization or other p53 activities. It is likely that this opposing activity on p53 weakens the potency of SKI in causing cellular transformation and limits its target cells only to avian embryo fibroblast cells. Moreover, it is conceivable that in a certain cellular context, SKI favors the p53 sumoylation, resulting in enhanced tumor suppressor activity, and thus SKI in this fashion acts as a tumor suppressor rather than an oncoprotein. The precise molecular circuitry that dictates the ultimate activity of SKI is not clear; nevertheless, our novel finding will provide a molecular guide to unravel its role in a particular biological context.

In contrast to cellular ubiquitination machinery, there are a limited number of core components mediating protein sumoylation. There are so far one SUMO-activating enzyme E1 and one conjugating enzyme E2, and a handful of SUMO E3s, including PIAS1–4, Polycomb protein Pc2, and RanGAP1. A recent report of the TRIM protein family likely will expand the SUMO E3 family (54). As with many cellular enzymes, there will be positive and negative regulators for their functions. RSUME and ASF2 have been shown to positively regulate Ubc9 activity, although with distinct molecular mechanisms. RSUME acts as an enhancer for Ubc9 activity leading to increased SUMO-Ubc9 thioester bond formation (24), although ASF2 does not lead to enhanced thioester bond formation while augmenting substrate sumoylation by Ubc9 (25). In this regard, SKI is shown to both enhance Ubc9-SUMO1 thioester bond formation as well as sumoylation of Ubc9 itself. Because it is known that Ubc9 sumoylation can alter substrate sumoylation, it is conceivable that SKI can indirectly alter substrate sumoylation in a more dramatic manner by also enhancing thioester bond formation thus providing more SUMO donor. In this regard, SKI can also be viewed as a SUMO E3 for Ubc9.

We have provided evidence that oncoprotein SKI can interact with Ubc9 protein, and up-regulate MDM2 activity through enhanced sumoylation with a consequent down-regulation of the p53 level. This activity of SKI likely is a major determinant of its transforming ability as it directly links to the central tumor suppressor, p53, in the cell. This finding suggests that in tumors where SKI is overexpressed but the p53 protein is intact, SKI may contribute to tumor initiation and progression through down-regulation of p53 via increased sumoylation. At the same time, a reduction of cellular sumoylation cascade might provide therapeutic benefits in causing inactivation of MDM2 protein with a reactivation of p53.

Acknowledgments—We thank Dr. Moshe Oren for sending expression plasmids for wild type MDM2; Dr. Xinhua Feng for expression plasmid of FLAG-Sumo1; Dr. Steven B. McMahon for FLAG-p53; and Dr. Bert Vogelstein for sending HCT-116 with or without Tp53.

REFERENCES

1. Li, Y., Turck, C. M., Teumer, J. K., and Stavnezer, E. (1986) Unique sequence, ski, in Sloan-Kettering avian retroviruses with properties of a new cell-derived oncogene. *J. Virol.* **57,** 1065–1072
2. Medrano, E. E. (2003) Repression of TGF-β signaling by the oncogenic protein SKI in human melanomas. Consequences for proliferation, survival, and metastasis. *Oncogene* **22,** 3123–3129
3. Ritter, M., Kattmann, D., Teichler, S., Hartmann, O., Samuelsson, M. K., Burchert, A., Bach, J. P., Kim, T. D., Berwanger, B., Thiede, C., Jäger, R., Ehninger, G., Schäfer, H., Ueki, N., Hayman, M. J., Eilers, M., and Neubauer, A. (2006) Inhibition of retinoic acid receptor signaling by Ski in acute myeloid leukemia. *Leukemia* **20,** 437–443
4. Buess, M., Terracciano, L., Reuter, J., Ballabeni, P., Boulay, J. L., Laffer, U., Metzger, U., Herrmann, R., and Rochlitz, C. (2004) Amplification of SKI is a prognostic marker in early colorectal cancer. *Neoplasia* **6,** 207–212
5. Heider, T. R., Lyman, S., Schoonhoven, R., and Behrns, K. E. (2007) Ski promotes tumor growth through abrogation of transforming growth factor-β signaling in pancreatic cancer. *Ann. Surg.* **246,** 61–68
6. Fukuchi, M., Nakajima, M., Fukai, Y., Miyazaki, T., Masuda, N., Sohda, M., Manda, R., Tsukada, K., Kato, H., and Kuwano, H. (2004) Increased expression of c-Ski as a co-repressor in transforming growth factor-β signaling correlates with progression of esophageal squamous cell carcinoma. *Int. J. Cancer* **108,** 818–824
7. Takahata, M., Inoue, Y., Tsuda, H., Imoto, I., Koinuma, D., Hayashi, M., Ichikura, T., Yamori, T., Nagasaki, K., Yoshida, M., Matsuoka, M., Morishita, K., Yuki, K., Hanyu, A., Miyazawa, K., Inazawa, J., Miyazono, K., and Imamura, T. (2009) SKI and MEL1 cooperate to inhibit transforming growth factor-β signal in gastric cancer cells. *J. Biol. Chem.* **284,** 3334–3344
8. Barkas, A. (1986) Ph.D. dissertation. New York University
9. Chen, D., Lin, Q., Box, N., Roop, D., Ishii, S., Matsuzaki, K., Fan, T., Hornyak, T. J., Reed, J. A., Stavnezer, E., Timchenko, N. A., and Medrano, E. E. (2009) SKI knockdown inhibits human melanoma tumor growth *in vivo*. *Pigment Cell Melanoma Res.* **22,** 761–772
10. Sutrave, P., Kelly, A. M., and Hughes, S. H. (1990) Ski can cause selective growth of skeletal muscle in transgenic mice. *Genes Dev.* **4,** 1462–1472
11. Berk, M., Desai, S. Y., Heyman, H. C., and Colmenares, C. (1997) Mice lacking the *ski* proto-oncogene have defects in neurulation, craniofacial, patterning, and skeletal muscle development. *Genes Dev.* **11,** 2029–2039
12. Colmenares, C., Heilstedt, H. A., Shaffer, L. G., Schwartz, S., Berk, M., Murray, J. C., and Stavnezer, E. (2002) Loss of the SKI proto-oncogene in individuals affected with 1p36 deletion syndrome is predicted by strain-dependent defects in Ski$^{-/-}$ mice. *Nat. Genet.* **30,** 106–109
13. Luo, K., Stroschein, S. L., Wang, W., Chen, D., Martens, E., Zhou, S., and Zhou, Q. (1999) The Ski oncoprotein interacts with the Smad proteins to repress TGFβ signaling. *Genes Dev.* **13,** 2196–2206
14. Sun, Y., Liu, X., Eaton, E. N., Lane, W. S., Lodish, H. F., and Weinberg, R. A. (1999) Interaction of the Ski oncoprotein with Smad3 regulates TGF-β signaling. *Mol. Cell* **4,** 499–509
15. Xu, W., Angelis, K., Danielpour, D., Haddad, M. M., Bischof, O., Campisi, J., Stavnezer, E., and Medrano, E. E. (2000) Ski acts as a co-repressor with Smad2 and Smad3 to regulate the response to type β transforming growth factor. *Proc. Natl. Acad. Sci. U.S.A.* **97,** 5924–5929
16. Kretzschmar, M., and Massagué, J. (1998) SMADs. Mediators and regulators of TGF-β signaling. *Curr. Opin. Genet. Dev.* **8,** 103–111
17. Nomura, T., Khan, M. M., Kaul, S. C., Dong, H. D., Wadhwa, R., Colmenares, C., Kohno, I., and Ishii, S. (1999) Ski is a component of the histone deacetylase complex required for transcriptional repression by Mad and thyroid hormone receptor. *Genes Dev.* **13,** 412–423
18. Ferrand, N., Atfi, A., and Prunier, C. (2010) The oncoprotein c-Ski functions as a direct antagonist of the transforming growth factor-β type I receptor. *Cancer Res.* **70,** 8457–8466
19. Colmenares, C., and Stavnezer, E. (1989) The *ski* oncogene induces muscle differentiation in quail embryo cells. *Cell* **59,** 293–303
20. Geiss-Friedlander, R., and Melchior, F. (2007) Concepts in sumoylation. A decade on. *Nat. Rev. Mol. Cell Biol.* **8,** 947–956
21. Bae, S. H., Jeong, J. W., Park, J. A., Kim, S. H., Bae, M. K., Choi, S. J., and

Kim, K. W. (2004) Sumoylation increases HIF-1α stability and its transcriptional activity. *Biochem. Biophys. Res. Commun.* **324,** 394–400
22. Desterro, J. M., Rodriguez, M. S., and Hay, R. T. (1998) SUMO-1 modification of IκBα inhibits NF-κB activation. *Mol. Cell* **2,** 233–239
23. Sun, Y., Perera, J., Rubin, B. P., and Huang, J. (2011) SYT-SSX1 (Synovial Sarcoma Translocated) regulates PIASy to cause overexpression of NCOA3. *J. Biol. Chem.* **286,** 18623–18632
24. Carbia-Nagashima, A., Gerez, J., Perez-Castro, C., Paez-Pereda, M., Silberstein, S., Stalla, G. K., Holsboer, F., and Arzt, E. (2007) RSUME, a small RWD-containing protein, enhances SUMO conjugation and stabilizes HIF-1α during hypoxia. *Cell* **131,** 309–323
25. Pelisch, F., Gerez, J., Druker, J., Schor, I. E., Muñoz, M. J., Risso, G., Petrillo, E., Westman, B. J., Lamond, A. I., Arzt, E., and Srebrow, A. (2010) The serine/arginine-rich protein SF2/ASF regulates protein sumoylation. *Proc. Natl. Acad. Sci. U.S.A.* **107,** 16119–16124
26. Subramaniam, S., Mealer, R. G., Sixt, K. M., Barrow, R. K., Usiello, A., and Snyder, S. H. (2010) Rhes, a physiologic regulator of sumoylation, enhances cross-sumoylation between the basic sumoylation enzymes E1 and Ubc9. *J. Biol. Chem.* **285,** 20428–20432
27. Hock, A., and Vousden, K. H. (2010) Regulation of the p53 pathway by ubiquitin and related proteins. *Int. J. Biochem. Cell Biol.* **42,** 1618–1621
28. Miyauchi, Y., Yogosawa, S., Honda, R., Nishida, T., and Yasuda, H. (2002) Sumoylation of Mdm2 by protein inhibitor of activated STAT (PIAS) and RanBP2 enzymes. *J. Biol. Chem.* **277,** 50131–50136
29. Lee, M. H., Lee, S. W., Lee, E. J., Choi, S. J., Chung, S. S., Lee, J. I., Cho, J. M., Seol, J. H., Baek, S. H., Kim, K. I., Chiba, T., Tanaka, K., Bang, O. S., and Chung, C. H. (2006) SUMO-specific protease SUSP4 positively regulates p53 by promoting Mdm2 self-ubiquitination. *Nat. Cell Biol.* **8,** 1424–1431
30. Buschmann, T., Lerner, D., Lee, C. G., and Ronai, Z. (2001) The Mdm-2 amino terminus is required for Mdm2 binding and SUMO-1 conjugation by the E2 SUMO-1 conjugating enzyme Ubc9. *J. Biol. Chem.* **276,** 40389–40395
31. Honda, R., Tanaka, H., and Yasuda, H. (1997) Oncoprotein MDM2 is a ubiquitin ligase E3 for tumor suppressor p53. *FEBS Lett.* **420,** 25–27
32. Hollstein, M., and Hainaut, P. (2010) Massively regulated genes. the example of Tp53. *J. Pathol.* **220,** 164–173
33. Brooks, C. L., and Gu, W. (2006) p53 ubiquitination. Mdm2 and beyond. *Mol. Cell* **21,** 307–315
34. Toledo, F., and Wahl, G. M. (2006) Regulating the p53 pathway. *In vitro* hypotheses, *in vivo veritas*. *Nat. Rev. Cancer* **6,** 909–923
35. Colmenares, C., Teumer, J. K., and Stavnezer, E. (1991) Transformation-defective v-ski induces MyoD and myogenin expression but not myotube formation. *Mol. Cell. Biol.* **11,** 1167–1170
36. Sui, G., Affar el, B., Shi, Y., Brignone, C., Wall, N. R., Yin, P., Donohoe, M., Luke, M. P., Calvo, D., Grossman, S. R., and Shi, Y. (2004) Yin Yang 1 is a negative regulator of p53. *Cell* **117,** 859–872
37. Linares, L. K., Hengstermann, A., Ciechanover, A., Müller, S., and Scheffner, M. (2003) HdmX stimulates Hdm2-mediated ubiquitination and degradation of p53. *Proc. Natl. Acad. Sci. U.S.A.* **100,** 12009–12014
38. Wu, C., Miloslavskaya, I., Demontis, S., Maestro, R., and Galaktionov, K. (2004) Regulation of cellular response to oncogenic and oxidative stress by Seladin-1. *Nature* **432,** 640–645
39. Aylon, Y., Michael, D., Shmueli, A., Yabuta, N., Nojima, H., and Oren, M. (2006) A positive feedback loop between the p53 and Lats2 tumor suppressors prevents tetraploidization. *Genes Dev.* **20,** 2687–2700
40. Pomerantz, J., Schreiber-Agus, N., Liégeois, N. J., Silverman, A., Alland, L., Chin, L., Potes, J., Chen, K., Orlow, I., Lee, H. W., Cordon-Cardo, C., and DePinho, R. A. (1998) The Ink4a tumor suppressor gene product, p19Arf, interacts with MDM2 and neutralizes MDM2's inhibition of p53. *Cell* **92,** 713–723
41. Dai, M. S., Shi, D., Jin, Y., Sun, X. X., Zhang, Y., Grossman, S. R., and Lu, H. (2006) Regulation of the MDM2-p53 pathway by ribosomal protein L11 involves a post-ubiquitination mechanism. *J. Biol. Chem.* **281,** 24304–24313
42. Mayo, L. D., and Donner, D. B. (2001) A phosphatidylinositol 3-kinase/Akt pathway promotes translocation of Mdm2 from the cytoplasm to the nucleus. *Proc. Natl. Acad. Sci. U.S.A.* **98,** 11598–11603
43. Long, J., Wang, G., Matsuura, I., He, D., and Liu, F. (2004) Activation of Smad transcriptional activity by protein inhibitor of activated STAT3 (PIAS3). *Proc. Natl. Acad. Sci. U.S.A.* **101,** 99–104
44. Tatham, M. H., Geoffroy, M. C., Shen, L., Plechanovova, A., Hattersley, N., Jaffray, E. G., Palvimo, J. J., and Hay, R. T. (2008) RNF4 is a poly-SUMO-specific E3 ubiquitin ligase required for arsenic-induced PML degradation. *Nat. Cell Biol.* **10,** 538–546
45. Lallemand-Breitenbach, V., Jeanne, M., Benhenda, S., Nasr, R., Lei, M., Peres, L., Zhou, J., Zhu, J., Raught, B., and de Thé, H. (2008) Arsenic degrades PML or PML-RARα through a SUMO-triggered RNF4/ubiquitin-mediated pathway. *Nat. Cell Biol.* **10,** 547–555
46. Zhang, X. W., Yan, X. J., Zhou, Z. R., Yang, F. F., Wu, Z. Y., Sun, H. B., Liang, W. X., Song, A. X., Lallemand-Breitenbach, V., Jeanne, M., Zhang, Q. Y., Yang, H. Y., Huang, Q. H., Zhou, G. B., Tong, J. H., Zhang, Y., Wu, J. H., Hu, H. Y., de Thé, H., Chen, S. J., and Chen, Z. (2010) Arsenic trioxide controls the fate of the PML-RARα oncoprotein by directly binding PML. *Science* **328,** 240–243
47. Knipscheer, P., Flotho, A., Klug, H., Olsen, J. V., van Dijk, W. J., Fish, A., Johnson, E. S., Mann, M., Sixma, T. K., and Pichler, A. (2008) Ubc9 sumoylation regulates SUMO target discrimination. *Mol. Cell* **31,** 371–382
48. Tokitou, F., Nomura, T., Khan, M. M., Kaul, S. C., Wadhwa, R., Yasukawa, T., Kohno, I., and Ishii, S. (1999) Viral ski inhibits retinoblastoma protein (Rb)-mediated transcriptional repression in a dominant negative fashion. *J. Biol. Chem.* **274,** 4485–4488
49. Inoue, Y., Iemura, S., Natsume, T., Miyazawa, K., and Imamura, T. (2011) Suppression of p53 activity through the cooperative action of Ski and histone deacetylase SIRT1. *J. Biol. Chem.* **286,** 6311–6320
50. Dahl, R., Wani, B., and Hayman, M. J. (1998) The Ski oncoprotein interacts with Skip, the human homolog of *Drosophila* Bx42. *Oncogene* **16,** 1579–1586
51. Akagi, T. (2004) Oncogenic transformation of human cells. Shortcomings of rodent model systems. *Trends Mol. Med.* **10,** 542–548
52. Shinagawa, T., Nomura, T., Colmenares, C., Ohira, M., Nakagawara, A., and Ishii, S. (2001) Increased susceptibility to tumorigenesis of ski-deficient heterozygous mice. *Oncogene* **20,** 8100–8108
53. Carter, S., and Vousden, K. H. (2008) p53-Ubl fusions as models of ubiquitination, sumoylation, and neddylation of p53. *Cell Cycle* **7,** 2519–2528
54. Chu, Y., and Yang, X. (2011) SUMO E3 ligase activity of TRIM proteins. *Oncogene* **30,** 1108–1116

Molecular Cancer Therapeutics

Combination of Rad001 (Everolimus) and Propachlor Synergistically Induces Apoptosis through Enhanced Autophagy in Prostate Cancer Cells

Sheng Tai, Yin Sun, Nan Liu, et al.

Mol Cancer Ther Published OnlineFirst April 5, 2012.

Published OnlineFirst on April 5, 2012; DOI:10.1158/1535-7163.MCT-11-0954

Therapeutic Discovery

Molecular Cancer Therapeutics

Combination of Rad001 (Everolimus) and Propachlor Synergistically Induces Apoptosis through Enhanced Autophagy in Prostate Cancer Cells

Sheng Tai[1,2], Yin Sun[2], Nan Liu[2,5], Boxiao Ding[2], Elaine Hsia[2], Sunita Bhuta[2], Ryan K. Thor[2], Robert Damoiseaux[4], Chaozhao Liang[1], and Jiaoti Huang[2,3]

Abstract

PI3K/AKT/mTOR pathway plays a key role in the tumorigenesis of many human cancers including prostate cancer. However, inhibitors of this pathway, such as Rad001, have not shown therapeutic efficacy as a single agent. Through a high-throughput screen of 5,000 widely used small molecules, we identified compounds that can synergize with Rad001 to inhibit prostate cancer cells. One of the compounds, propachlor, synergizes with Rad001 to induce apoptosis of castration-resistant prostate cancer cells via enhanced autophagy. This enhanced autophagic cell death is accompanied by increased Beclin1 expression as well as upregulation of Atg5–Atg12 conjugate and LC3-2. Rad001 and propachlor can also synergistically inhibit tumors in a xenograft animal model of prostate cancer. These findings provide a novel direction to develop combination therapies for advanced and metastatic prostate cancer that has failed the currently available therapies. *Mol Cancer Ther; 11(6); 1–12. ©2012 AACR.*

Introduction

Prostate cancer is the most common malignancy and the second most common cause of cancer-related death among men in Western countries (1, 2). Although prostate cancer in early stages can be cured by local therapies, there is no cure for advanced and metastatic prostate cancer. Therefore, there is an urgent need to develop novel and effective systemic therapies. As has been observed in many human cancers, growth factor signaling pathways, particularly PI3K/AKT/mTOR pathway, are critical for the development of prostate cancer. A genomic survey of prostate cancer identified mutations in this pathway, leading to its hyperactivity (3). Inactivation of PTEN, a negative regulator of this pathway, has been found in a significant portion of human prostate cancer (3), and tissue-specific deletion of PTEN is sufficient to initiate prostate cancer in a mouse model (4). Thus, inhibition of the PI3K/AKT/mTOR pathway will likely suppress prostate cancer and provide therapeutic benefits. Rapamycin or its derivative, Rad001 (Everolimus; Fig. 1B), can specifically and potently inhibit mTORC1. Indeed, rapamycin (we will refer to Rad001, which is a more stable derivative, thereafter) has been approved to treat advanced kidney cancer as well as neuroendocrine pancreatic cancer. However, efforts to expand its use in more prevalent cancers including prostate cancer have been unsuccessful. It is postulated that inhibition of mTORC1 by Rad001 leads to activation of compensatory signaling pathways thus countering the growth-inhibitory effects (5). Novel compounds that simultaneously inhibit several signaling pathways, including mTORC1, have been identified, promising to more effectively suppress the tumor growth (6). Alternatively, identification of compounds that synergize with Rad001 may enhance the potency of Rad001 to treat human cancers. We conducted a high-throughput screen of 5,000 compounds including more than 1,000 U.S. Food and Drug Administration (FDA)-approved drugs as well as purified natural products and other compounds with known safety profiles. We identified propachlor (Fig. 1B) as a compound that synergizes with Rad001 to induce cell death in prostate cancer cells.

Materials and Methods

Materials

PC3 cells were obtained from the American Type Culture Collection (ATCC), and the C4-2 cells were kindly provided by Dr. Lily Wu at UCLA (Los Angeles, CA). Both

Authors' Affiliations: [1]Department of Urology and Anhui Geriatric Institute, The First Affiliated Hospital of Anhui Medical University, Hefei, Anhui, China; [2]Department of Pathology, [3]Jonsson Comprehensive Cancer Center and Broad Center for Regenerative Medicine and Stem Cell Biology; [4]Molecular Screening Shared Resource, David Geffen School of Medicine at UCLA, Los Angeles, California; and [5]Department of Obstetrics and Gynecology, Nanfang Hospital, Southern Medical University, Guangzhou, China

Note: S. Tai and Y. Sun contributed equally to this work.

Corresponding Authors: Jiaoti Huang, Department of Pathology and Laboratory Medicine, David Geffen School of Medicine at UCLA, 10833 Le Conte Ave., 13-229 CHS, Los Angeles, CA 90095. Phone: 310-267-2264; Fax: 310-794-4161; E-mail: JiaotiHuang@mednet.ucla.edu; and Chaozhao Liang, Department of Urology and The Geriatric Institute of Anhui, The First Affiliated Hospital of Anhui Medical University, 218 Jixi Avenue, Hefei, Anhui, China 230022. E-mail: Liang_chaozhao@163.com

doi: 10.1158/1535-7163.MCT-11-0954

Published OnlineFirst on April 5, 2012; DOI:10.1158/1535-7163.MCT-11-0954

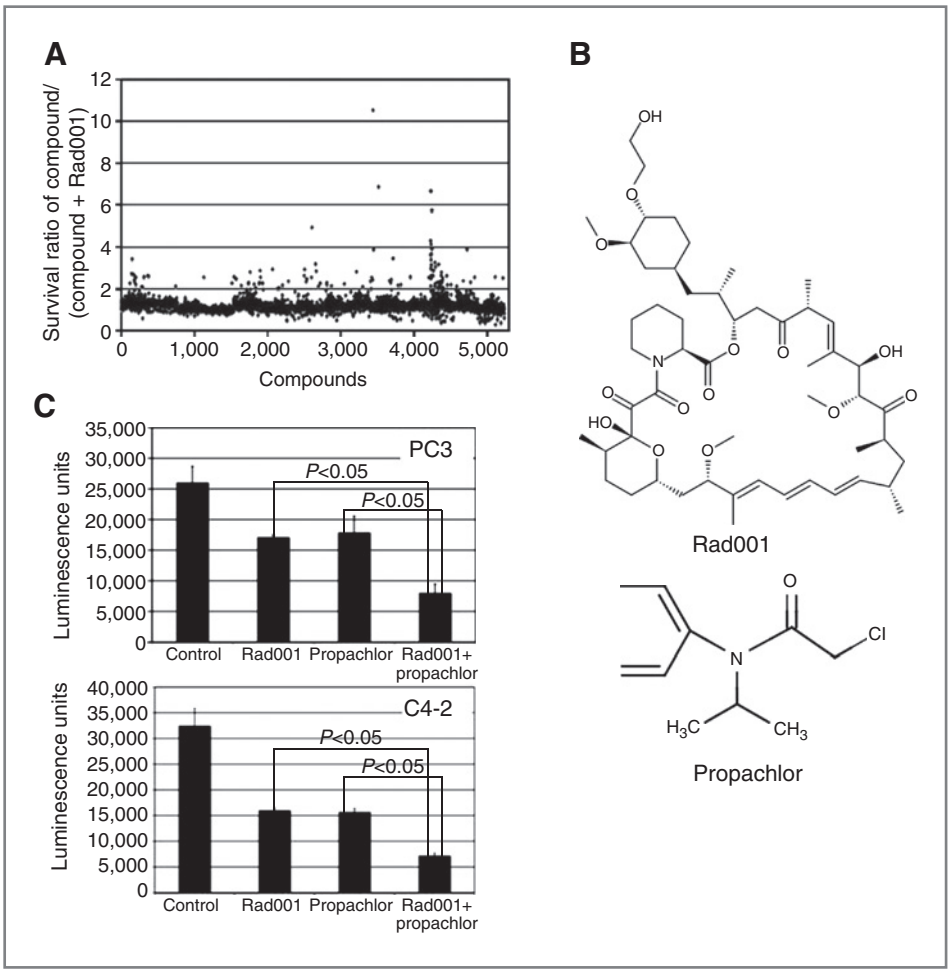

Figure 1. Identification of propachlor as a collaborating compound with Rad001. A, five thousand compounds were added alone or together with 20 nmol/L Rad001 in C4-2 cells, the survival ratio gauged by ATP measurement between cells that are treated with single compound or combination with Rad001 is plotted. B, the chemical structures of Rad001 and propachlor. C, propachlor can collaborate with Rad001 to inhibit PC3 and C4-2 cells. Single compounds or combination with Rad001 were used to treat PC3 or C4-2 cells for 72 hours followed by CellTiter-Glo measurement to measure cell number. The 2-way *t* test showed $P < 0.05$ between the 2 groups.

cell lines were passaged for fewer than 6 months after resuscitation. The PC3 cells were tested and authenticated by the ATCC, and no authentication for either cell line was done by the authors. FBS, RPMI medium 1640, Dulbecco's Modified Eagle's Medium (DMEM), sodium pyruvate, L-glutamine, penicillin, and streptomycin were purchased from Hyclone; propachlor and Rad001 were from Sigma; CellTiter assay was from Promega; Caspase-3/7 Assay Kit was from Anaspec; Annexin V Apoptosis Detection Kit was from eBioscience; DharmaFECT transfection reagent was from Thermo Scientific Life Science; Lipofectamine 2000 transfection reagent was from Invitrogen; *Beclin1*-siRNA (5′-rGrGrA rArUrGrGrArArUrGrArrGrArUrUrArA, 5′-rArGrCrArGrCrArUrUrArArUrCrUrCrArUrU) and control-siRNA (5′-rGrArArArArArCrUrCrArUrArUrArArArUrCr, 5′-rGrUrGrGrGrGrCrGrA rUrUrUrArUrArUrGrA) were from IDT; and reverse transcriptase PCR (RT-PCR) primers for *Beclin1*, 5′-GGCCAATAAGATGGGTCTGA-3′ and 5′-CTGCACACAGTCCAGGAAAG-3′, for *GAPDH* 5′-CATGGGTGTGAACCATGAGA-3′ and 5′-CAGTGATGGCATGGACTGTG-3′, were from ValueGene. Rabbit anti-LC-3 polyclonal antibody was from GenScript; rabbit anti-Beclin1, rabbit anti-cleaved caspase-3, and rabbit anti-PARP1 polyclonal antibodies were from Cell Signaling; rabbit anti-caspase-3 polyclonal antibody was from Abgent; rabbit anti-Atg5 monoclonal antibody was from Epitomics; and mouse anti-β-actin antibody was from Sigma.

High-throughput screen

C4-2 cells were seeded in 384-well plate at 1,000 cells per well. After overnight incubation, compounds were delivered to the plates by SAGIAN Core System with a Biomek FX equipped with 500 nL pin tool, and Rad001 was added to a final concentration of 20 nmol/L using a Multidrop 384. The concentration of the compounds from the compound libraries was 10 μmol/L final, whereas the total volume was 50 μL and the dimethyl sulfoxide (DMSO) concentration was 1% or less. Ninety-six hours later, cell number was determined using CellTiter-Glo (Promega) on a VICTOR 3V (PerkinElmer), according to the manufacturers' instructions. The potential hits were identified as those that led to 50% or more reduction of cell number with the combination of Rad001 and the compound than with the compound alone. The hits were further tested in conventional tissue culture settings to verify their synergistic effects with Rad001 in decreasing cell viability.

Published OnlineFirst on April 5, 2012; DOI:10.1158/1535-7163.MCT-11-0954

Cell culture

The PC3 cells were maintained in the DMEM containing 10% FBS penicillin-streptomycin, L-glutamine, sodium pyruvate; and the C4-2 cells were maintained in RPMI-1640 supplemented with 10% FBS and penicillin-streptomycin. Cells were grown at 37°C with 5% CO_2.

Cell viability, combination index, and growth curves

The cells were seeded into the 96-well plate at 3×10^3 cells per well. After 48 hours, PC3 cells were treated with DMSO, 0.055 to 0.88 μmol/L Rad001 for 24 hours, and 0.89 to 14.25 μmol/L propachlor or their combination for 24 hours. The C4-2 cells were treated with DMSO, 0.041 to 0.65 μmol/L Rad001 for 24 hours, and 0.25 to 4.08 μmol/L propachlor or their combination for 24 hours. Triplicates were used for each treatment group. The cell viability/relative cell number was measured with the Promega CellTiter-Glo Assay according to manufacturer's instructions. The compound interactions were analyzed with CalcuSyn software (version2.1, BIOSOFT) to determine the combination index (CI) for Rad001 and propachlor.

Equal numbers of cells were seeded into 96-well plate and maintained with normal medium. After 48 hours, the PC3 cells were treated with DMSO (control), Rad001 (0.70 μmol/L), propachlor (6.15 μmol/L), or their combination, respectively. The C4-2 cells were treated with DMSO (control), Rad001 (0.56 μmol/L), propachlor (7.05 μmol/L), or their combination, respectively. The cell viability/relative cell number was measured on days 1, 2, 3, and 4 after compound addition by CellTiter-Glo. All the experiments were carried out in triplicates. The PC3 and C4-2 cells were also treated with compounds for 1 day and analyzed with trypan blue staining.

GFP-LC3 analysis

Cells were transfected with GFP-LC3 plasmid using Lipofectamine 2000 transfection reagent. After 24 hours, the medium was changed, and the PC3 cells were treated with DMSO (control), Rad001 (0.7 μmol/L), propachlor (6.15 μmol/L), or their combination, respectively, for 1 day. The C4-2 cells were treated with DMSO (control), Rad001 (0.56 μmol/L), propachlor (7.05 μmol/L), or their combination, respectively, for 1 day. The cells were fixed in 4% paraformaldehyde for 30 minutes, washed twice with PBS and stained with 4′,6–diamidino–2–phenylindole (DAPI), and observed under a fluorescence microscope (Eclipse 90i slide scope) with ×40 lens.

Protein analysis

The cultured cells were washed with cold PBS and lysed with lysis buffer (20 mmol/L KCl, 150 mmol/L NaCl, 1% NP-40, 50 mmol/L NaF, 50 mmol/L Tris-HCl, pH 7.5, 1 mmol/L dithiothreitol, 1 mmol/L EGTA, 1 × Protease Inhibitor, 10% glycerol) for 10 minutes on ice. The cells were centrifuged for 15 minutes at 4°C. The protein concentration in the supernatant was determined with the Bradford Assay (Bio-Rad). Equal amount of protein was loaded on 8% or 15% SDS-PAGE and transferred to polyvinylidene fluoride membrane. The membrane was blocked with nonfat dry milk for 1 hour, incubated with primary antibody in nonfat dry milk overnight, washed with PBS for 30 minutes, incubated with secondary antibody for 30 minutes, washed with PBS/0.1%Tween-20 for 2 hours, and detected with enhanced chemiluminescence (Pierce).

Caspase-3/7 activity analysis

Equal number of PC3 and C4-2 cells was seeded into the 96-well plates. After 48 hours, cells were treated the DMSO, Rad001, propachlor, or their combination for 15 hours. The caspase-3/7 activity was measured by the SensoLyte Homogeneous AMC Caspase-3/7 Assay Kit after reaction for 8 hours. All the experiments were carried out in triplicates.

Analysis of apoptosis

After 15-hour treatment, the PC3 and C4-2 cells were collected. The apoptosis was quantified by fluorescence-activated cell-sorting (FACS) analysis (BD FACSDiva Software v6) with Annexin-V/7-AAD staining following the manufacturer's guidelines. The percentage of Annexin-V–positive cells was analyzed by FlowJo (Version 7.6.4).

Quantitative RT-PCR

The PC3 and C4-2 were treated with compounds for 1 day and total RNA was purified from the cells with Fermentas Gene RNA Purification Kit. Equal amounts of RNA were reverse-transcribed by reverse transcriptase (Fermentas) according to the manufacturer's instructions. Quantitative real-time PCR was carried out with SA Biosciences RT^2 Real-time SYBR Kit with the following parameters: 15 μL, 95°C for 8 minutes for one cycle followed by 43 cycles of 95°C for 15″/60°C for 60″.

siRNA transfection

A total of 4×10^3 of cells were seeded into the 96-well plates and transfected with siRNA (100 nmol/L) by the DharmaFECT General Transfection Reagent. The combination of Rad001 and propachlor was added to the cells for 1 day after transfection followed by cell viability/relative cell number measurement. To determine the knockdown efficiency, cells were seeded into the 12-well plate followed by transfection with *Beclin1*-siRNA and control-siRNA, respectively, and collected after another 24 hours.

Beclin1 mRNA half-life analysis

To determine the metabolic stability of *Beclin1* mRNA, the C4-2 cells were treated with DMSO, Rad001, propachlor, and their combination. Actinomycin D was added at 10 μg/mL to inhibit transcription. After 0, 1, 2, and 4 hours, cells were collected and washed with PBS, and total RNA was extracted. Relative levels of mRNAs were determined by real-time PCR and normalized to that of glyceraldehyde-3-phosphate

Published OnlineFirst on April 5, 2012; DOI:10.1158/1535-7163.MCT-11-0954

dehydrogenase (*GAPDH*). All the experiments were carried out in triplicates.

Cell-cycle analysis

After 24-hour treatment, PC3 and C4-2 cells were harvested, washed with PBS, and fixed in 70% ethanol. After 1-day fixation, the cells were washed with PBS twice, treated with RNase (50 μg/mL), and stained with propidium iodide (50 μg/mL) for 30 minutes at 37°C. The cell-cycle phase distribution was determined by Flow Cytometry (BD FACSDiva Software v6). The percentage of cells in each phase was analyzed by FlowJo (Version 7.6.4).

Prostate cancer xenograft

Five- to 6-week-old SCID (severe combined immunodeficient) mice were obtained from the UCLA Division of Laboratory Animal Medicine. All the mice were inoculated with 100 μL (50% Matrigel/PBS) of PC3 cells suspension (7×10^6) to each dorsal flank with 25-gauge syringe. When the tumor size reached between 90 and 100 mm^3, the mice were divided into the control, Rad001, propachlor, and combination group, with 6 mice per group. The Rad001 and propachlor were delivered intraperitoneally (i.p.) 1 and 5 mg/kg daily. The tumor size and mouse weight were measured every 4 days. These tumor measurements were converted to tumor volume using the formula, $V = 0.52 \times L \times W^2$, where W and L are the smaller and larger diameters. At the 44th day, all mice were sacrificed; tumors were dissected and collected. All the animal experiments were conducted according to the protocol approved by the UCLA Animal Research Committee.

Statistical analysis

The normalized isobologram analysis and bars were conducted with CalcuSyn software (version 2.1, BIOSOFT) and Microsoft Excel 2003, respectively. With median effects model described by Chou (7), the multiple compound dose–effect calculations were conducted. CI values of <0.9, >0.9 to <1.2, >1.2 were considered as being synergistic, additive, and antagonistic, respectively. Statistical analysis was conducted by 2-sided t test. P value less than 0.05 was considered to be statistically significant.

The statistical significance of different tumor sizes between each treatment and control group was determined by one-way ANOVA followed by the Dunnett test. Statistical analyses on body weights were conducted by one-way ANOVA followed by Tukey test. The level of significance was set at $P < 0.05$. Statistical calculations were carried out by the SPSS version 13.0.

Results

Identification of compounds that synergize with Rad001 to inhibit prostate cancer cells

PI3K/AKT/mTOR signaling pathway plays a central role in many human cancers including prostate cancer. However, inhibitors of this pathway, such as Rad001, have failed to show efficacy for prostate cancer as a single agent likely due to activation of compensatory pathways (5). We reasoned that certain chemical compounds may synergize with Rad001 to inhibit multiple pathways and thus restore the full therapeutic potential of Rad001, a clinically useful drug with known safety profiles. Therefore, we chose 5,000 compounds available through our screening facility and conducted a screen in castration-resistant prostate cancer (CRPC) cells using individual compound alone or in combination with Rad001 (Fig. 1A). The primary screen yielded a number of compounds that decreased cell numbers by more than 50% in the presence of Rad001 compared with when the compounds were used alone. Several compounds collaborated with Rad001 in reducing the cell numbers in secondary and tertiary screens, and propachlor (Fig. 1B) was chosen for detailed studies.

Synergy of Rad001 and propachlor in inhibiting prostate cancer cell lines PC3 and C4-2

To confirm that Rad001 and propachlor can synergistically inhibit prostate cancer cells, we added each of them at varying concentrations and monitored the effects in PC3 and C4-2 cells, 2 prostate cancer cell lines that resist androgen withdrawal. As shown in Fig. 2A, dose-dependent decrease of cell numbers was seen in both cell lines treated with either Rad001 or propachlor. For PC3 cells, the ED_{50} for propachlor was 6.55 μmol/L, and we did not reach ED_{50} for Rad001 under the experimental conditions. For C4-2 cells, we did not reach ED_{50} for propachlor, whereas the ED_{50} for Rad001 was 0.43 μmol/L. However, when the cells were treated with the combination of the 2 compounds, there was significantly more decrease in cell numbers in both cell lines (z-axis) compared with treatment with either Rad001 or propachlor alone (Fig. 2A). CI, a measure of synergistic activity, was determined with the CalcuSyn software program, which confirmed significant synergism of the 2 compounds (Fig. 2B). For example, for PC3 cells, treatment with 0.44 μmol/L Rad001 or 3.56 μmol/L propachlor alone resulted in 10.45% and 17.15% reduction in the cell number, respectively. However, when the 2 compounds were combined, the cell number was reduced by 67.21% (CI < 0.9). Mixture-algebraic estimate analysis, conducted with CalcuSyn software, showed a strong synergism for most of the combinations of 2 compounds at various concentrations for the 2 cell lines, suggesting that the synergism is not limited to a particular threshold concentration of either compound. We also determined whether these compounds synergize at different time points after compound addition. As shown in Fig. 2C, both PC3 and C4-2 cells exhibited pronounced reduction of cell numbers after combination treatment at multiple time points.

Combination of Rad001 and propachlor synergistically induces apoptosis in PC3 and C4-2 cells

The synergistic reduction of cell number can be the result of a cell-cycle block or an induction of cell death or

Published OnlineFirst on April 5, 2012; DOI:10.1158/1535-7163.MCT-11-0954

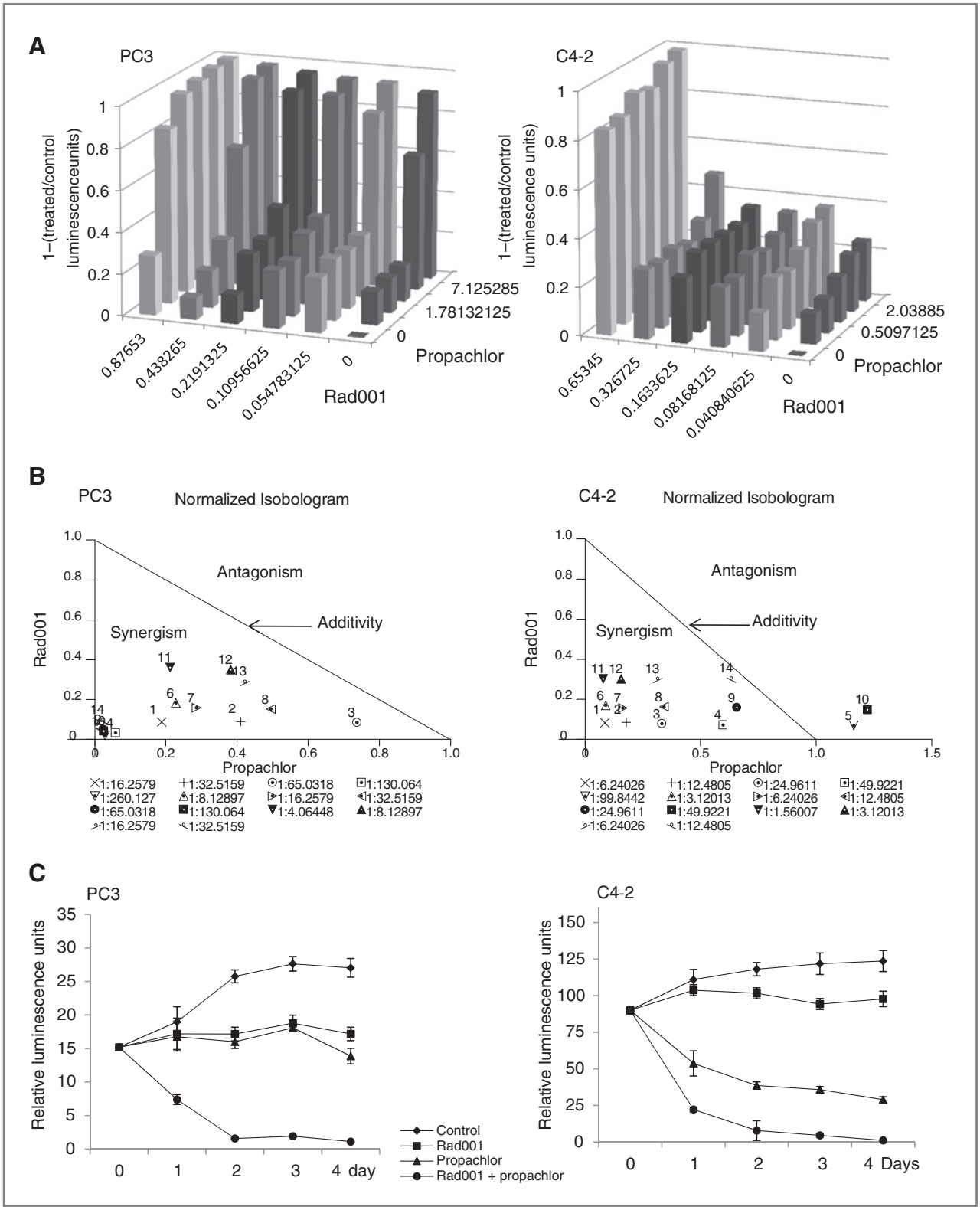

Figure 2. The combination of Rad001 and propachlor induces a synergistic reduction of cell number in prostate cancer cells. A, decreasing doses of Rad001 alone, propachlor alone, and their combination were used, and cell numbers measured as in Fig. 1 (*x*-axis, Rad001 μmol/L; *y*-axis, propachlor μmol/L; *z*-axis, 1 − (treatment luminescence unit/control luminescence). B, normalized isobologram analysis showed synergistic interactions in PC3 and C4-2 cells. The analysis was done with CalcuSyn software, which conducts the drug dose–effect calculation with the median effect method described by Chou (7). A large number of combination groups were below the line, indicating synergism. C, growth curves by measuring ATP level shows more reduction of cell number when cells were treated with the drug combination.

Published OnlineFirst on April 5, 2012; DOI:10.1158/1535-7163.MCT-11-0954

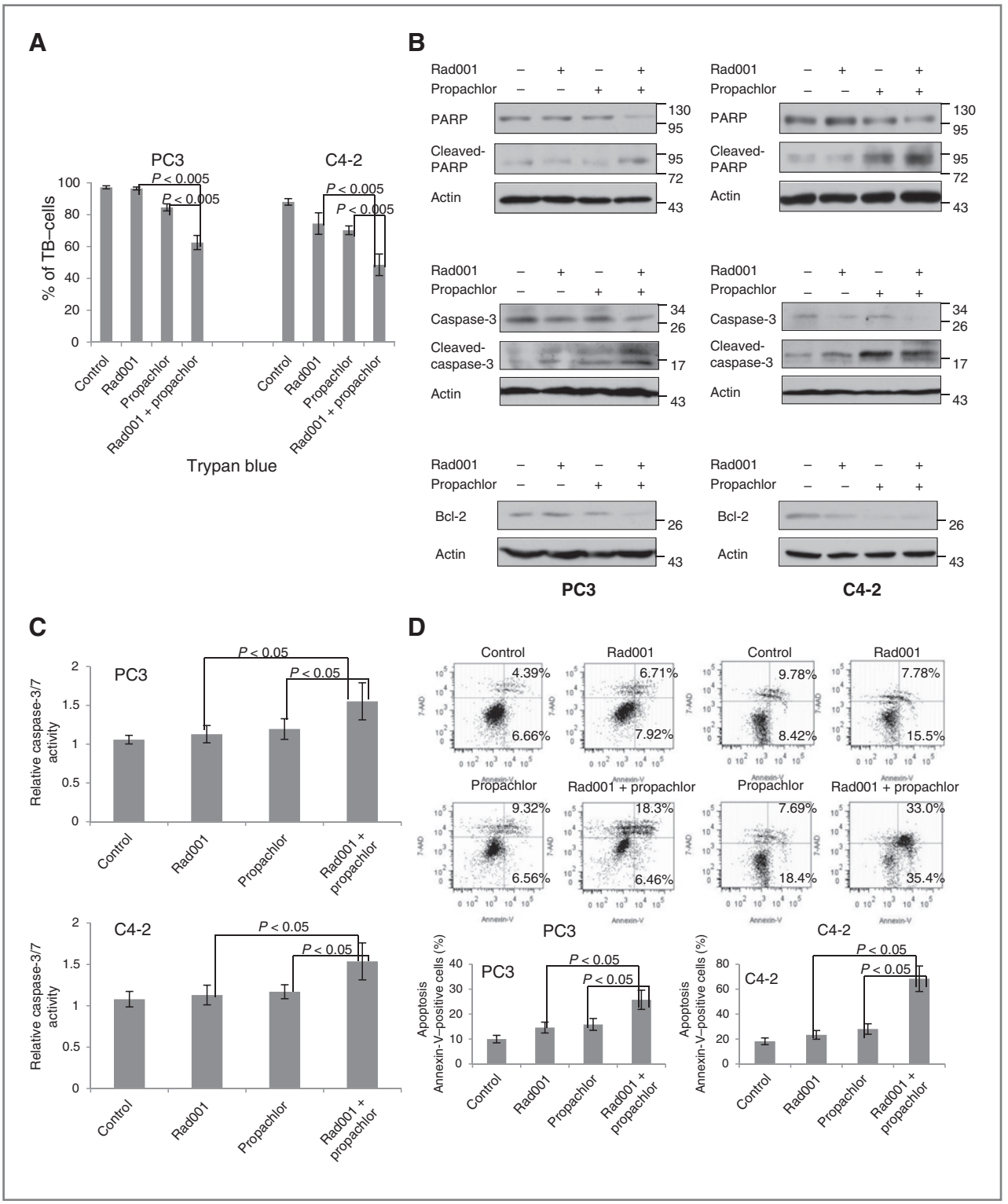

Figure 3. Combination of Rad001 and propachlor synergistically induces cell death in prostate cancer cells. PC3 cells were treated with DMSO (control), Rad001 (0.70 μmol/L), propachlor (6.15 μmol/L), or their combination, and C4-2 cells were treated with DMSO (control), Rad001 (0.56 μmol/L), propachlor (7.05 μmol/L), or their combination. A, trypan blue (TB) assay. Combination treatment resulted in lower cell viability than either compound alone (2-way *t* test: $P < 0.005$). B, increased levels of cleaved PARP1 and caspase-3 and decreased Bcl-2 in PC3 and C4-2 cells treated for 15 hours with the combination of Rad001 and propachlor. Lysates from cells were separated by SDS-PAGE followed by immunoblotting with respective antibodies. C, higher activities of caspase-3/7 in PC3 and C4-2 cells treated for 15 hours with the drug combination. D, flow cytometric analysis of apoptosis with Annexin-V and 7-AAD staining. There was a significant increase in the percentage of apoptotic cell after combination treatment versus single compound ($P < 0.05$).

Published OnlineFirst on April 5, 2012; DOI:10.1158/1535-7163.MCT-11-0954

their combination. We conducted a cell-cycle analysis of the cells treated with the compounds but did not detect a significant change in the distribution of cell-cycle phases. We conducted trypan blue staining of the cells after the drug treatment. As shown in Fig. 3A, there was a significant decrease in the percentage of cells negative for intracellular blue staining in both PC3 and C4-2 cells compared with single compound treatment ($P < 0.005$), suggesting that the combination treatment resulted in decreased cell viability. This was further confirmed with the semiquantitative analysis of the abundance of proteins involved in cell apoptosis. As shown in Fig. 3B, when PC3 and C4-2 cells were treated with vehicle (DMSO), Rad001, propachlor, or their combination for 15 hours, there was a significant increase of the cleaved form of apoptosis marker PARP1 (Fig. 3B, top; ref. 8). This was accompanied by the induction of cleaved caspase-3 (Fig. 3B, middle), reduced expression of Bcl-2 (Fig. 3B, bottom), and induced activity of caspase-3/7 (Fig. 3C), suggesting that apoptotic pathway was activated in response to the combination

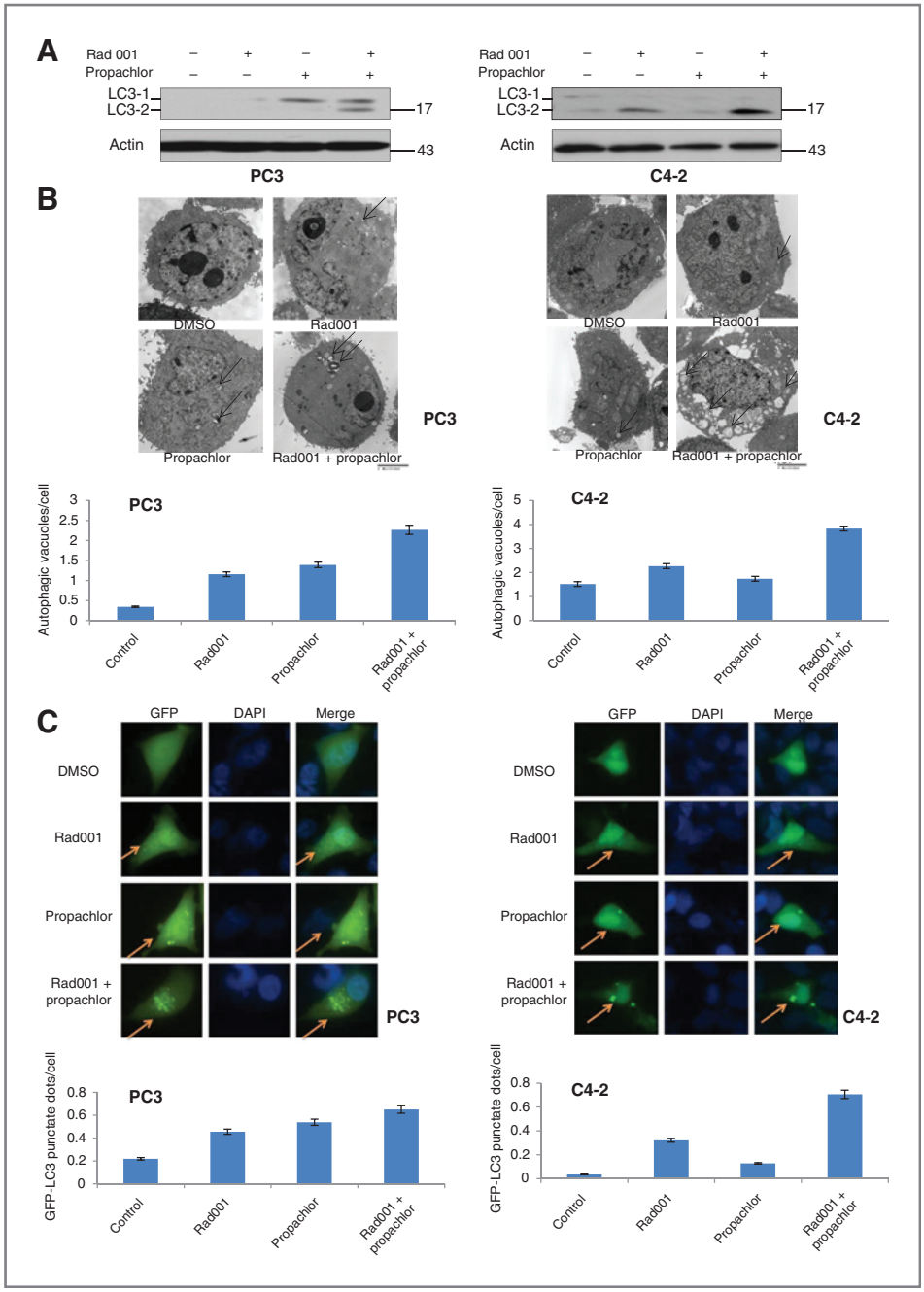

Figure 4. Rad001 and propachlor combination synergistically induces autophagy in PC3 and C4-2 cells. Autophagy was analyzed after 1 day of treatment. PC3 cells were treated with DMSO (control), Rad001 (0.70 μmol/L), propachlor (6.15 μmol/L), or their combination, and C4-2 cells were treated with DMSO (control), Rad001 (0.56 μmol/L), propachlor (7.05 μmol/L), or their combination. A, upregulation of LC3-2 in PC3 and C4-2 cells treated with combination of the 2 compounds. Immunoblotting was conducted as in Fig. 3. B, increased autophagosomes (arrows) were observed by electron microscopy in cells treated with Rad001/propachlor compared with each compound alone. Quantified data from 30 cells are shown in the bottom. C, autophagosome analysis through GFP-LC3 expression. C4-2 and PC3 cells expressing GFP-LC3 were treated with DMSO, Rad001, propachlor, or their combination for 24 hours. The cells were fixed with paraformaldehyde and visualized with epifluorescence. Yellow arrows indicate the punctate pattern of GFP-LC3, representative of autophagosome, and nuclei were visualized through DAPI staining. The number of GFP-LC3 punctuate dots/cells was quantitated in 50 GFP^+ cells from each group (bottom).

Published OnlineFirst on April 5, 2012; DOI:10.1158/1535-7163.MCT-11-0954

treatment. To provide another level of confirmation, we conducted flow cytometric analysis of cells stained with Annexin-V and 7-AAD to examine the population level of apoptotic response to the compounds. As shown in Fig. 3D, combination of Rad001 and propachlor increased the fraction of apoptotic cells significantly more than single treatment, as quantified by the percentage of both early and late apoptotic cells in the 2 cell lines. These data strongly suggest that combination of Rad001 and propachlor results in synergistic cytotoxicity through the activation of the apoptotic pathway.

Combination of Rad001 and propachlor synergistically induces autophagy in PC3 and C4-2 cells

It is important to understand the mechanism by which the combination of the 2 compounds synergistically activates the apoptotic pathway. Because programmed cell death can be induced by autophagy, we determined whether the 2 compounds synergistically induce autophagy. Enhanced conversion of microtubule-associated protein 1 light chain 3 (LC3-1) to its faster-migrating form LC3-2 is a hallmark of autophagy induction (9). As shown in Fig. 4A, there was substantially more LC3-2 conversion after combination treatment compared with Rad001 or propachlor treatment alone in both PC3 and C4-2 cell lines, suggesting that they can synergistically induce autophagy. We also examined the abundance of autophagosomes induced by the compounds. Autophagosomes are characterized by membranous structures with double or multiple membrane layers. Transmission electron microscopic analysis of the cells treated with various compounds showed that the cells treated with the 2 compounds in combination had increased number of autophagosomes in comparison with single-agent treatment (Fig. 4B, top), again confirming that there was a synergistic induction of autophagy. The quantification of this increase is shown in Fig. 4B (bottom).

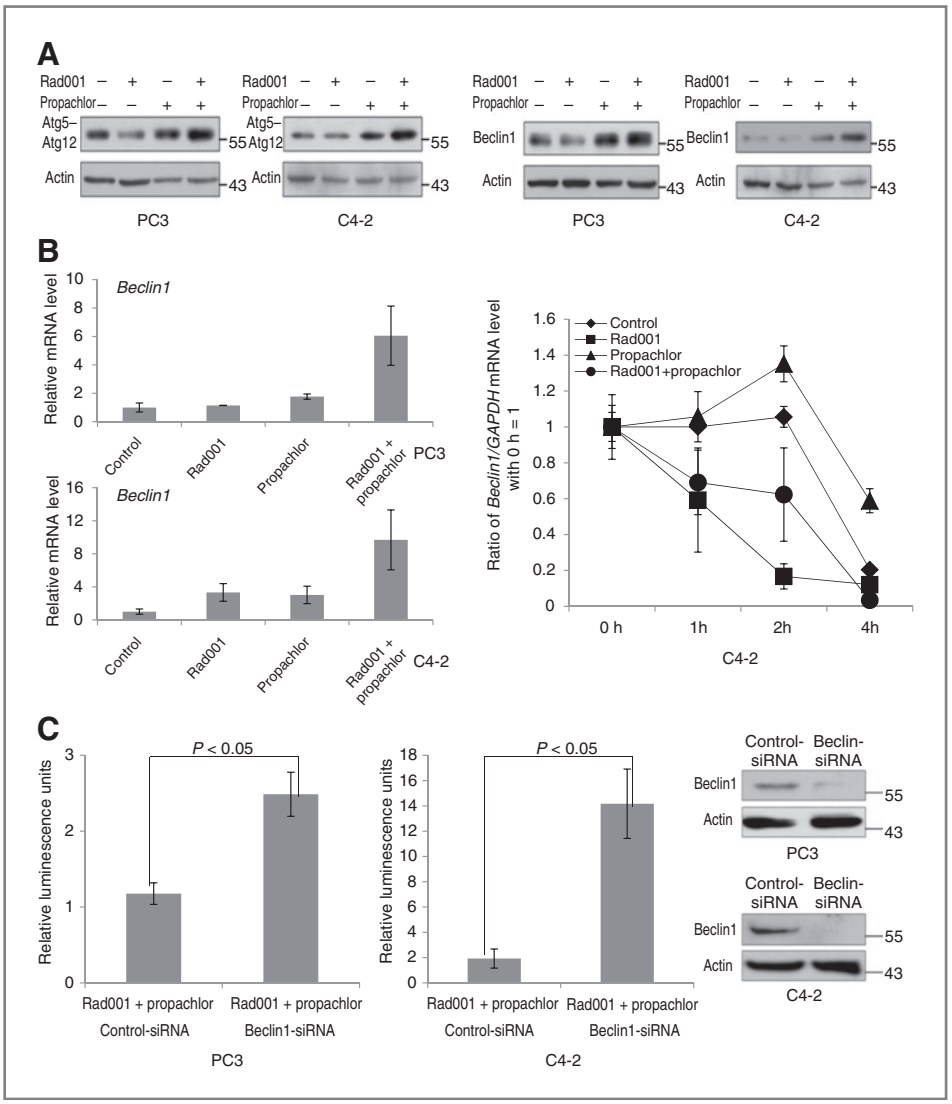

Figure 5. Regulation of autophagy proteins in response to combination treatment of Rad001 and propachlor. A, Atg5–Atg12 conjugates and Beclin1 were induced in response to combination treatment for 24 hours. Immunoblotting was conducted as in Fig. 3. B, *Beclin 1* mRNA was more significantly upregulated by the combination treatment as shown by qRT-PCR analyses (left). Right, shows that *Beclin1* mRNA stability does not increase in response to the combination treatment. C, Beclin1 is critical for the autophagic death induced by the combination treatment. PC3 and C4-2 cells were transfected with control siRNA or siRNA for *Beclin1* (right). Cells were treated with combination of Rad001 and propachlor 24 hours after transfection. The cell number was determined with ATP measurement 24 hours after the combination treatment.

Published OnlineFirst on April 5, 2012; DOI:10.1158/1535-7163.MCT-11-0954

Autophagosomes can also be visualized through the expression of GFP-LC3, which upon autophagosome formation becomes clustered on the membrane vesicles and visible as a ring structure under a fluorescent microscope. Figure 4C (top) shows that there were more punctuate GFP-positive vesicles in response to the combination treatment in both PC3 and C4-2 cells, and the quantification of the results is shown in Fig. 4C (bottom). Consistent with the increase of autophagy in response to the combination treatment, we also found that Atg5–Atg12 conjugate, which is involved in the first of the two ubiquitination-like reactions that control autophagy (10), was increased in the 2 cell lines treated with the 2 compounds in combination (Fig. 5A). Taken together, we conclude that there is a synergistic induction of autophagy in response to the combinatorial treatment of Rad001 and propachlor, resulting in autophagic cell death.

Combination of Rad001 and propachlor increases the expression of Beclin1, which is important for the induced autophagy and apoptosis

Beclin1 (Atg6) is critical for the initiation of autophagy pathway (11). Accordingly, we found that Beclin1 protein levels increased in response to the combination treatment (Fig. 5A, right). The increase of Beclin1 protein is likely the result of increased mRNA levels of *Beclin1* as shown by qRT-PCR analysis (Fig. 5B, left). To determine whether the increase of mRNA level is the result of enhanced transcription of *Beclin1* gene or increased stability of *Beclin1* mRNA, we examined the metabolic stability of *Beclin1* mRNA by measuring its half-life. As shown in Fig. 5B (right), Rad001 decreased *Beclin1* mRNA stability, whereas propachlor slightly increased its stability and the combination of the 2 compounds did not increase *Beclin1* mRNA stability as compared with the control group, suggesting that the increase of *Beclin1* mRNA is likely the result of increased transcription of the gene.

To determine whether the induced autophagy is necessary for the increased cell death induced by the combination treatment, we used siRNA to reduce the expression of Beclin1 and examined whether its loss of function impacts on the cell death induced by the combination treatment. As shown in Fig. 5C, the Beclin1 level was markedly reduced by siRNA treatment (right) and reduction of Beclin1 protein led to a significant rescue of cell death in response to the combination treatment (left and middle). These results suggest that synergistic induction of autophagy is likely the underlying mechanism for the increased cell death induced by the 2 compounds used in combination. Taken together, these results suggest that Beclin1 is induced in response to the combination treatment, and the enhanced autophagy plays an essential role in the synergistic induction of cell death.

Rad001 and propachlor combination inhibits prostate cancer xenograft tumor

We next determined whether the synergism also exists in a preclinical prostate cancer xenograft mouse model. The toxicity of propachlor is relatively low with LD_{50} at 550 mg/kg (12), so we used it at 5 mg/kg D^{-1} while using Rad001 at 1 mg/kg D^{-1}, which has been commonly reported (13). We initiated tumor with s.c. injection of PC3 cells on both flanks of SCID mice. When tumor size reached approximately 100 mm^3, we started daily intraperitoneal injection of the 2 compounds and measured tumor size and body weight on every fourth day. As shown in Fig. 6A, the combination of Rad001 and propachlor inhibited the growth of PC3 xenograft tumor significantly more than either compound alone (**, $P < 0.05$ compared with one compound administration; *, $P < 0.05$ compared with control). In addition, combination treatment showed no adverse effect on body weights (Fig. 6A, right; $P > 0.05$) and daily activities. No complications such as anaphylaxis and skin necrosis were observed throughout the course of the study. We also examined autophagosome formation in the xenograft tumors by transmission electron microscopy. Consistent with the *in vitro* results, combination of the 2 compounds increased autophagosome formation in the xenograft tumors (Fig. 6B and C). In addition, there was a significant increase of LC3-1, LC3-2, and Beclin1 levels in the combination treatment group, compared with groups that received either compound alone (Fig. 6D). Therefore, we have shown that propachlor can synergize with Rad001 to induce apoptosis of prostate cancer cells through synergistic induction of autophagy *in vitro* and *in vivo*, establishing a foundation for potential clinical trials of similar combinations in patients with prostate cancer.

Discussion

Hormonal therapy has been the main treatment modality for advanced or metastatic prostate cancer for decades. However, hormonal therapy, including the newest drugs such as abiraterone and MDV3100, is palliative and nearly all patients will eventually experience tumor recurrence, for which there is no effective therapy. Thus, there is an urgent need to develop novel therapies targeting additional pathways for CRPC. It has been found that androgen enhances mTOR activity in an androgen receptor–dependent manner (14), and active mTOR signaling suppresses autophagy. Autophagosome formation is increased in the rat prostate epithelial cells upon castration (15, 16). More recently, it was reported that prostate cancer cells can enhance autophagy to survive androgen deprivation treatment (17). Therefore, it is likely that autophagy plays an important role in the development of prostate cancer, and targeting this pathway may be a novel therapeutic strategy.

Propachlor is a herbicide first marketed by Monsanto in 1965 (18) with well-established safety profile. Although this particular compound may or may not be used in patients with prostate cancer, its synergy with Rad001 and the underlying mechanism provide us novel therapeutic targets and an opportunity to increase

Published OnlineFirst on April 5, 2012; DOI:10.1158/1535-7163.MCT-11-0954

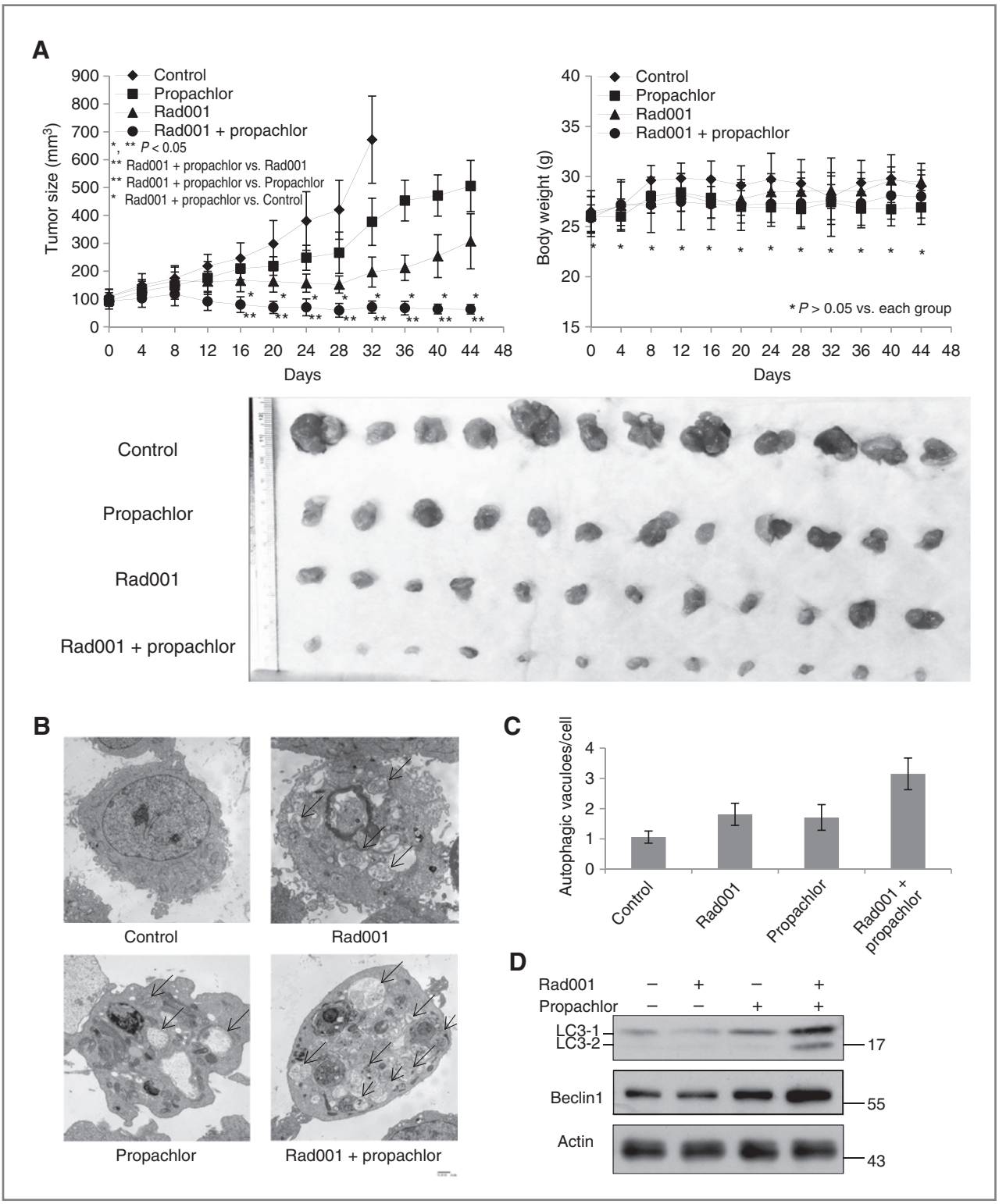

Figure 6. Combination of Rad001 and propachlor significantly inhibits the PC3 xenograft tumors in mice. A, antitumor activity on PC3 xenografts by various compounds. Mice were administered daily i.p. with Rad001 (1 mg/kg), propachlor (5 mg/kg), or both (6 mice/group). The tumor sizes (left) and body weights (right) were measured every 4 days. Tumors treated with 2 drugs were much smaller than single compound treatment or control. B, electron microscopic analysis of the tumors collected from various treatment groups. Arrows indicate autophagosomes. C, quantitation of the number of autophagosomes in 30 cells from the xenograft tumors. D, immunoblot analysis for LC3 and Beclin1 from the xenograft tumors.

Published OnlineFirst on April 5, 2012; DOI:10.1158/1535-7163.MCT-11-0954

the therapeutic efficacy and reduce the side effects of existing drugs. In this regard, the recent identification of combination treatment of rapamycin and thapsigargin for ras-driven cancer represents another excellent example (19). Identification of novel compounds that synergize with existing molecules will also expand our understanding of the molecular mechanisms of induced cancer cell death.

The main finding of our study is that the combination of Rad001 and propachlor induces apoptosis of CRPC cells in a synergistic manner, and enhanced autophagy is likely the underlying mechanism. Autophagy or macroautophagy is a major intracellular pathway for degrading and recycling cellular macromolecules, including proteins, ribosomes, and cytoplasmic organelles (20). In normal cells, autophagy functions to maintain cellular homeostasis by disposing of damaged or aged organelles. Autophagy is induced in response to stresses such as nutrient starvation, hormone treatment, chemotherapeutic agents, as well as in pathologic conditions, including neurodegenerative diseases such as Alzheimer disease, Parkinson disease, Huntington disease, hereditary myopathies, infectious diseases, and cancer (20–23). More recently, it was found that excessive autophagy can lead to cell death, especially in the absence of functional apoptotic molecules such as Bax/Bak (24). This type of cell death is termed the second type of programmed cell death (20). Thus, it is conceivable that the induction of autophagy is cell context–dependent, and the extent of autophagy dictates the cellular outcome. At an appropriate level, autophagy protects cells by recycling and disposing of toxic and nonfunctional cellular proteins and organelles, whereas excessive autophagy or a particular kind of autophagy may result in damage of the cells, ultimately leading to cell death. As such, agents have been identified that can cause tumor cell death and reduce tumor burden by causing autophagic cell death, suggesting that modulation of autophagy is a new avenue for anticancer therapeutics (25, 26). In gastric cancer cells, inhibition of caspase-3 enhances the autophagic cell death, suggesting that inhibition of apoptosis results in induction of autophagy (27). For prostate cancer, induction of autophagy and caspase-independent apoptosis by arginine deiminase appears to be a novel therapeutic modality (28). It has also been reported that inhibition of autophagy can lead to induction of apoptosis (29). Simultaneous induction of autophagy and apoptosis seems to be responsible for cell death in response to the combination treatment of histone deacetylase inhibitor and the Bcl-2 homology domain-3 mimetic GX15-070 (30). Rad001 induces autophagy but is not potent (31). Because propachlor can synergize with Rad001 to enhance autophagy and induce cell death in 2 CRPC cell lines, this may represent a new direction to develop therapies for advanced prostate cancer that has failed both traditional (e.g., LH-RH analog, casodex) and newer (e.g., abirateron, MDV3100) forms of hormonal therapy for which no effective treatment exists.

C4-2 was derived from LNCaP cells and has features of castration-resistant adenocarcinoma, such as expressing androgen receptor and prostate-specific antigen. PC3 cells are negative for androgen receptor and prostate-specific antigen but express neuroendocrine markers, similar to human prostate small cell carcinoma (32), which represents the most aggressive form of late-stage prostate cancer. Although the 2 cell lines are similarly resistant to androgen deprivation, they appear to have different sensitivities to the agents used in this study, which may have clinical implications.

In summary, we have shown that Rad001 and propachlor can synergize with each other to cause death of CRPC cells, thus providing a novel therapeutic possibility for this incurable disease. Our findings also establish autophagy induction as a novel direction of prostate cancer therapy.

Disclosure of Potential Conflicts of Interest

No potential conflicts of interests were disclosed.

Acknowledgments

The authors thank Dr. Hong Zhang for helpful discussions.

Grant Support

J. Huang is supported by UCLA SPORE in Prostate Cancer (PI: Robert Reiter), Department of Defense Prostate Cancer Research Program (PC101008), a challenge award from the Prostate Cancer Foundation (PI: O. Witte), a creativity award from the Prostate Cancer Foundation (PI: Matthew Rettig), Cal-Tech-UCLA Joint Center for Translational Medicine Program, and National Cancer Institute (1R01CA158627-01; PI: Leonard Marks).

The costs of publication of this article were defrayed in part by the payment of page charges. This article must therefore be hereby marked *advertisement* in accordance with 18 U.S.C. Section 1734 solely to indicate this fact.

Received November 23, 2011; revised March 13, 2012; accepted March 28, 2012; published OnlineFirst April 5, 2012.

References

1. Morgan TM, Welty CJ, Vakar-Lopez F, Lin DW, Wright JL. Ductal adenocarcinoma of the prostate: increased mortality risk and decreased serum prostate specific antigen. J Urol 2010;184:2303–7.
2. Andriole GL, Crawford ED, Grubb RL III, Buys SS, Chia D, Church TR, et al. Mortality results from a randomized prostate-cancer screening trial. N Engl J Med 2009;360:1310–9.
3. Berger MF, Lawrence MS, Demichelis F, Drier Y, Cibulskis K, Sivachenko AY, et al. The genomic complexity of primary human prostate cancer. Nature 2011;470:214–20.
4. Wang S, Gao J, Lei Q, Rozengurt N, Pritchard C, Jiao J, et al. Prostate-specific deletion of the murine Pten tumor suppressor gene leads to metastatic prostate cancer. Cancer Cell 2003;4:209–21.
5. Carracedo A, Baselga J, Pandolfi PP. Deconstructing feedback-signaling networks to improve anticancer therapy with mTORC1 inhibitors. Cell Cycle 2008;7:3805–9.
6. Santiskulvong C, Konecny GE, Fekete M, Chen KY, Karam A, Mulholland D, et al. Dual targeting of phosphoinositide 3-kinase and mammalian target of rapamycin using NVP-BEZ235 as a novel therapeutic

Published OnlineFirst on April 5, 2012; DOI:10.1158/1535-7163.MCT-11-0954

approach in human ovarian carcinoma. Clin Cancer Res 2011;17:2373–84.
7. Chou TC. Drug combination studies and their synergy quantification using the Chou-Talalay method. Cancer Res 2010;70:440–6.
8. Tewari M, Quan LT, O'Rourke K, Desnoyers S, Zeng Z, Beidler DR, et al. Yama/CPP32 beta, a mammalian homolog of CED-3, is a CrmA-inhibitable protease that cleaves the death substrate poly(ADP-ribose) polymerase. Cell 1995;81:801–9.
9. Tanida I, Ueno T, Kominami E. LC3 and Autophagy. Methods Mol Biol 2008;445:77–88.
10. Ravikumar B, Futter M, Jahreiss L, Korolchuk VI, Lichtenberg M, Luo S, et al. Mammalian macroautophagy at a glance. J Cell Sci 2009;122:1707–11.
11. Smith DM, Patel S, Raffoul F, Haller E, Mills GB, Nanjundan M. Arsenic trioxide induces a beclin-1-independent autophagic pathway via modulation of SnoN/SkiL expression in ovarian carcinoma cells. Cell Death Differ 2010;17:1867–81.
12. Hertfordshire, UK: University of Hertfordshire. Available from: http://sitem.herts.ac.uk/aeru/footprint/en/Reports/543.htm.
13. Stelzer MK, Pitot HC, Liem A, Lee D, Kennedy GD, Lambert PF. Rapamycin inhibits anal carcinogenesis in two preclinical animal models. Cancer Prev Res (Phila) 2010;3:1542–51.
14. Xu Y, Chen SY, Ross KN, Balk SP. Androgens induce prostate cancer cell proliferation through mammalian target of rapamycin activation and post-transcriptional increases in cyclin D proteins. Cancer Res 2006;66:7783–92.
15. Kwong J, Choi HL, Huang Y, Chan FL. Ultrastructural and biochemical observations on the early changes in apoptotic epithelial cells of the rat prostate induced by castration. Cell Tissue Res 1999;298:123–36.
16. Wilson MJ, Whitaker JN, Sinha AA. Immunocytochemical localization of cathepsin D in rat ventral prostate: evidence for castration-induced expression of cathepsin D in basal cells. Anat Rec 1991;229:321–33.
17. Li M, Jiang X, Liu D, Na Y, Gao GF, Xi Z. Autophagy protects LNCaP cells under androgen deprivation conditions. Autophagy 2008;4:54–60.
18. Zheng W, Yates SR, Papiernik SK, Guo M. Propachlor herbicide residue studies in cabbage using modified analytical procedure. Cornell University: Springerlink; 2009.
19. De Raedt T, Walton Z, Yecies JL, Li D, Chen Y, Malone CF, et al. Exploiting cancer cell vulnerabilities to develop a combination therapy for ras-driven tumors. Cancer Cell 2011;20:400–13.
20. Levine B. Cell biology: autophagy and cancer. Nature 2007;446:745–7.
21. Kuma A, Hatano M, Matsui M, Yamamoto A, Nakaya H, Yoshimori T, et al. The role of autophagy during the early neonatal starvation period. Nature 2004;432:1032–6.
22. Mizushima N, Levine B, Cuervo AM, Klionsky DJ. Autophagy fights disease through cellular self-digestion. Nature 2008;451:1069–75.
23. Shintani T, Klionsky DJ. Autophagy in health and disease: a double-edged sword. Science 2004;306:990–5.
24. Shimizu S, Kanaseki T, Mizushima N, Mizuta T, Arakawa-Kobayashi S, Thompson CB, et al. Role of Bcl-2 family proteins in a non-apoptotic programmed cell death dependent on autophagy genes. Nat Cell Biol 2004;6:1221–8.
25. Zhang XQ, Huang XF, Hu XB, Zhan YH, An QX, Yang SM, et al. Apogossypolone, a novel inhibitor of antiapoptotic Bcl-2 family proteins, induces autophagy of PC-3 and LNCaP prostate cancer cells *in vitro*. Asian J Androl 2010;12:697–708.
26. Lian J, Wu X, He F, Karnak D, Tang W, Meng Y, et al. A natural BH3 mimetic induces autophagy in apoptosis-resistant prostate cancer via modulating Bcl-2-Beclin1 interaction at endoplasmic reticulum. Cell Death Differ 2010;18:60–71.
27. Kim MS, Jeong EG, Ahn CH, Kim SS, Lee SH, Yoo NJ. Frameshift mutation of UVRAG, an autophagy-related gene, in gastric carcinomas with microsatellite instability. Hum Pathol 2008;39:1059–63.
28. Kim RH, Coates JM, Bowles TL, McNerney GP, Sutcliffe J, Jung JU, et al. Arginine deiminase as a novel therapy for prostate cancer induces autophagy and caspase-independent apoptosis. Cancer Res 2009;69:700–8.
29. Amaravadi RK, Yu D, Lum JJ, Bui T, Christophorou MA, Evan GI, et al. Autophagy inhibition enhances therapy-induced apoptosis in a Myc-induced model of lymphoma. J Clin Invest 2007;117:326–36.
30. Wei Y, Kadia T, Tong W, Zhang M, Jia Y, Yang H, et al. The combination of a histone deacetylase inhibitor with the BH3-mimetic GX15-070 has synergistic antileukemia activity by activating both apoptosis and autophagy. Autophagy 2010;6:976–8.
31. Tsvetkov AS, Miller J, Arrasate M, Wong JS, Pleiss MA, Finkbeiner S. A small-molecule scaffold induces autophagy in primary neurons and protects against toxicity in a Huntington disease model. Proc Natl Acad Sci U S A 2010;107:16982–7.
32. Tai S, Sun Y, Squires JM, Zhang H, Oh WK, Liang CZ, et al. PC3 is a cell line characteristic of prostatic small cell carcinoma. Prostate 2011;71:1668–79.